APPARENT ELECTRICAL CONDUCTIVITY MAPPING IN MANAGED PODZOLS USING MULTI-COIL AND MULTI-FREQUENCY EMI SENSOR MEASUREMENTS

By

EMMANUEL ADEDAMOLA BADEWA

A Thesis submitted to the School of Graduate Studies

in partial fulfillment of the requirements for the degree of

Master of Science

Boreal Ecosystems and Agricultural Sciences

School of Science and Environment

Grenfell Campus

Memorial University of Newfoundland

October, 2017

St. John's Newfoundland and Labrador

APPARENT ELECTRICAL CONDUCTIVITY MAPPING IN MANAGED PODZOLS USING MULTI-COIL AND MULTI-FREQUENCY EMI SENSOR MEASUREMENTS

by

EMMANUEL ADEDAMOLA BADEWA

A Thesis submitted to the School of Graduate Studies

in partial fulfillment of the requirements for the degree of

Master of Science

In

Boreal Ecosystems and Agricultural Sciences

Approved:

____

Dean of the Graduate School

____

Advisor

____

Date

Committee Members:

Dr. Adrian Unc

Dr. Mumtaz Cheema

ABSTRACT

Apparent Electrical Conductivity Mapping in managed Podzols using Multi-coil and Multi-frequency EMI sensor measurements

by

Emmanuel Badewa, Master of Science

Memorial University, 2017

Advisor: Dr. Lakshman W. Galagedara

Department: Boreal Ecosystems and Agricultural Sciences

The research focused on utilizing apparent electrical conductivity (ECa) survey protocols in characterizing the spatial and temporal variability of soil physical and hydraulic properties in Western Newfoundland, Canada. In this study, two different non-invasive multi-coil and multi-frequency EMI sensors; CMD Mini-explorer and GEM-2, respectively were used to collect ECa data under different nutrient management systems at Pynn's Brook Research Station, Pasadena. Results showed that due to the differences in investigation depths of the two EMI sensors, the linear regression models generated for SMC using the CMD Mini-explorer were statistically significant with the highest R^2 = 0.79 and the lowest RMSE = 0.015 $m^3\ m^{-3}$ and not significant for GEM-2 with the lowest R^2 = 0.17 and RMSE = 0.045 $m^3\ m^{-3}$. Furthermore, there is a significant relationship between the ECa mean relative differences (MRD) versus SMC MRD (R^2 = 0.33 to 0.70) for both multi-Coil and multi-Frequency sensors. In addition, the spatial variability of the

ECa predicted soil properties are relatively consistent with lower variability compared to the measured soil properties. Conclusively, the ECa measurements obtained through either multi-coil or multi-frequency sensors have the potential to be successfully employed for soil physical and hydraulic properties at the field scale.

ACKNOWLEDGMENTS

My sincere appreciation to the almighty God for the grace and strength He gave me to successfully complete my masters course. First, I would like to thank my advisor, Dr. Lakshman Galagedara for inviting me to work on this topic with his research team and my co-advisor, Dr Adrian Unc for his purposeful advice and encouragement throughout my programme and Dr. Mumtaz Cheema as the advisory committee member for his supports and comments.

I equally thank Dr. Daniel Altdorff for his support in all phases of my research particularly for his expertise on the EMI instruments. Special Thanks to the Agro-physics research team members for their support during lab and field works. Special Thanks to Research and Development Corporation, NL (RDC-Ignite) and Research Office of Grenfell Campus, Memorial University of Newfoundland for their financial supports.

I am also grateful to my friends in Corner Brook particularly Corner Brook Baptist Church members, Ifeoma Emana Edet, Emmanuel Adeyemo, Emmanuel Ogunkunle. Kamaleswaran Sadatcharam, Akin Akinsanya, Okusipe Obafemi, Dorcas Adesiyan, Edidiong Emmanuel Udonyah and Emiko Victoria.

I specially thank all my family members, my parents Prince and Mrs. Badewa, my siblings Adedeji, Adedayo and Gbeminiyi Badewa for their support and encouragement. I also want to thank my special friend Busola Kolade for her support and understanding.

Emmanuel Badewa

TABLE OF CONTENTS

LIST OF TABLES

LIST OF FIGURES

LIST OF ABBREVIATIONS AND SYMBOLS

Ae horizon - Light coloured eluviated horizon

AWC - Available water content

BC – Biochar

CV - Coefficient of variation

DM - Dairy manure

DOE - Depth of exploration

EC - Electrical conductivity

ECa - Soil apparent electrical conductivity

ECa-L - CMD Mini-explorer vertical coplanar (VCP) configuration

ECa-H - CMD Mini-explorer horizontal coplanar (HCP) configuration

ECa-38kHz – GEM-2 horizontal coplanar (HCP) configuration

EC_t - ECa data collected

ECw – Soil salinity

EC_{25} - Temperature corrected ECa

EMI - Electromagnetic induction

f - Frequency

GPR - Ground penetrating radar

GPS – Global positioning system

Ha – Hectares

HCP - Horizontal coplanar

H_p - Primary magnetic field at the receiver coil

H_s - Secondary magnetic field at the receiver coil

LRM(s) – Linear regression model

MLR - Multiple linear regression

MRD - Mean relative differences

n – number of sample

N - Number of surveys

ODM - oven-drying method

θ_g - Gravimetric soil moisture content

θ_v - Volumetric soil moisture content

PA - Precision agriculture

PBRS - Pynn's Brook Research Station

PD(s) - Pseudo-depth(s)

Q - Quadrature (90° out of phase)

R^2 - Coefficient of determination

RD - Relative differences

RMSE - Root mean square error

RMSEP - Root mean square error of prediction

Rx – Receiver coil

SDRD - standard deviation of the relative differences

SMC – Soil moisture content

SOC - Soil organic carbon

Sp - Saturated percentage

SSM - Site specific management

Std Dev/SD – Standard deviation

t - Measured soil temperature (°C)

TDR - Time domain reflectometry

Tx – Transmitter coil

TRIME - Time domain reflectometry with intelligent micro elements)

VCP - Vertical coplanar

z - Depth (cm) from the soil surface

CHAPTER 1

1.0 INTRODUCTION AND OVERVIEW:

1.1 Introduction

Mapping the spatial variability in apparent electrical conductivity (ECa) is key to understand the variability of soil properties. The links between human needs, soil based ecosystem services, functions and soil natural capital presented by Brevik et al. (2016) established that soil properties can be used to represent the soil natural capital (Dominati et al., 2010). Understanding the variability of these soil properties is key to effective soil management so as to improve soil function (USDA-NRCS, 2015). In addition, precision agriculture (PA) encompasses the use of spatial and temporal information to determine where, how and when an input such as fertilizers is needed (Corwin and Lesch, 2005a). Furthermore, large spatial data are essential in achieving the adoption of conservation agriculture (FAO Soils Portal, 2016). Hence, a better understanding of the spatial and temporal variability of soil properties is one of the expectations of future soil mapping (Ibáñez et al., 2005; 2015).

ECa measurements can effectively delineate the variability in soil properties at field scale. The potential techniques for the characterization of soil spatio–temporal variability includes: ground penetrating radar (GPR), aerial photography, multi- and hyper-spectral imagery, time domain reflectometry (TDR), and soil's apparent electrical conductivity (ECa). Of these approaches, ECa is recognized as one of the most efficient methods used in agriculture for mapping the spatial variability of soil properties at field and landscape scales (Corwin and Lesch, 2005b; Corwin et al., 2006; Corwin, 2008; Lück et al., 2009; Doolittle and Brevik, 2014). This is because ECa increases with high clay content, water, temperature and soluble salt (Rhoades et al., 1976; McNeill, 1980; Kachanoski et al., 1988; Brevik and Fenton, 2002).

Due to the non-invasive nature, various electromagnetic induction (EMI) sensors have been adopted for the measurement of ECa. EMI can measure changes in the ECa of the subsurface without direct contact with the sampled volume (Daniels et al., 2003; Allred et al., 2008; Doolittle and Brevik, 2014). There are numerous commercially available sensors. EMI sensors commonly used in agriculture and soil investigations include the DUALEM-1 and DUALEM-2 meters (Dualem, Inc, Milton, Ontario); the EM31, EM38, EM38-DD, and EM38-MK2 meters (Geonics Limited, Mississauga, Ontario), and the profiler EMP-400 (Geophysical Survey Systems, Inc., Salem, New Hampshire). Notably, the introduction of multi-coil and multi-frequency EMI sensors is well suited for agricultural purposes especially for soil studies (Doolittle and Brevik, 2014).

Currently, research efforts are targeted at utilizing EMI-ECa measurements to map soil properties especially the soil moisture content (SMC) and develop varying site-specific management (Corwin, 2008; Toushmalani, 2010; Doolittle and Brevik, 2014). Furthermore, the future expectation is that mapping of the variability of the soil properties will be carried out using multi-coil and multi-frequency EMI sensors and various combinations of these instruments (Triantafilis and Monteiro Santos, 2013; Doolittle and

Brevik, 2014). This study examines the spatial variability of ECa as an effective means to map soil properties especially SMC using CMD Mini-explorer (GF Instruments, 2011) and GEM-2 (GEM-2, Geophex, Ltd), a multi-coil and a multi-frequency EMI sensor, respectively. The result will help guide soil management decisions and provide soil physical information for Western Newfoundland.

Podzols cover 55.2% of the landmass of Newfoundland (Sanborn et al., 2011). They are soils with an ash-grey subsurface horizon, with accumulation of underlain black organic matter and/or reddish Fe oxides horizon (IUSS Working Group WRB, 2014). Podzols are undesirable for arable farming due to low nutrient status, low level of available moisture, low pH, aluminium toxicity and phosphorus deficiency. However, liming and fertilization have been effectively used to reclaim podzols for arable farming (FAO Soils Portal, 2017).

1.1.1 Purpose of the thesis

The thesis focuses on the application of ECa measurements from two EMI sensors for mapping the spatial variability of soil physical properties such as soil texture and bulk density and hydraulic properties such as SMC and available water content (AWC) at Pynn's Brook Research Station (PBRS), Pasadena, Newfoundland.

1.1.2 Thesis aim and objectives

The principal aim of this thesis was to explore the potential of CMD Mini-explorer and GEM-2 for mapping ECa on a managed agricultural podzols study site. This involved comparing CMD Mini-explorer and GEM-2 to soil physical properties such as texture, bulk density and hydraulic properties such as SMC and AWC.

In other to accomplish this study, the following specific objectives were formulated:

i. Comparison of SMC from the oven drying method and precise moisture measurement TDR.

ii. Comparison of CMD Mini-explorer and GEM-2 ECa measurements.

iii. Calibration of CMD Mini-explorer and GEM-2 with in-situ measurements of SMC. Validation of SMC prediction model from CMD Mini-explorer and GEM-2.

iv. Characterization of the spatial variability of SMC predicted from different CMD Mini-explorer and GEM-2 surveys.

v. Establishment of the relationship between ECa and ECa predicted soil physical and hydraulic properties such as SMC, soil texture, bulk density, and available water content.

vi. Temporal stability analysis of ECa in relation to soil physical and hydraulic properties such as texture, bulk density, SMC and AWC.

1.1.3 Thesis organization

This thesis is divided into four chapters, with the relevant literature being reviewed at the start of each experimental chapter.

Chapter One: provides a brief overview on soil mapping, EMI, ECa and a description of the primary aim and objectives of the thesis. Describes podzols, the theory of EMI, CMD Mini-explorer, GEM-2, HD2-TDR.

Chapter Two: describes a comparative study between CMD Mini-explorer and GEM-2 ECa measurements. The chapter also evaluates the accuracy of precise SMC measurement using TDR with the the oven drying method in-situ measurements for field use. Thus, this point measurements from the TDR would be used to evaluate the performance of models developed from CMD Mini-explorer and GEM-2. Calibration and prediction of CMD Mini-explorer and GEM-2 ECa measurements are also determined.

Chapter Three: establishes the relationship between ECa and ECa predicted soil properties on a managed agricultural podzols study site. The chapter also evaluates the temporal stability of ECa in relation to soil physical properties using CMD Mini-explorer and GEM-2 ECa measurements.

Chapter Four: general discussion, conclusions and recommendations for the study.

1.1.4 Definitions

Apparent Electrical Conductivity (ECa): The measured electrical conductivity that represents the true value for the entire bulk soil volume when soil electrical conductivity is assumed homogeneous. It is the measurement of the electrical conductivity for a bulk volume of soil using resistivity and electromagnetic induction geophysical methods.

Electromagnetic Induction (EMI) Methods: Geophysical investigation methods used to measure subsurface electrical conductivity or electrical resistivity. The operation is based on the applied principle of EMI theory.

Site Specific Management (SSM): The application of variable conditions information within a farm field for effective crops, soil and pest management.

1.1.5 Delimitations, limitations, and assumptions

Delimitations – The research was carried out on an experimental field for in depth study of the dynamic nature of soil especially the soil physical properties in a managed podzol.

Limitations – The EMI instruments measure the ECa assuming the soil EC is homogenous, but EC is more likely to be heterogeneous due to the dynamic nature of the soil.

Assumptions –

I. ECa is a function of several soil properties. Therefore, ECa measurements can be used to provide indirect measures of these properties if the contribution of the other affecting soil properties to the ECa measurement are known or can be estimated.

II. For accurate interpretation of the large amounts of ECa data collected from EMI sensors, it is necessary to understand and consider issues related to how the data were collected and its intended application. This is particularly true in non-saline soils, where the variation in ECa across a field will generally be much smaller than in saline soils, and therefore more affected by operational differences.

1.2 Podzols

Podzols are soils with an ash-grey subsurface horizon, bleached by organic acids, on top of a dark accumulation horizon. They occur more in the humid areas in the Boreal and Temperate zone (Sanborn et al., 2011). According to Soil Classification Working Group (1998), Podzols have B horizons in which the dominant accumulation product is amorphous material composed mainly of humified organic matter combined in varying degrees with Al and Fe. Typically, Podzolic soils occur in coarse- to medium-textured, acid parent materials, under forest or heath vegetation in cool to very cold humid to per humid climates. They are easily recognised in the field through the dark colored organic surface horizons. Soils of the Podzolic order are defined based on a combination of morphological and chemical criteria of the B horizons.

1.3 Electromagnetic Induction (EMI)

EMI principle is governed by the fundamental laws of Ampere's and Faraday for all EMI theory. A transmitter coil located at one end of the EMI instrument induces circular eddy-current loops in the soil with the magnitude of these loops directly proportional to the EC near that loop. Each current loop generates a secondary electromagnetic field that is proportional to the value of the current flowing within the loop. A fraction of the secondary induced electromagnetic field from each loop is intercepted by the receiver coil of the instrument and the sum of these signals is amplified and formed into an output voltage which is related to a depth-weighted soil EC (Corwin, 2008). Due to the influence of soil properties (*e.g.,* clay content, moisture content, salinity), spacing of the coils and their orientation, frequency, and distance from the soil surface, the amplitude and phase of the secondary field will differ from those of the primary field (Hendrickx and Kachanoski, 2002).

The accuracy and precision of the EMI sensors is important for effective soil EC mapping. The accuracy of EMI-ECa sensor instrument and data acquisition system accuracies is one of the issues believed to be important when using EMI sensor for soil ECa data collection (Fig. 1.1). Sudduth et al. (2001) reported that it is important to understand and consider issues related to how the large amounts of ECa data were collected and its intended application for accurate interpretation. He found out that variations in sensor operating speed and height did not affect the sensitivity of ECa. The author further presented the relative effects of various operational and ambient parameters on ECa readings that can serve as a guide for successfully planning and interpreting ECa surveys in PA. The drifting of the sensor which occur due to the temperature effect of the sensor (Robinson et al., 2004), contribute significantly to the within field ECa variation (Sudduth et al., 2001). The drift can be adjusted through a regular drift runs, the distance from the sensor to the GPS antenna and the data acquisition system time lags results in positional offset (Corwin and Lesch, 2005c).

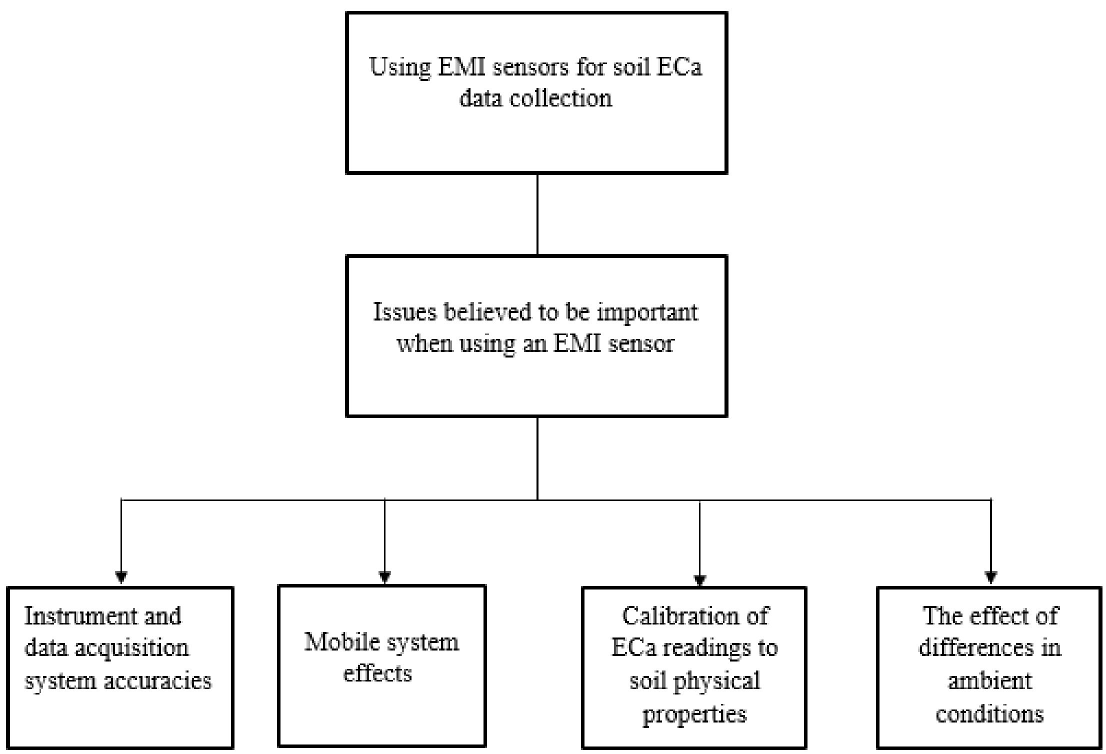

Figure 1.1 Issues believed to be important in soil ECa data collection using EMI sensor (Sudduth et al., 2001).

Several factors need to be considered for the selection, operation and interpretation of suitable EMI sensor for field application. These includes the mode of sensor transport, station spacing, depth of penetration, interference effects, instrument height, speed and orientation (Corwin, 2008).

EMI measures the ECa which is determined by the ratio of the magnitudes of the out-of-phase secondary to primary magnetic fields as shown in Equation 1.1. This implies that ECa is a weighted average value over a certain depth range that depends on the coil separation and coil orientation (McNeill, 1980). According to McNeill (1980), EMI sensor works based on low induction numbers *i.e.* the value generated for the ratio of the distance between transmitter and receiver coils to the shallow depth of exploration.

$$\sigma_a = \frac{4}{i\omega\mu_0\sigma s^2}\left(\frac{H_s}{H_p}\right)_Q \tag{1.1}$$

Where $\left(\frac{H_s}{H_p}\right)_Q$ is the ratio of the out-of-phase secondary to primary magnetic fields.

Q = Quadrature (90^o out of phase)

H_s = Secondary magnetic field at the receiver coil

H_p = Primary magnetic field at the receiver coil

σ_a = Apparent electrical conductivity

$\omega = 2\pi f$ – angular frequency

f = Frequency

μ_o = Permeability of free space

S= Inter-coil spacing (m) *i.e.* 32 cm, 71 cm and 118 cm

I = √-1

To understand the integrated response of the surface measurement of EMI, it is assumed that the current loops generated below the ground are not influenced by others nearby (McNeill, 1980). This resulted in the following Equations 1.2 and 1.3 for horizontal and vertical dipole configurations *i.e.* vertical coplanar (VCP) and horizontal coplanar (HCP) coil configuration, respectively (Kaufman, 1983).

$$\varphi^H(z) = 2 - \frac{4z}{(4z^2 + 1)^{1/2}} \tag{1.2}$$

$$\varphi^v(z) = \frac{4z}{(4z^2 + 1)^{3/2}} \tag{1.3}$$

Where $\varphi^H(z)$ and $\varphi^v(z)$ are the sensitivity function of the EMI sensor (VCP and HCP, respectively) with depth and z is the depth (cm) from the soil surface.

1.3.1 The CMD Mini-explorer

CMD Mini-explorer is a multi-coil EM sensor, which consists of a probe in conjunction with a control unit, connected via Bluetooth. The CMD Mini-explorer operates at 30 kHz and has one transmitter and three coplanar receiver coils with different separations (32 cm, 71 cm, and 118 cm) that can be oriented in low or high depth range *i.e.* VCP or HCP coil configuration, respectively (Fig. 1.2). The CMD Mini-explorer can be used to simultaneously sense different integral depths (Fig. 1.3) of Pseudo-depths (PD) 25, 50 and 90 cm from VCP; 50, 100, 180 cm from HCP (Altdorff et al., 2016).

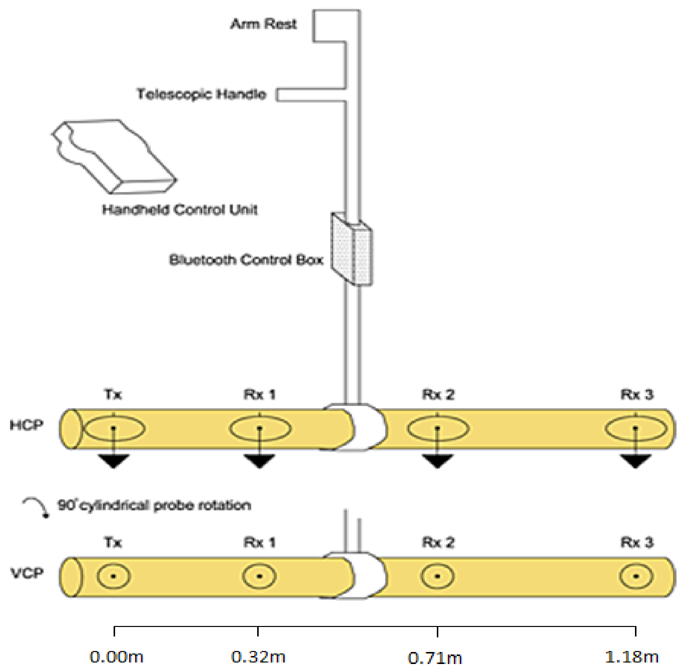

Figure 1.2 The schematic diagram of CMD Mini-explorer at low (VCP) and high (HCP) depth range showing the positions of the transmitter coil (Tx), receiver coils (Rx), coil geometry, spacing and orientation (Bonsall et al., 2013).

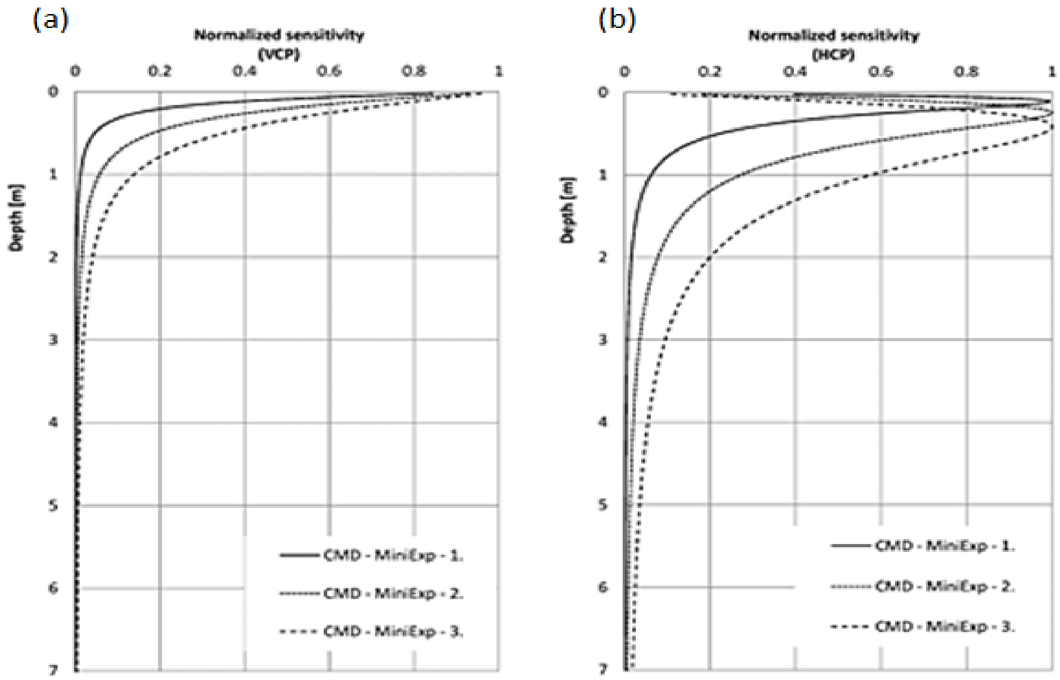

Figure 1.3 The sensitivity function curves based on simplified Maxwell equations for the CMD Mini-explorer, as derived from GF Instrument's information (a) low (VCP) and (b) high (HCP) depth range (GF Instruments, 2011).

1.3.2 The GEM-2

GEM-2 (Fig 1.4) is a broadband multi-frequency EM sensor with one transmitter coil and a receiver coil separated by 166 cm, which consists of a ski that can operate in a frequency band between 30 Hz to about 93 kHz. The sensor frequency is inversely proportional to the depth of measurement *i.e.* high frequency travel short distance and vice versa (Won, 1980). The GEM-2 sensor operates in both HCP and VCP coil configurations. The sensor has a factory set of three and five highs, medium and low frequency file that can be adjusted to the desired frequency (Geophex Ltd., 2004).

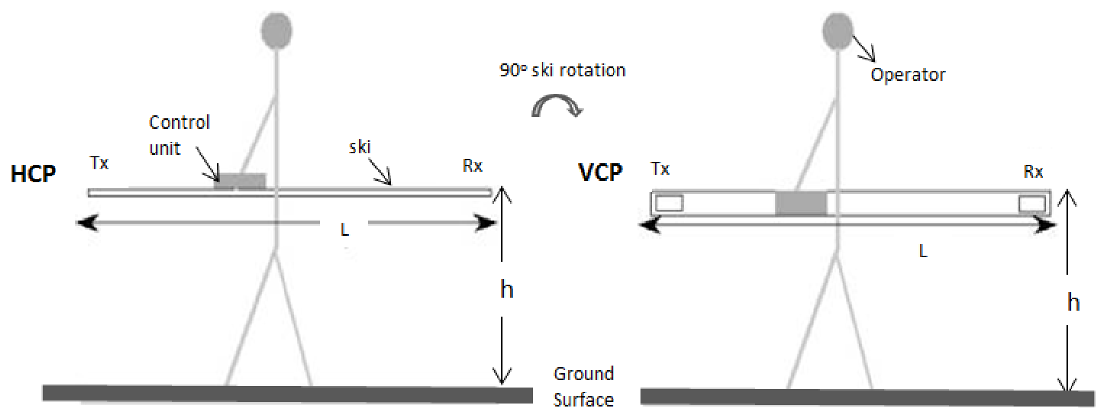

Figure 1.4 (a) GEM-2 in HCP coils configurations (b) GEM-2 in VCP coils configurations (Won, 1980).

1.4 Soil Moisture Content Measurements

HD2 meter (IMKO Micromodultechnik, Ettlingen, Germany); an integrated TDR known as the TRIME (Time domain Reflectometry with Intelligent MicroElements), for in situ monitoring of volumetric moisture in soils are often used instead of the conventional TDR. TRIME is cost and labour effective with precise excellent spatial resolution (IMKO, 2016). For large-scale SMC measurement, TRIME-TDR sensor has inside network capability that are not limited by cable length and wet surroundings induce considerable measurement deviation compared to conventional TDR (IMKO, 2016).

Figure 1.5 The wave transmission around the metal rod (IMKO, 2016).

HD2 meter is based on the TDR-technique (Time-Domain-Reflectometry), and was developed to measure the dielectric constant (ε) of a material (Topp et al., 1980; Ferré and Topp, 2002; Jones et al., 2002). The measurement of ε can be used to determine SMC through calibration (Dalton, 1992). Furthermore, the relationship between SMC and ε is approximately linear and is influenced by soil type, bulk density, clay content and organic matter (Jacobsen and Schjønning, 1993).

The metal rods, strips or plates are used as wave guides for the transmission of the TDR-signal as shown in Fig 1.5. The HD2-TDR meter generates a high-frequency-pulse (up to 1 GHz) which propagates along the wave guides generating an electromagnetic field around the HD2-TDR probe (Fig 1.5). At the end of the wave-guides, the pulse is reflected back to its source. The resulting transit time and dielectric constant are dependent on the moisture content of the material (Schaap et al., 1996; Robinson et al., 2003; Topp et al., 1980). The SMC is calculated and display on the HD2-TDR meter via the RS232/V24 connected to the device.

1.5 Conclusion

Aa a result of the above reviews, I concluded to assess the potential of EMI surveys for mapping SMC and selected soil properties at field scale using;

(i) small field study and large field study for detailed investigation which was carried out on a silage corn variety plot (Fig. 1.6) with different nutrient management.

(ii) Two EMI sensors; multi-coil and multi-frequency; CMD Mini-explorer and GEM-2, respectively and HD2-TDR adopted for the study are shown in Fig 1.6.

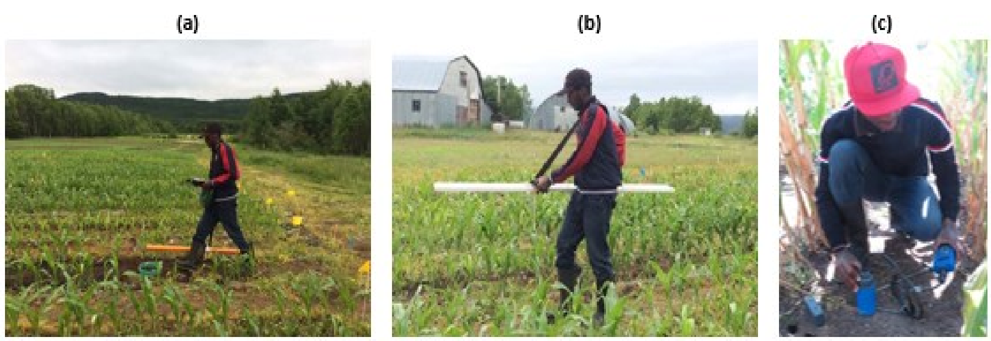

Figure 1.6 Field operation of (a) CMD Mini-explorer (b) GEM-2 (c) HD2-TDR at PBRS, Pasadena, Newfoundland.

1.6 References

Allred, B. J., Ehsani, M. R., & Daniels, J. J. (2008). General considerations for geophysical methods applied to agriculture. *Handbook of Agricultural Geophysics. CRC Press, Taylor and Francis Group, Boca Raton, Florida*, 3-16.

Altdorff, D., Bechtold, M., van der Kruk, J., Vereecken, H., & Huisman, J. A. (2016). Mapping peat layer properties with multi-coil offset electromagnetic induction and laser scanning elevation data. *Geoderma*, 261, 178–189.

Bonsall, J., Fry, R., Gaffney, C., Armit, I., Beck, A., & Gaffney, V. (2013). Assessment of the CMD Mini-Explorer, a New Low-frequency Multi-coil Electromagnetic Device, for Archaeological Investigations. *Archaeological Prospection*, 20(3), 219–231.

Brevik, E. C., Calzolari, C., Miller, B. A., Pereira, P., Kabala, C., Baumgarten, A., & Jordán, A. (2016). Soil mapping, classification, and pedologic modeling: History and future directions. *Geoderma,* 264, 256-274.

Brevik, E. C., & Fenton, T. E. (2002). The relative influence of soil water, clay, temperature, and carbonate minerals on soil electrical conductivity readings with an EM-38 along a Mollisol catena in central Iowa. *Soil Survey Horizon*, 43, 9–13.

Corwin, D. L., & Lesch, S. M. (2005a). Characterizing soil spatial variability with apparent soil electrical conductivity Part II. Case study. *Computers and Electronics in Agriculture, 46*, 135–152.

Corwin, D. L., & Lesch, S. M. (2005b). Apparent soil electrical conductivity measurements in agriculture. *Computers and electronics in agriculture, 46*(1), 11-43.

Corwin, D. L., & Lesch, S. M. (2005c). Characterizing soil spatial variability with apparent soil electrical conductivity: I. Survey protocols. *Computers and Electronics in Agriculture, 46*(1), 103-133.

Corwin, D. L., Lesch, S. M., Oster, J. D., & Kaffka, S. R. (2006). Monitoring management-induced spatio–temporal changes in soil quality through soil sampling directed by apparent electrical conductivity. *Geoderma, 131*(3), 369-387.

Corwin, D. L. (2008). Past, present, and future trends in soil electrical conductivity measurements using geophysical methods. *In: Allred, B.J., Daniels, J.J., Ehsani, M.R. (Eds.), Handbook of Agricultural Geophysics. CRC Press, Taylor and Francis Group, Boca Raton, Florida,* pp. 17–44.

Dalton, F. N. (1992). Development of time domain reflectometry for measuring soil water content and bulk soil electrical conductivity. *In: Topp, G.C., Reynolds,W.D., Green, R.E. (Eds.),* *Advances in Measurement of Soil Physical Properties: Bringing Theory into Practice. SSSA Spec. Publ. 30. Soil Science Society of America, Madison, WI, USA*, 143–167.

Daniels, J. J., Allred, B., Collins, M., & Doolittle, J. (2003). Geophysics in soil science. Encyclopedia of Soil Science, *Second edition. Marcel Dekker, New York*, 1-5.

Dominati, E., Patterson, M., & Mackay, A. (2010). A framework for classifying and quantifying the natural capital and ecosystem services of soils. *Ecological Economics, 69*(9), 1858-1868.

Doolittle, J. A., & Brevik, E. C. (2014). The use of electromagnetic induction techniques in soils studies*. Geoderma, 223*, 33-45.

FAO Soils Portal (2016). Soil survey. *Retrieved from http://www.fao.org/soils-portal/soil-survey/en/*

FAO Soils Portal (2017). Acid soils. *Retrieved from http://www.fao.org/soils-portal/soil-management/management-of-some-problem-soils/acid-soils/en/*

Ferré, P. A., & Topp, G. C. (2002). Time domain reflectometry. *In: Dane, J.H., Topp, G.C. (Eds.), Methods of Soil Analysis. Part 4. Physical Methods. American Society of Agronomy, Madison, WI,* 434–445.

Geophex Ltd. (2004). GEM-2 User’s Manual, Version 3.8. Geophex Ltd., Raleigh, USA. *Available at: http://www.geophex.com/Downloads/GEM-2%20Operator's%20Manual.pdf.*

GF Instruments (2011). CMD Electromagnetic conductivity meter user manual V. 1.5. Geophysical Equipment and Services, Czech Republic. *Available at: http://www.gfinstruments.cz/index.php?menu=gi&smenu=iem&cont=cmd_&ear=ov.*

Hendrickx, J. M. H., & Kachanoski, R. G. (2002). Nonintrusive electromagnetic induction. *Methods of soil analysis. Part, 4,* 1297-1306.

Ibáñez, J. J., Sánchez Díaz, J., De Alba, S., López Árias, M., & Boixadera, J. (2005). Collection of Soil Information in Spain: a review in 2003. *Soil Resources of Europe, second edition. Jones, RJA, Houšková, B., Bullock, P. et Montanarella, L.(eds). European Soil Bureau Research Report,* (9), 345-356.

Ibáñez, J. J., Pérez-Gómez, R., Oyonarte, C., & Brevik, E. C. (2015). Are there arid land soilscapes in Southwestern Europe? *Land Degradation & Development, 26*(8), 853-862.

IMKO (2016). About TRIME-TDR. *Retrieved from https://imko.de/en/about-trime-tdr*

IUSS Working Group WRB (2014). World reference base for soil resources 2014. *International soil classification system for naming soils and creating legends for soil maps. FAO, Rome. World Soil Resources Reports No*. 106.

Jacobsen, O. H., & Schjønning, P. (1993). A laboratory calibration of time domain reflectometry for soil water measurement including effects of bulk density and texture. *Journal of Hydrology, 151*(2-4), 147-157.

Jones, S. B., Wraith, J. M., & Or, D. (2002). Time domain reflectometry measurement principles and applications. *Hydrological processes, 16*(1), 141-153.

Kachanoski, R. G., Wesenbeeck, I. V., & Gregorich, E. G. (1988). Estimating spatial variations of soil water content using non-contacting electromagnetic inductive methods. *Canadian Journal of Soil Science, 68*(4), 715-722.

Kaufman, A. (1983). Geophysical field theory and method: Part C, *Electromagnetic Fields II. Elsevier, New York, USA.*

Kirby, G. E. (1988). Soils of the Pasadena-Deer Lake area, Newfoundland. St. John's. *Retrieved from http://sis.agr.gc.ca/cansis/publications/surveys/nf/nf17/nf17_report.pdf*

Lück, E., Gebbers, R., Ruehlmann, J., & Spangenberg, U. (2009). Electrical conductivity mapping for precision farming. *Near Surface Geophysics, 7*(1), 15-25.

McNeill, J. D. (1980). Electromagnetic terrain conductivity measurement at low induction numbers. *(Geonics Ltd., Mississauga, Ontario, Canada, Technical Note TN-5).*

Rhoades, J. D., Raats, P. A. C., & Prather, R. J. (1976). Effects of liquid-phase electrical conductivity, water content, and surface conductivity on bulk soil electrical conductivity. *Soil Science Society of America Journal, 40*(5), 651-655.

Robinson, D. A., Jones, S. B., Wraith, J. M., Or, D., & Friedman, S. P. (2003). A review of advances in dielectric and electrical conductivity measurement in soils using time domain reflectometry. *Vadose Zone Journal, 2*(4), 444-475.

Robinson, D. A., Lebron, I., Lesch, S. M., & Shouse, P. (2004). Minimizing drift in electrical conductivity measurements in high temperature environments using the EM-38. *Soil Science Society of America Journal, 68*(2), 339-345.

Sanborn, P., Lamontagne, L., & Hendershot, W. (2011). Podzolic soils of Canada: Genesis, distribution, and classification. *Canadian Journal of Soil Science, 91*(5), 843-880.

Schaap, M. G., De Lange, L., & Heimovaara, T. J. (1997). TDR calibration of organic forest floor media. *Soil Technology, 11*(2), 205-217.

Sudduth, K. A., Drummond, S. T., & Kitchen, N. R. (2001). Accuracy issues in electromagnetic induction sensing of soil electrical conductivity for precision agriculture. *Computers and electronics in agriculture, 31*(3), 239-264.

Terraplus Inc. (2013). Gem 2 Multi-Frequency EM Sensor. *http://terraplus.ca/products/electromagnetics/gem2.aspx*

Topp, G. C., Davis, J. L., & Annan, A. P. (1980). Electromagnetic determination of soil water content: Measurements in coaxial transmission lines. *Water resources research, 16*(3), 574-582.

Toushmalani, R. (2010). Application of geophysical methods in agriculture. *Australian Journal of Basic and Applied Sciences, 4*(12), 6433–6439.

Triantafilis, J., & Santos, F. M. (2013). Electromagnetic conductivity imaging (EMCI) of soil using a DUALEM-421 and inversion modelling software (EM4Soil). *Geoderma, 211*, 28-38.

USDA-NRCS. (2015). Soil Health Literature Summary – Effects of Conservation practices on soil properties in Areas of Croplands. Retrieved from https://www.nrcs.usda.gov/wps/portal/nrcs/detailfull/soils/health/mgnt/?cid=stelprdb1257753

Won, I. J. (1980). A wide-band electromagnetic exploration method—Some theoretical and experimental results. *Geophysics, 45(*5), 928-940.

1.7 Co-authorship Statement

A manuscript based on the Chapter 2, entitled "*Soil Moisture Mapping Using Multi-frequency and Multi-coil Electromagnetic Induction Sensors on Managed Podzols*" has been submitted to Precision Agriculture (Badewa, E., Unc, A., Cheema, M., Kavanagh, V. and Galagedara, L., 2017). Emmanuel Badewa, the thesis author was the primary author and Dr. Galagedara (supervisor), was the corresponding and the fifth author. Dr. Unc (co-supervisor) and Dr. Cheema (committee member) were second and third authors, respectively. Dr. Kavanagh, a collaborative researcher of this project from the Department of Fisheries and Land Resources of the Government of NL was the fourth author. All authors were part of the same research project on "*Hydrogeophysical Characterization of Agricultural Fields in Western Newfoundland using Integrated GPR-EMI*", which was led by Dr. Galagedara. For the work in Chapter 2, the design of the research was developed by Dr. Galagedara with input from all members of the group. Mr. Badewa was responsible for the data collection, analysis, and interpretation and writing of the manuscript. Dr. Unc provided specific guidance on statistical analysis, data interpretation and manuscript writing. Drs. Cheema and Kavanagh provided inputs for the field experiment, data interpretation and manuscript editing.

For the remainder of the thesis including introduction, literature review, data collection, analysis and interpretation and writing, was performed by Mr. Badewa. The Chapter 3 is on "*Soil Apparent Electrical Conductivity (ECa): A Proxy for Determination of Soil Properties in Managed Podzols*". has been submitted to Pedosphere (Badewa, E., Unc, A., Cheema, M. and Galagedara, L., 2017). Emmanuel Badewa, the thesis author was the primary author and Dr. Galagedara (supervisor), was the corresponding and the fourht author. Dr. Unc (co-supervisor) and Dr. Cheema (committee member) were second and third authors, respectively. All authors were part of the same research project on "*Hydrogeophysical Characterization of Agricultural Fields in Western Newfoundland using Integrated GPR-EMI*", which was led by Dr. Galagedara. For the work in Chapter 3, the design of the research was developed by Dr. Galagedara with input from all members of the group. Mr. Badewa was responsible for the data collection, analysis, and interpretation and writing of the manuscript. Dr. Unc provided specific guidance on statistical analysis, data interpretation and manuscript writing. Dr. Cheema provided inputs for the field experiment, data interpretation and manuscript editing. Dr. Galagedara as the project lead and the main supervisor, provided research plans and guidance for the entire process.

CHAPTER 2

2.0 SOIL MOISTURE MAPPING USING MULTI-FREQUENCY AND MULTI-COIL ELECTROMAGNETIC INDUCTION SENSORS ON MANAGED PODZOLS[1].

Abstract

Precision agriculture (PA) involves the management of agricultural fields including spatial information of soil properties derived from soil apparent electrical conductivity (ECa) measurements. While this approach is gaining ground in agricultural management, farmed podzols are under-represented in the relevant literature. We: (i) established the relationship between ECa and measured soil moisture content (SMC) by the gravimetric method and time domain reflectometry (TDR); and (ii) compared SMC with ECa measurements obtained with two different electromagnetic induction (EMI) sensors, multi-Coil and multi-Frequency. Measurements were taken in different sampling plots at Pynn's Brook Research Station (PBRS), Pasadena, Newfoundland. The mean ECa measurements were calculated for the same sampling location in each plot. Due to the difference in the depth of investigation of the two EMI sensors, the linear regression models generated for SMC using the CMD Mini-explorer were statistically significant with the highest $R^2 = 0.79$ and lowest RMSE = 0.015 $m^3\ m^{-3}$ and not significant for GEM-2 with the lowest $R^2 = 0.17$ and RMSE = 0.045 $m^3\ m^{-3}$. The validation of the SMC model results for the two EMI sensors produced the highest $R^2 = 0.54$ with lowest RMSE

foot note: [1]"Badewa, E., Unc, A., Cheema, M., Kavanagh, V. and Galagedara, L. (2017). Soil Moisture Mapping Using Multi-frequency and Multi-coil Electromagnetic Induction Sensors on Managed Podzols (Submitted to Precision Agriculture)".

prediction = 0.031 m^3 m^{-3} given by by CMD Mini-explorer. We concluded that CMD Mini-explorer based measurements better predicted shallow SMC, while deeper SMC was better predicted by GEM-2 measurements. In addition, the ECa measurements obtained through either multi-Coil or multi-Frequency sensors have the potential to be successfully employed for SMC mapping at the field scale.

Keywords

Apparent electrical conductivity, Precision agriculture, Soil moisture content, Electromagnetic induction

2.1 Introduction

Development of site-specific management (SSM) over large fields is the goal of precision agriculture (PA). PA encompasses the use of spatial and temporal information to support decisions on agronomic practices that best match soil and crop requirements as they vary in the field (Corwin and Lesch, 2005a; Peralta and Costa, 2013). Lesch et al. (2005) have shown that different types of spatial information derived from bulk apparent electrical conductivity (ECa) obtained by electromagnetic induction (EMI) surveys can offer significant support to the development of accurate management decisions for agricultural fields. PA provides a way to automate SSM using information technology, thereby making SSM practical in commercial agriculture. It includes all those agricultural production practices that use information technology either to tailor input to achieve desired outcomes, or to monitor those outcomes (*e.g.* variable rate application, yield monitors, remote sensing) (Bongiovanni and Lowenberg-DeBoer, 2004). Also, PA has proven to be the most viable approach for achieving sustainable agriculture (Khosla et al., 2008). ECa technology has been proposed as an effective, rapid response methodology in support of PA (Kyaw et al., 2008; Fortes et al., 2015).

Literature shows that ECa has the potential to become a widely-adopted means for characterizing the spatial variability of soil properties at field and landscape scales (Corwin and Lesch, 2005b; Doolittle and Brevik, 2014). Spatial variability of soil properties can also be characterized by other means such as ground penetrating radar (GPR) (Galagedara et al., 2005; Wijewardana and Galagedara, 2010), time domain reflectometry (TDR) (Topp et al., 1980; Ferré, et al., 1998), cosmic-ray neutrons (Desilets et al., 2010; Franz et al., 2013), aerial photography (Kyaw et al., 2008; Mondal and Tewari, 2007), or multi- and hyper-spectral imagery (Jay et al., 2010; Zhang et al., 2013). Nevertheless, ECa, once calibrated with spatial imagery to plant responses, can be cost effective and robust (Corwin and Lesch, 2005c).

High clay content, soil moisture content (SMC), temperature and soluble salts affect ECa (Rhoades et al., 1976; McNeill, 1980; Kachanoski et al., 1988; Brevik and Fenton, 2002). SMC affects ECa through the three pathways of conductance in the soil (Rhoades et al., 1989; Corwin and Lesch, 2005b), namely soil salinity (Lesch et al., 1995; Goff et al., 2014), saturated percentage (Lesch and Corwin, 2003; Corwin and Lesch, 2005b) and soil bulk density (Walter et al., 2015; Altdorff et al., 2016). When salinity, texture and mineralogy are constant ECa is a direct function of SMC (Corwin and Lesch, 2003; Friedman, 2005); under such conditions several authors have established that there is a linear relationship between SMC and ECa (Brevik et al., 2006; Serrano et al., 2013; Huang et al., 2016). Furthermore, SMC is widely recognized as a driving factor for agricultural productivity as it governs germination and growth (Bittelli et al., 2011). Given the time, labour, and cost of traditional soil sampling (Huang et al., 2014), the development of an accurate proxy alternative for measuring the spatio-temporal variability of SMC, such as EMI, is essential for efficient soil and crop management at large scales (Vereecken et al., 2014).

CMD Mini-explorer is a multi-coil EMI sensor, which operates at 30 kHz and has one transmitter and three coplanar receiver coils with different distances (32 cm, 71 cm, and 118 cm) (GF Instruments, 2011). GEM-2 is a broadband multi-frequency EMI sensor with one transmitter coil and a receiver coil separated by 166 cm, which can be operated in a frequency band between 30 Hz to about 93 kHz (Geophex Ltd., 2004). Both sensors operate in vertical coplanar (VCP) or horizontal coplanar (HCP) coil configurations and support GPS communication with a control unit connected via bluetooth. The difference between the two sensors is that the depth of exploration (DOE) of CMD Mini-explorer is known (GF Instruments, 2011) while that of GEM-2 is yet to be determined even though arguably it can measure deeper than CMD Mini-explorer (Won et al., 1980).

Podzols are formed from acidic parent material with coarse to medium textured soils, and are distinctively characterized by illuvial B horizons where humified organic matter combined in varying degrees with Al and Fe accumulate, often overlain by a light coloured eluviated (Ae) horizon (Soil Classification Working Group 1998). Globally, podzolic soils are widely spread in the temperate and boreal regions on the Northern Hemisphere and they occupy approximately 4% (485 million ha) of the earth's total land surface (Driessen et al. 2001). The adaptation of podzolic soils for agriculture is on the increase because of the demand on the agricultural land base, application of intensive mechanization, fertilization, and water management practices (Sanborn et al. 2011). In addition, Podzolic soils have distinctive morphology and agricultural land use conversion can significantly affect their hydrologic parameters (Wang et al. 1984; Altdorff et al. 2017a). Despite their uniqueness there is limited information available to inform the water management for effective agricultural production (Sanborn et al. 2011).

The objectives of this study was to: (i) comparatively investigate the potential of multi-coil (CMD Mini-explorer) and multi-frequency EMI (GEM-2) sensors and the various combinations of these instruments for agricultural systems on managed podzols; (ii) develop a relationship between ECa, as measured by both instruments, and SMC measured using in-situ gravimetric and HD2-TDR; and (iii) compare the performance between the ECa and SMC based projections.

2.2 Materials and Methods

2.2.1 Study site

The study was carried out at Pynn's Brook Research Station (PBRS) (49° 04' 20" N, 57° 33' 35" W), Pasadena, Newfoundland (Fig. 1), Canada. The soil, reddish brown to brown, has developed on gravelly sandy fluvial deposit of mixed lithology, with >100 cm depth to bedrock, and a 2 – 5% slope (Kirby, 1988). Soil samples (n = 7) analyzed for the study site revealed a gravelly loamy sand soil (sand = 82.0% (±3.4); silt = 11.6% (±2.4); clay = 6.4% (±1.2)), which is classified as orthic Humo-ferric podzol (Kirby, 1988). The average bulk density and porosity for the site (n = 28) were 1.31 g cm^{-3} (±0.07) and 51% (±0.03), respectively. Based on the 30-year data (1986 – 2016) of a nearby Deer Lake weather station from Environment Canada (http://climate.weather.gc.ca/), the area receives an average precipitation of 1113 mm per year with less than 410 mm falling as snow, and has an annual mean temperature of 4 °C.

Initially, a large field survey (0.45 ha) was conducted to evaluate the variability in measurements between the CMD Mini-explorer and GEM-2 versus SMC. The field is split between grass, silage corn and soybean plots. Here, a portion of the silage corn experimental field consisting of one variety was selected for a detailed, small-field study (Fig. 1). The small-field study was used to calibrate and validate the SMC against the proximally sensed ECa across an area of 45 m x 8.5 m with gridded plots. A large field study was conducted to apply the calibration at the same site on a large scale, GPS integrated.

2.2.2 SMC data recording and HD2-TDR calibration

SMC was measured using two methods; namely gravimetrically, via oven drying (OD), and by TDR. While OD measures SMC gravimetrically (θ_g), TDR measures SMC volumetrically (θ_v). For OD, soil core sections were dried at 105 °C for 48 h; θ_g was determined for 0 – 10 cm ($\theta_{g(0\text{-}10)}$), 10 – 20 cm ($\theta_{g(10\text{-}20)}$) and 0 – 20 cm ($\theta_{g(0\text{-}20)}$) depth ranges. We employed an integrated TDR, known as HD2-TDR, with probe lengths of 11 cm ($\theta_{v(0\text{-}11)}$), 16 cm ($\theta_{v(0\text{-}16)}$) and 30 cm ($\theta_{v(0\text{-}30)}$) (IMKO, 2016). The θ_v values obtained by TDR were correlated to calculate θ_v values obtained by multiplying θ_g with the measured average soil bulk density of 1.30 g cm^{-3}. Also, the mean soil temperature measured from the HD2-TDR precision soil moisture probe was used for the temperature conversion of ECa. Twenty seven geo-referenced SMC data points ($\theta_{v(0\text{-}16)}$) were collected using HD2-TDR 16 cm length probe and hand held GPS according to the stratified sampling locations.

2.2.3 EMI survey

ECa was measured using the multi-coil CMD Mini-explorer (GF instruments, Brno, Czech Republic) and the multi-frequency GEM-2 (Geophex, Ltd., Raleigh, USA). CMD Mini-explorer has 3 coil separations, which at VCP and HCP coil configurations, respectively can generate six pseudo depths (PDs) namely; 25, 50 and 90 cm from VCP; 50, 100, 180 cm from HCP (Altdorff et al., 2016). However, DOE of GEM-2 frequencies are yet to be determined even though it has the potential to measure at a deeper depths compared to CMD Mini-explorer (Won et al., 1980). Based on the preliminary data obtained on the site, we decided to employ the CMD Mini-explorer with the largest coil separation (coil 3 = 118 cm) with PDs 90 and 180 and a 38-kHz frequency (the coil separation is 166 cm). CMD Mini-explorer at VCP configuration was represented with ECa-L and at HCP configuration was represented with ECa-H while GEM-2 at a HCP configuration was represented with ECa-38kHz. The surveys with CMD Mini-explorer were carried out at a height of 15 cm above ground. The GEM-2 device was carried with the supplied shoulder strap at an average height of 100 cm above the ground.

The ECa measurements were carried out on 30 September and 6 October in fall 2016 and 31 May in spring 2017. To ensure high data quality, both sensors were allowed a warm up period of at least 30 min before measurements (Robinson et al., 2004). However, no instrumental drift was expected in the ECa due to the high temperature stability of the CMD Mini-explorer and GEM-2 (Allred et al., 2005; GF Instruments, 2011). Several studies suggested temperature conversion of raw ECa to a standard soil temperature (25 ^{o}C) (*e.g.* Corwin and Lesch, 2005a; Ma et al., 2011) using Eq. 2.1:

$$EC_{25} = EC_t \ast \times (0.4470 + 1.4034\ e^{-t/26.815}) \qquad \text{Eq. 2.1}$$

where EC_t is the ECa data collected, t is the measured soil temperature (°C) and EC_{25} is the temperature corrected ECa.

To test ECa response to SMC at a larger spatial scale, one additional survey each using the CMD Mini-explorer and GEM-2 was carried out by walking across the field using GPS to obtained geo-referenced data on 18 November, 2016.

For the analysis, the mean ECa measurements (n = 20) were generated from CMD Mini-explorer and GEM-2 survey data collected on the same day along each of the selected twenty sampling locations similar to Zhu et al. (2010). Field calibration of CMD Mini-explorer and GEM-2 survey data were carried out using data collected on September 30, 2016, while the validation was carried out using data collected on October 6, 2016. To establish the relationship between CMD Mini-explorer and GEM-2, a 45 m transect in the study site was used to evaluate the ECa patterns and trends of CMD Mini-explorer and GEM-2.

2.2.4 Soil sampling

The selected silage corn plots received different nutrient management treatments using biochar (BC), dairy manure (DM) and inorganic fertilizer or a combination of these. Soil sampling at the study site was done by selecting twenty sampling locations based on the BC and DM application. Each sampling location was made up of approximately a 4 m x 1 m grid. Soil samples were collected using a gouge auger and a hammer, from the depths of 0 − 10 cm and 10 − 20 cm. The samples were placed in airtight bags and transferred into a thermally insulated, cooled, styrofoam box until measurements were made in the laboratory.

2.2.5 Data analysis

The descriptive statistics (min, max, mean, median, skewness, kurtosis and coefficient of variation, CV), paired samples t-test, Pearson's correlation coefficients, coefficient of determination (R^2), root mean square error (RMSE) and root mean square error of prediction (RMSEP), simple linear regression and backward stepwise multiple linear regression (MLR) were performed with Minitab 17 (Minitab 17 statistical software). ECa maps were generated using Surfer 8 (Golden Software, 2002).

2.3 Results

2.3.1 SMC results

A good match between volume based SMC (θ_v) from HD2-TDR and mass based SMC (θ_g) from OD methods was obtained with a R^2 of > 0.8 and a RMSE < 0.04 $m^3 m^{-3}$ (Fig. 2.3 and Table 2.1). HD2-TDR for 16 cm probe length is similar to the standard error of estimate of 0.013 $m^3 m^{-3}$ by Topp et al. (1980) while HD2-TDR 11 and 30 cm probe lengths have RMSE values of 0.040 $m^3 m^{-3}$ and 0.018 $m^3 m^{-3}$, respectively (Fig. 2.3 and Table 2.1).

Table 2.1 Liner regression, R^2 and RMSE for HD2-TDR calibration at PBRS using calculated θ_v from θ_g (n = 10).

SMC	Regression Equation	R^2	RMSE
$\theta_{v(0-11)}$	$1.1524(\theta_v)$	0.79	0.040
$\theta_{v(0-16)}$	$1.0117(\theta_v)$	0.88	0.013
$\theta_{v(0-30)}$	$1.0260(\theta_v)$	0.87	0.018

2.3.2 EMI results

The ECa patterns and trends along a 45 m transect were similar for CMD Mini-explorer and GEM-2, despite different DOE and orientations (Figs. 2.2 and 2.4). The CMD Mini-explorer data plotted against GEM-2 data (Fig. 2.5) shows that ECa values of ECa-H is closely related to that of GEM-2 (R^2 = 0.71) compared to ECa-L (R^2 = 0.40). The possibility of integrating the mean ECa measurements from CMD Mini-explorer and

GEM-2 were evaluated with the average of ECa-L, ECa-H and ECa-38kHz calculated and analyzed using the backward stepwise MLR. The results (see appendix 1) indicated that they are redundant.

ECa data were spatially mapped across the study site by variogram analysis and ordinary block kriging using Surfer 8 (Golden Software, USA). The trends of ECa data from CMD Mini-explorer and GEM-2 show similar patterns despite the different DOE (or sampling volume) and ECa values (Fig. 2.7). For instance, larger ECa values were measured at the north west and south east portion of the study site while lower ECa values were found on the north eastern portion, which stretches across the middle area of the field. The map of SMC predicted using the ECa-L and the 27 georeferenced measurements (Fig. 2.8) show similar patterns with lower values (< 0.28 m^3 m^{-3}) across the center of the study site.

2.3.3 Basic statistics

The descriptive statistics of the ECa measurements from CMD Mini-explorer and GEM-2 and the SMC in the study site are presented in Table 2.2. According to the classification of Warrick and Nielsen (1980), CVs of CMD Mini-explorer were low (CV < 12%) while that of GEM-2 were moderate (12 < CV < 62%). The CVs of SMC were moderate except for $\theta_{v(0-11)}$, which was low (Table 2).

Table 2.2 Descriptive statistics of the ECa (mS m^{-1}) measurements of CMD Mini-explorer and GEM-2 and SMC at the study site (n = 20).

Depth	Min	Max	Mean	Median	Skewness	Kurtosis	CV
ECa-L	2.79	3.99	3.58^a	3.68	-0.9	0.5	9.0
ECa-H	3.45	4.88	4.14^a	4.14	-0.1	-1.0	11.3
ECa-38kHz	2.15	4.58	3.21^b	3.2	0.2	-0.9	22.4
$\theta_{v(0\text{-}11)}$	0.23	0.34	0.29^c	0.30	-0.5	-0.6	11.3
$\theta_{v(0\text{-}16)}$	0.16	0.31	0.25^d	0.26	-0.7	0.2	14.6
$\theta_{v(0\text{-}30)}$	0.16	0.35	0.25^d	0.26	0.1	-0.4	20.5

Means that do not share a letter are significantly different at 5% probability.

A paired samples t-test was carried out on a sample of 20 ECa data points (see appendix 2) to determine whether there was a statistically mean difference in ECa from CMD Mini-explorer and GEM-2. ECa means were significantly different for ECa-38kHz (3.214 ± 0.718) when compared to ECa-L (3.576 ± 0.323) and ECa-H (4.139 ± 0.466) with p = 0.050 and, p = 0.000, respectively.

A paired-samples t-test was also carried out on a sample of 20 SMC data (see appendix 2) to determine whether there was a statistically mean difference in SMC at different depths. SMC mean was statistically significant for $\theta_{v(0\text{-}11)}$ (0.28755 ± 0.03241) compared to $\theta_{v(0\text{-}16)}$ (0.25268 ± 0.03690) and $\theta_{v(0\text{-}30)}$ (0.2471 ± 0.0507) with the same p = 0.000. Also, correlation coefficient among ECa measurements and SMC are shown in Table 2.3. At a p-value < 0.1, ECa data (CMD Mini-explorer and GEM-2) were significantly correlated with SMC.

Table 2.3 Pearson's correlation coefficients of the ECa measurements of CMD Mini-explorer and GEM-2 and SMC at the study site (n = 20). Significance is reported at the 0.1 (*), 0.05 (**), and 0.001 (***) p-values for correlation.

	ECa-L	ECa-H	ECa-38kHz	$\theta_{v(0-11)}$	$\theta_{v(0-16)}$	$\theta_{v(0-30)}$
ECa-L	1					
ECa-H	0.88^{***}	1				
ECa-38kHz	0.63^{**}	0.84^{***}	1			
$\theta_{v(0-11)}$	0.89^{***}	0.74^{***}	0.54^{**}	1		
$\theta_{v(0-16)}$	0.86^{***}	0.68^{***}	0.50^{**}	0.95^{***}	1	
$\theta_{v(0-30)}$	0.59^{**}	0.42^{*}	0.41^{*}	0.75^{***}	0.79^{***}	1

2.3.4 Regression analysis

The LRM results for SMC in relation to CMD Mini-explorer and GEM-2 data are summarized in Table 2.4. The SMC estimation using ECa-L (R^2_p = 0.38 and 0.54) is higher than ECa-H and ECa-38kHz with RMSEP 0.033 and 0.031 m^3 m^{-3}, respectively, which is about 9% of the total SMC variability (Table 2.4). Table 2.5 also presents an overview of the backward stepwise MLR analyses using all the EMI data variables to select the best models for SMC prediction at the study site. LRMs for $\theta_{v(0-11)}$ and $\theta_{v(0-16)}$ show a high prediction accuracy via ECa-L (R^2_p = 0.68 and 0.66) with RMSEP of 0.018 and 0.021 m^3 m^{-3}, respectively (Table 2.5).

Because the purpose of the large field study was to evaluate the ECa response to variability in SMC at a larger spatial scale, only $\theta_{v(0\text{-}16)}$ with the highest precision accuracy for the study site (Table 2.1) was measured at 27 geo-referenced locations on the field. The LRM for $\theta_{v(0\text{-}16)}$ at ECa-L on the small field was used for the large field study. The SMC estimation of $\theta_{v(0\text{-}16)}$ using ECa-L at the large field study is lower compared to the small field study estimation (RMSEP = 0.076 $m^3\ m^{-3}$), which equals 21% of the total SMC variability.

Furthermore, the models were applied to a 30 m transect on the corn-silage plot and the grass plot at the study site (Table 2.6). The SMC estimation via ECa-L for the grass plot is lower with a relatively lower R^2 values (from 0.07 to 0.32) and higher RMSEP (from 0.039 to 0.074 $m^3\ m^{-3}$) than corn-silage plot (R^2 = from 0.30 to 0.59; RMSEP = from 0.041 to 0.072 $m^3\ m^{-3}$. Overall, LRM developed between ECa and SMC in this study show higher prediction accuracy for ECa-L compared to ECa-H and ECa-38kHz.

Table 2.4 LRMs between ECa data from CMD Mini-explorer and GEM-2 with SMC (n = 20).

			Calibration		Validation	
ECa	SMC	Regression Equation	R^2	RMSE	R^2_p	RMSEP
ECa-L	$\theta_{v(0-11)}$	0.0888 ECa-L - 0.0301	0.79	0.015	0.38	0.033
	$\theta_{v(0-16)}$	0.0983 ECa-L - 0.0988	0.74	0.018	0.54	0.031
	$\theta_{v(0-30)}$	0.0925 ECa-L - 0.0836	0.35	0.040	-	-
ECa-H	$\theta_{v(0-11)}$	0.0515 ECa-H + 0.0743	0.55	0.021	0.15	0.032
	$\theta_{v(0-16)}$	0.0542 ECa-H + 0.0284	0.47	0.026	0.32	0.031
	$\theta_{v(0-30)}$	0.0462 ECa-H + 0.056	0.18	0.045	-	-
ECa-38kHz	$\theta_{v(0-11)}$	0.0243 ECa-38kHz + 0.2095	0.29	0.027	0.01	0.036
	$\theta_{v(0-16)}$	0.0257 ECa-38kHz + 0.1701	0.25	0.031	0.05	0.040
	$\theta_{v(0-30)}$	0.0292 ECa-38kHz + 0.1533	0.17	0.045	-	-

Table 2.5 Summary MLR model's quality by means RMSE, R^2, RMSEP, and R^2 of the cross validation (R^2_P).

	Calibration		Validation	
SMC	R^2	RMSE	R^2_P	RMSEP
$\theta_{v(0\text{-}11)}$	0.79	0.028	0.68	0.018
$\theta_{v(0\text{-}16)}$	0.74	0.030	0.66	0.021
$\theta_{v(0\text{-}30)}$	0.49	-	0.17	0.045

Table 2.6 Validation of LRMs in Table 4 using ECa data from CMD Mini-explorer and GEM-2 with SMC on a 30 m transect (n = 11).

		Silage Corn Plot		Grass Plot	
SMC	ECa	R^2_p	RMSEP	R^2_p	RMSEP
$\theta_{v(0\text{-}11)}$	ECa-L	0.30	0.046	0.13	0.066
	ECa-H	0.35	0.054	0.32	0.062
	ECa-38kHz	0.30	0.041	0.30	0.074
$\theta_{v(0\text{-}16)}$	ECa-L	0.55	0.070	0.07	0.071
	ECa-H	0.58	0.044	0.26	0.053
	ECa-38kHz	0.59	0.072	0.23	0.061
$\theta_{v(0\text{-}30)}$	ECa-L	-	-	0.07	0.062
	ECa-H	-	-	0.18	0.039
	ECa-38kHz	-	-	0.14	0.040

2.4 Discussion

The factory calibration of TDR would not be sufficient for field applications as it was carried out in a repacked soil with uniform temperature and low bulk electrical conductivity (IMKO, 2016). Also, low representative elemental volume of soils, which affects the variability of SMC have been reported for many current sensor technologies as well as direct sampling methods (Hignett and Evett, 2008). This has been attributed to several factors such as gravel content and position in landscape, which influences water content variation across the field (Hignett and Evett, 2008). In our study, highly disturbed soil surface and high gravel content at the 0 – 10 cm soil depth and positions of measurement (point measurements) within the study area might be the potential reasons for differences between 11 cm HD2-TDR probe data and OD data (Fig. 2.3). This behaviour implies that it is not a field error (Std Dev = 0.037 m^3 m^{-3}), but a high spatial variability of field water content within the shallow depth.

Khan et al. (2016) reported a low ECa between 2.1 and 35.5 mS m^{-1} on an orthic Humo-ferric podzol while Pan et al. (2014) indicated low ECa between 1.36 and 3.29 mS m^{-1} in sandy soil. Martini et al. (2017) also observed a low ECa, between 0 and 24 mS m^{-1}, with a very small range of spatial variation which was predominantly attributed to the small heterogeneity of soil texture (Sand = 6 – 28%, Silt = 55 – 79%, Clay = 13 – 25%). This is similar to the result from our study site classified as orthic Humo-ferric podzol with a lower ECa range between 0 and 7 mS m^{-1} and also a low textural variation (Sand = 80.10 – 83.75%, Silt = 10.44 – 12.58%, Clay = 5.81 – 7.32%). Although the report by

Martini et al. (2017) has low percentage variations of sand, and the clay content (which is one of the factors that can influence ECa; McNeill, 1980) is lower at both sites.

The depth range (0 – 30 cm) considered in our study, also includes the Podzolic Ae horizons with texture that is coarser than the adjacent horizons (Soil Classification Working Group, 1998). The known depth-response function of CMD Mini-explorer has been used by various authors to calibrate the sensor, even though not all coil separations exhibit low signal to noise level (Altdorff et al., 2016; Bonsall et al., 2013).

Arguably, the multi-frequency GEM-2 sensor measures at a deeper depth of exploration compared to the multi-coil CMD Mini-explorer sensor. ECa measurements from the GEM-2 sensor has lower values compared to the CMD Mini-explorer sensor ECa measurements with known depth of exploration of 90 cm and 180 cm for low and high coil 3 dipole configurations, respectively. Evaluating the ECa measurements by GEM-2 with the site description using the EMI skin depth Nomogram (Won et al., 1980) also confirmed that the DOE is greater than 180 cm. When the DOE increases, lower signals are observed and the soil is less conductive, whereby higher signals are observed with increasing DOE (Callegary et al., 2007; Delefortrie et al., 2014). Additionally, the CMD Mini-explorer coil 3 dipole configuration adopted for the study shows the highest local sensitivity between 35 and 75 cm depth according to the sensitivity function by McNeil (1980) which provides a reasonable match between the sensing volume of EMI and the depth range sampled by the HD2-TDR precision soil moisture probe. The largest coil separation in vertical dipole orientation was also less sensitive to variations in instrument height that inevitably occur when EMI measurements were carried out.

Warrick and Nielsen (1980) proposed the use of CV categories, which have been widely adopted to assess the soil's spatial variability. This procedure allows for comparisons across samples and measurements that employ different units of measurement (Souza et al., 2009). However, the geostatistical techniques must be carried out to understand the spatial dependence among the variables (Liu et al., 2006). Molin and Faulin (2013) found CVs for ECa and SMC to be moderate (43% and 57%). These findings are similar to my results even though CVs are less than 23% (Table 2.2). This implies that ECa response to vertical heterogeneity of soil properties (Neely et al., 2016) such as SMC.

Other researchers also found considerable site-to-site variability in the relationship between ECa and SMC (*e.g.* Brevik et al., 2006), similar to this study. The R^2 and RMSE of validation models are not consistent compared to that of calibration models (Table 2.4). For instance, calibration using $\theta_{v(0\text{-}16)}$ produces an $R^2 = 0.74$ and RMSE = 0.018 m^3 m^{-3} while validation produces $R^2 = 0.54$ and RMSEP = 0.031 m^3 m^{-3}. The R^2 generated when the detailed field study models were applied to the grass plot showed the need for site-specific calibration to establish the relationship between ECa and SMC (Table 2.6). Also, the R^2 and the RMSE values for SMC presented in Figure 6 for ECa-L, ECa-H and ECa-38kHz measurements varies by 0.01 and 0.54 and 0.031 m^3 m^{-3} and 0.040 m^3 m^{-3}

respectively. This implies that the variation in SMC can be attributed to the maximum sensitivity of the ECa.

Martini et al. (2017) observed that SMC monitoring using ECa requires the determination of the temporal variations of all other state variables that induce codependences on ECa (*e.g.* temperature and ECw) while Altdorff et al. (2017b) reported that EMI has the potential to account for the strong influence of SMC on ECa. Even though our study did not account for all variables, the data set used was sufficient for the site-specific calibration of SMC at the study site.

This study confirms the linear relationship between ECa and SMC through the correlation between the spatial pattern of ECa (Fig. 2.7) and SMC (Fig. 2.8). Regions of low ECa correspond to regions of low SMC and vice versa. For instance, the region with the ECa > 4 mS m^{-1} corresponds to SMC region > 0.28 m^3 m^{-3}. The spatial variability of geo-referenced SMC is lower than ECa-L predicted SMC (Fig. 2.8) as expected. This can be attributed to the inability of the number of sampling locations used in this study to capture the spatial variability of SMC and its effects on the map interpolation.

2.5 Conclusions

Analysis of the relationships between ECa measurements using two EMI sensors (CMD Mini-explorer and GEM-2), and SMC using OD and HD2-TDR methods were carried out on a podzolic soil at an experimental site in western Newfoundland. Linear regression analysis used to estimate SMC from the two EMI-ECa sensors at the study site gave the best prediction models for SMC at 0 – 11 cm and 0 –16 cm depth ranges.

Mapping of SMC at field scale required site-specific calibration to derive reasonably accurate models to predict SMC from EMI measurements. In our study, the validation of site specific calibration of SMC on the corn-silage plot was significant ($R^2 = 0.30 \sim 0.59$), but results were relatively poor ($R^2 = 0.07 \sim 0.32$) for the grass plot. A LRM was found to justifiably describe the site-specific calibration of ECa-SMC on the small field. This can be attributed to the potential of CMD Mini-explorer and GEM-2 to measure the strong influence of SMC on ECa implying that the SMC is a major driver of ECa measurement at the study site.

A good relationship was found between measured ECa from CMD Mini-explorer and GEM-2 at the study site. The plot of CMD Mini-explorer and GEM-2 was observed to have similar values for the selected coil and frequency used in the study. Though the temperature effect is minimal, it is important to conduct the direct measurements and EMI measurements from the two EMI sensors within a short time difference when there will be minor changes of SMC.

Further research on the prediction of profile depth and sampling volume of the field needs to be carried out to confirm if SMC is the basic driver of CMD Mini-explorer and GEM-2 response along the depth and horizontal variation at large scale.

2.6 Acknowledgments

Financial supports from Research and Development Corporation, NL (RDC-Ignite) for field research and Research Office of Grenfell Campus, Memorial University of Newfoundland for equipment purchase are greatly appreciated. An MSc-BEAS graduate fellowship from Memorial University to E. Badewa, and data-collection support by Marli Vermooten, Dinushika Wanniarachchi and Kamaleswaran Sadatcharam are acknowledged.

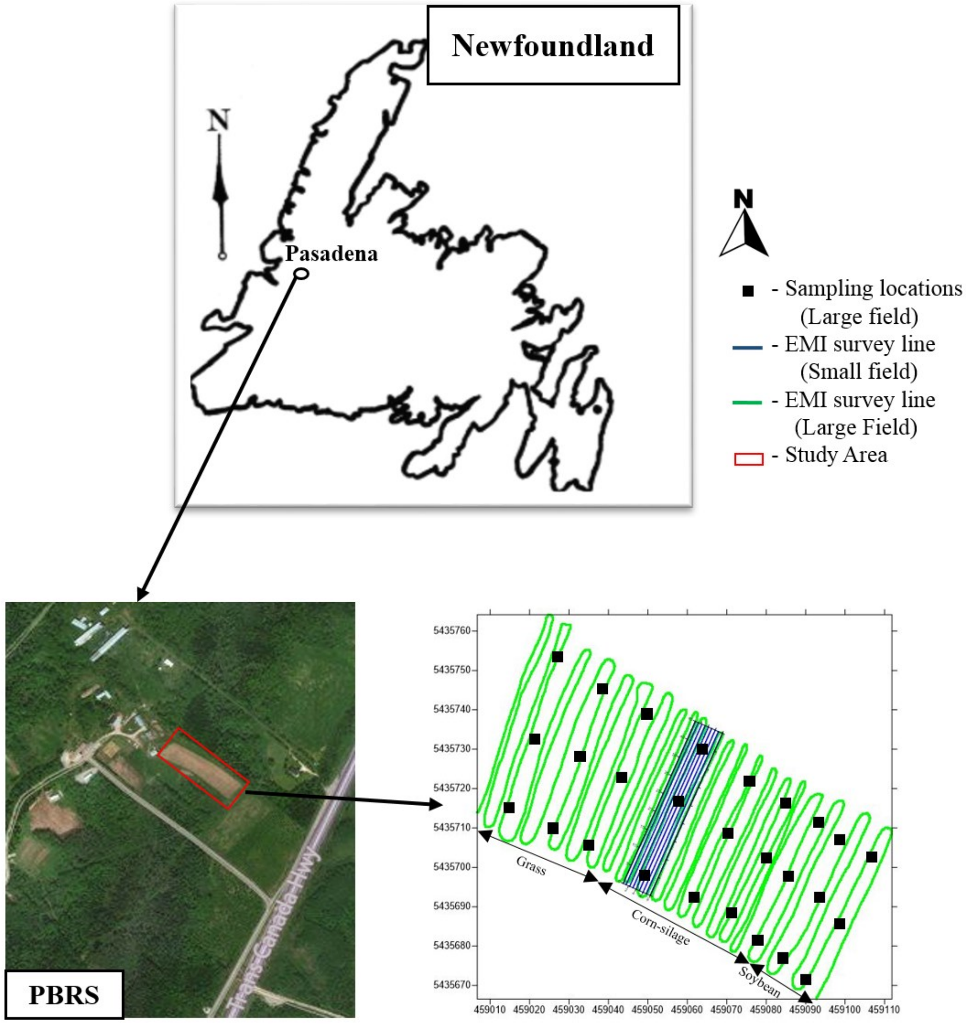

Figure 2.1 The location of Pynn's Brook Research Station (PBRS), Pasadena (49° 04' 20" N, 57° 33' 35" W) in Newfoundland, Canada and the study site.

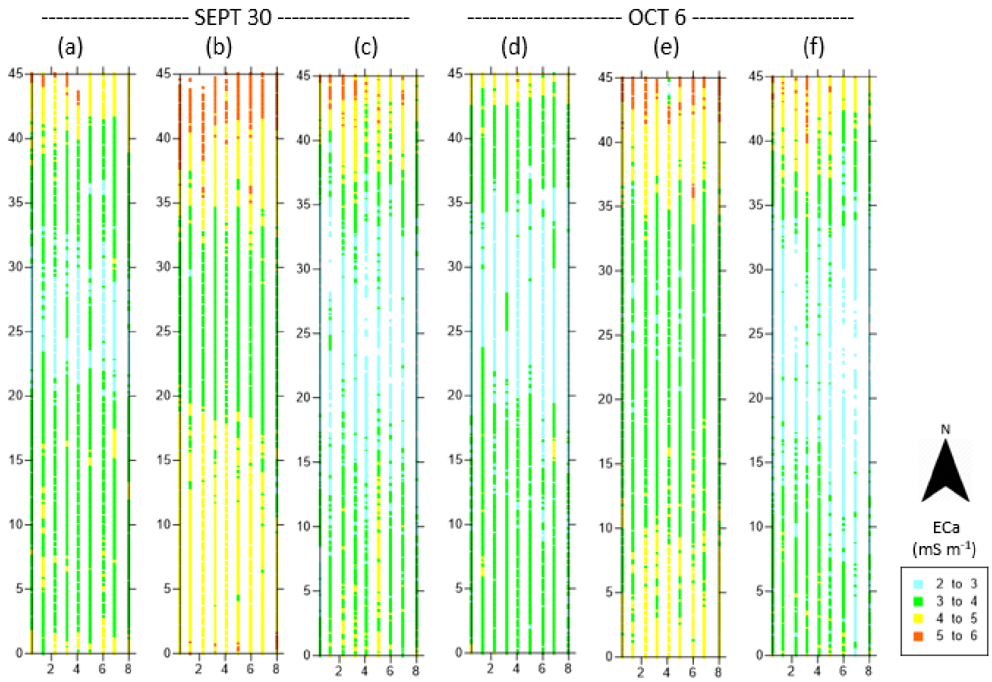

Figure 2.2 Measured soil ECa on 30 September (a) to (c) and on 6 October (d) to (f) for ECa-L, ECa-H and ECa-38kHz surveys, respectively during the detailed small field study.

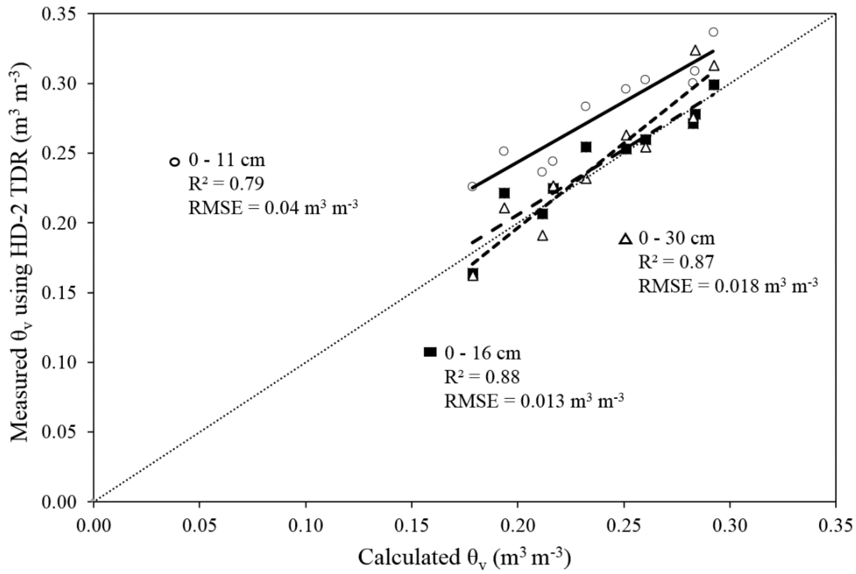

Figure 2.3 . HD2-TDR calibration at PBRS using the calculated θ_v by using the measured θ_g and bulk density.

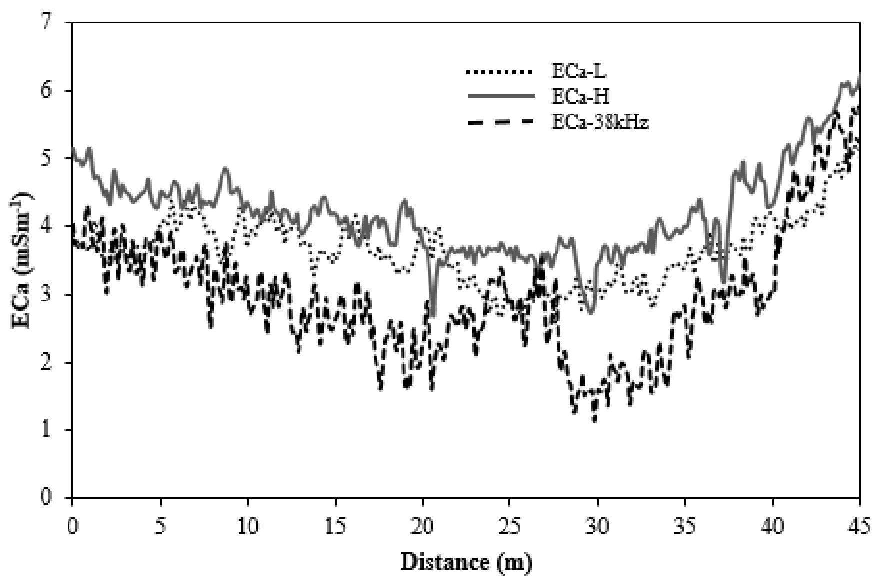

Figure 2.4 ECa measurements by the two EMI sensors on a 45 m transect on the experimental field.

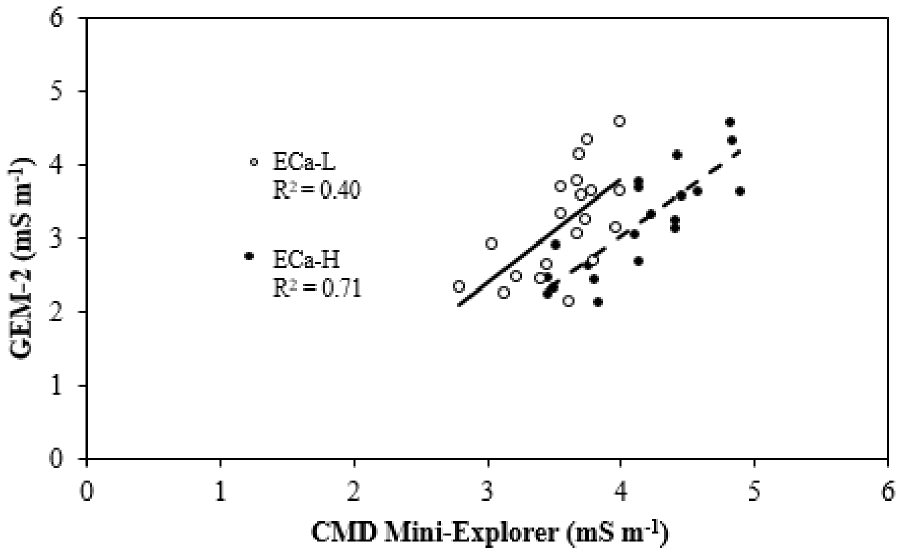

Figure 2.5 Scatter-plot of ECa measured using CMD Mini-explorer and GEM-2.

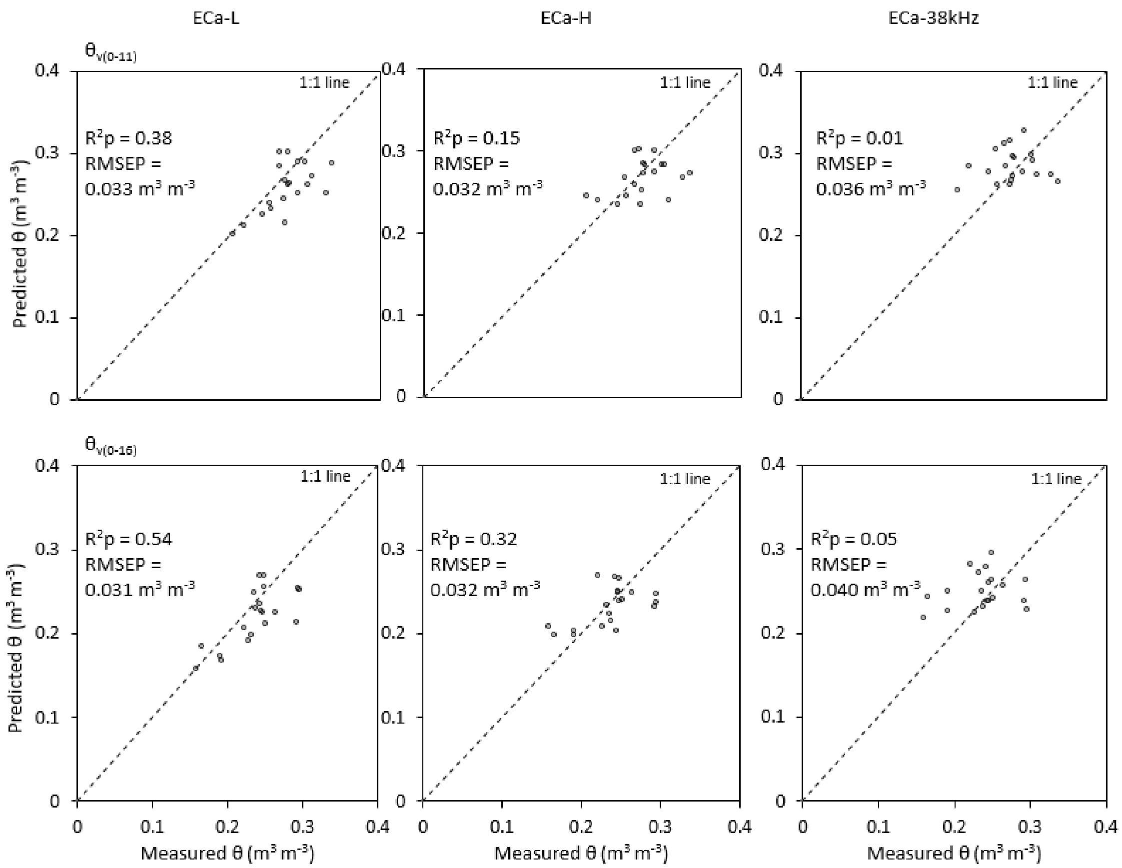

Figure 2.6 Plots of predicted θ_v (m^3 m^{-3}) versus measured θ_v (m^3 m^{-3}) for the LRMs given in Table 4 for ECa-L, ECa-H and ECa-38kHz.

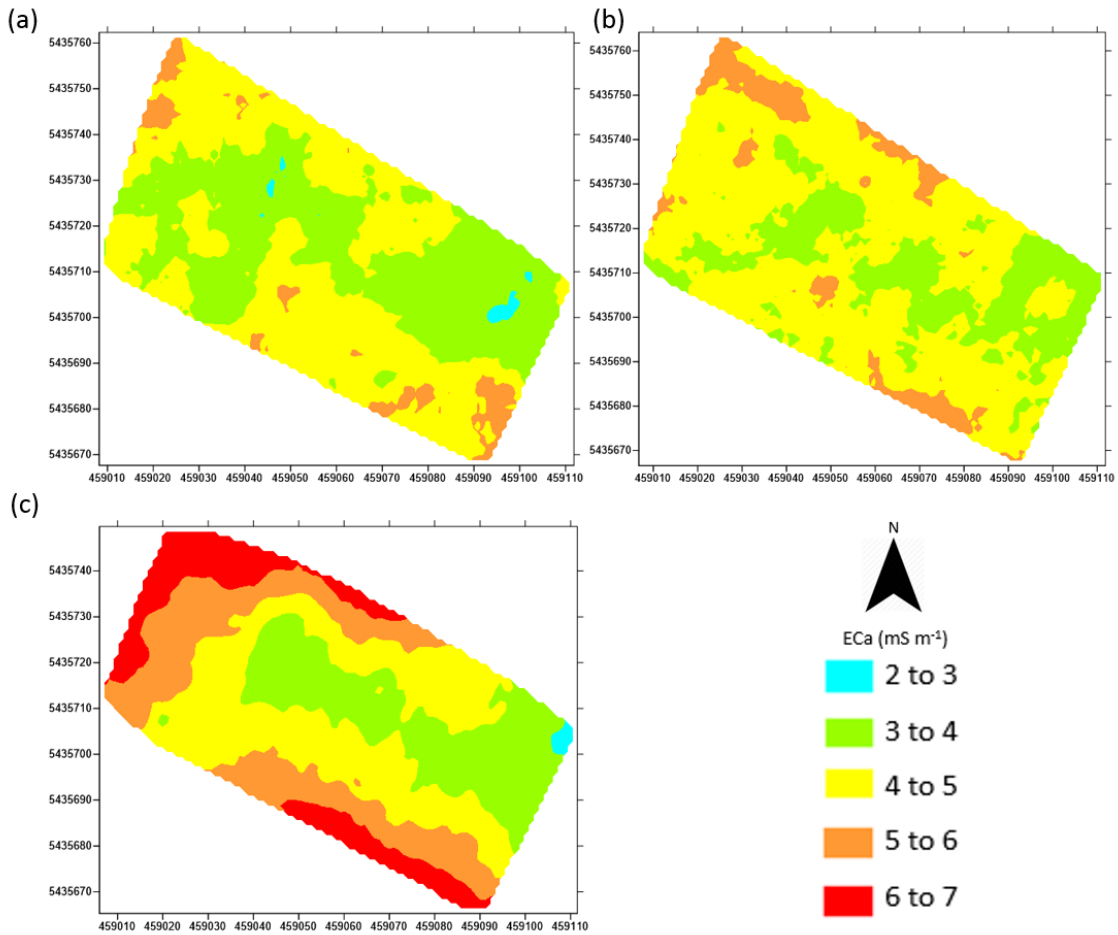

Figure 2.7 ECa variability maps for the large field study (a) ECa-L (b) ECa-H (c) ECa-38kHz.

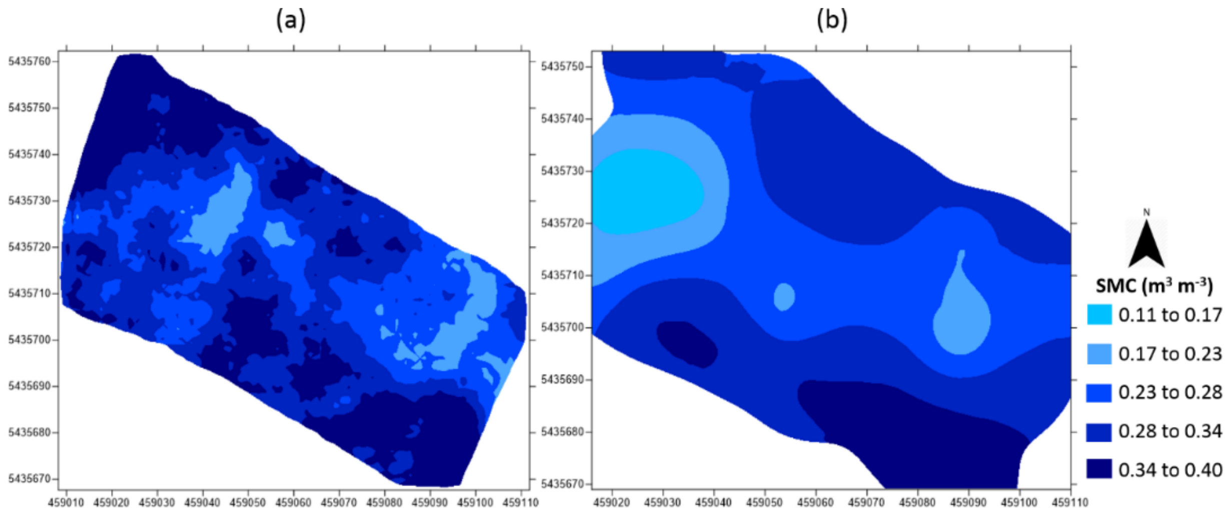

Figure 2.8 SMC variability maps for the large field study estimated using ECa-L measurements (a) and 27 geo-referenced point measurements (b).

2.7 References

Allred, B. J., Ehsani, M. R., & Saraswat, D. (2005). The Impact of Temperature and Shallow Hydrologic Conditions on The Magnitude and Spatial Pattern Consistency of Electromagnetic Induction Measured Soil Electrical Conductivity. *American Society of Agricultural Engineers, 48*(6), 2123–2135.

Altdorff, D., Bechtold, M., van der Kruk, J., Vereecken, H., & Huisman, J. A. (2016). Mapping peat layer properties with multi-coil offset electromagnetic induction and laser scanning elevation data. *Geoderma, 261*, 178–189.

Altdorff D, Galagedara L, & Unc A. (2017). Impact of projected land conversion on water balance of boreal soils in western Newfoundland. *Journal of Water and Climate Change,* (In press).

Altdorff, D., von Hebel, C., Borchard, N., van der Kruk, J., Bogena, H. R., Vereecken, H., & Huisman, J. A. (2017b). Potential of catchment-wide soil water content prediction using electromagnetic induction in a forest ecosystem. *Environmental Earth Sciences, 76*(3), 111.

Bittelli, M. (2011). Measuring soil water content: A review. *HortTechnology, 21*(3), 293-300.

Bonsall, J., Fry, R., Gaffney, C., Armit, I., Beck, A., & Gaffney, V. (2013). Assessment of the CMD Mini-Explorer, a New Low-frequency Multi-coil Electromagnetic Device, for Archaeological Investigations. *Archaeological Prospection, 20*(3), 219–231.

Brevik, E. C., & Fenton, T. E. (2002). The relative influence of soil water, clay, temperature, and carbonate minerals on soil electrical conductivity readings with an EM-38 along a Mollisol catena in central Iowa. *Soil Survey Horizon, 43*, 9–13.

Brevik, E. C., Fenton, T. E., & Lazari, A. (2006). Soil electrical conductivity as a function of soil water content and implications for soil mapping. *Precision Agriculture, 7*(6), 393–404.

Callegary, J. B., Ferré, T. P. A., & Groom, R.W. (2007). Vertical spatial sensitivity and exploration depth of low-induction-number electromagnetic induction instruments. *Vadose Zone Journal, 6*, 158–167.

Corwin, D. L., & Lesch, S. M. (2003). Application of soil electrical conductivity to precision agriculture. *Agronomy Journal, 95*(3), 455–471.

Corwin, D. L., & Lesch, S. M. (2005a). Characterizing soil spatial variability with apparent soil electrical conductivity Part II. Case study. *Computers and Electronics in Agriculture, 46*, 135–152.

Corwin, D. L., & Lesch, S. M. (2005b). Apparent soil electrical conductivity measurements in agriculture. *Computers and electronics in agriculture, 46*(1), 11-43.

Corwin, D. L., & Lesch, S. M. (2005c). Characterizing soil spatial variability with apparent soil electrical conductivity: I. Survey protocols. *Computers and Electronics in Agriculture, 46*(1), 103-133.

Delefortrie, S., Saey, T., Van De Vijver, E., De Smedt, P., Missiaen, T., Demerre, I., & Van Meirvenne, M. (2014). Frequency domain electromagnetic induction survey in the intertidal zone: Limitations of low-induction-number and depth of exploration. *Journal of Applied Geophysics, 100,* 14-22.

Desilets, D., Zreda, M., & Ferre, T. P. A. (2010). Nature's neutron probe: Land surface hydrology at an elusive scale with cosmic rays. *Water Resource Research 46,* W11505, doi:10.1029/2009WR008726.

Doolittle, J. A., & Brevik, E. C. (2014). The use of electromagnetic induction techniques in soils studies. *Geoderma, 223,* 33–45.

Driessen, P., Deckers, J., Spaargaren, O., & Nachtergaele, F. (2001). Lecture notes on the major soils of the world. Food and Agriculture Organization of the United Nations. World Soil Resources Report No. 94. 334 pp.

Ferré, P. A., Redman, J. D., Rudolph, D. L., & Kachanoski, R. G. (1998). The Dependence of the Electrical Conductivity Measured by Time Domain Reflectometry on the Water Content of a Sand. *Water Resources Research, 34*(5), 1207-1213.

Franz, T. E., Zreda, M., Ferre, P. A., & Rosolem, R. (2013). An assessment of the effect of horizontal soil moisture heterogeneity on the area-average measurement of cosmic-ray neutrons. *Water Resources Research, 49*(10), 1-10.

Fortes, R., Millán, S., Prieto, M. H., & Campillo, C. (2015). A methodology based on apparent electrical conductivity and guided soil samples to improve irrigation zoning. *Precision Agriculture, 16*(4), 441–454.

Friedman, S. P. (2005). Soil properties influencing apparent electrical conductivity: a review. *Computers and electronics in agriculture, 46*(1), 45-70.

Galagedara, L. W., Parkin, G. W., Redman, J. D. von Bertoldi, P., & Endres, A. L. (2005). Field studies of the GPR ground wave method for estimating soil water content during irrigation and drainage. *Journal of Hydrology, 301,* 182-197.

Geophex Ltd., 2004. GEM-2 User's Manual, Version 3.8. Geophex Ltd., Raleigh, USA. *Available at: http://www.geophex.com/Downloads/GEM-2%20Operator's%20Manual.pdf.*

GF Instruments., 2011. CMD Electromagnetic conductivity meter user manual V. 1.5. Geophysical Equipment and Services, Czech Republic. *Available at: http://www.gfinstruments.cz/index.php?menu=gi&smenu=iem&cont=cmd_&ear=ov.*

Goff, A., Huang, J., Wong, V. N. L., Monteiro Santos, F. A., Wege, R., & Triantafilis, J. (2014). Electromagnetic Conductivity Imaging of Soil Salinity in an Estuarine–Alluvial Landscape. *Soil Science Society of America Journal, 78*(5), 1686.

Hignett, C., & Evett, S. (2008). Direct and surrogate measures of soil water content (*No. IAEA-TCS--30).*

Huang, J., Nhan, T., Wong, V. N. L., Johnston, S. G., Lark, R. M., & Triantafilis, J. (2014). Digital soil mapping of a coastal acid sulfate soil landscape. *Soil Research, 52,* 327–339.

Huang, J., Scudiero, E., Bagtang, M., Corwin, D. L., & Triantafilis, J. (2016). Monitoring scale-specific and temporal variation in electromagnetic conductivity images. *Irrigation Science, 34*(3), 187–200.

IMKO. (2016). TRIME-TDR user manual. *Retrieved from https://imko.de/en/about-trime-tdr*

Jay, S. C., Lawrence, R. L., Repasky, K. S., & Rew, L. J. (2010 July). Detection of leafy spurge using hyper-spectral-spatial-temporal imagery. *In Geoscience and Remote Sensing Symposium (IGARSS) 2010 IEEE International* (pp. 4374-4376). IEEE.

Kachanoski, R. G., Gregorich, E. G., & vanWesenbeeck, I. J. (1988). Estimating spatial variations of soil water content using non-contacting electromagnetic inductive methods. *Canadian Journal of Soil Science, 68*, 715–722.

Khan, F. S., Zaman, Q. U., Chang, Y. K., Farooque, A. A., Schumann, A. W., & Madani, A. (2016). Estimation of the rootzone depth above a gravel layer (in wild blueberry fields) using electromagnetic induction method. *Precision agriculture, 17*(2), 155-167.

Khosla, R., Inman, D., Westfall, D. G., Reich, R. M., Frasier, M., Mzuku, M., Koch, B., & Hornung, A. (2008). A synthesis of multi-disciplinary research in precision agriculture: site-specific management zones in the semi-arid western Great Plains of the USA. *Precision Agriculture, 9*(1-2), 85-100.

Kyaw, T., Ferguson, R. B., Adamchuk, V. I., Marx, D. B., Tarkalson, D. D., & McCallister, D. L. (2008). Delineating site-specific management zones for pH-induced iron chlorosis. *Precision Agriculture, 9*(1–2), 71–84.

Lesch, S. M., Strauss, D. J., & Rhoades, J. D. (1995). Spatial prediction of soil salinity using electromagnetic induction techniques. Part 1. Statistical prediction models: a comparison of multiple linear regression and cokriging. *Water Resources Research, 31,* 373–386.

Lesch, S. M., & Corwin, D. L. (2003). Predicting EM/soil property correlation estimates via the dual pathway parallel conductance model. *Agronomy Journal, 95*(2), 365–379.

Lesch, S. M., Corwin, D. L., & Robinson, D. A. (2005). Apparent soil electrical conductivity mapping as an agricultural management tool in arid zone soils. *Computers and Electronics in Agriculture, 46*(1), 351-378.

Liu, T. L., Juang, K. W., & Lee, D. Y. (2006). Interpolating soil properties using kriging combined with categorical information of soil maps. *Soil Science Society of America Journal, 70*(4), 1200-1209.

Ma, R., McBratney, A., Whelan, B., Minasny, B., & Short, M. (2011). Comparing temperature correction models for soil electrical conductivity measurement. *Precision Agriculture, 12*(1), F55–F66.

Martini, E., Werban, U., Zacharias, S., Pohle, M., Dietrich, P., & Wollschläger, U. (2017). Repeated electromagnetic induction measurements for mapping soil moisture at the field scale: validation with data from a wireless soil moisture monitoring network. *Hydrology and Earth System Sciences, 21*(1), 495.

McNeill, J. D. (1980). Electromagnetic terrain conductivity measurement at low induction numbers. *(Geonics Ltd., Mississauga, Ontario, Canada, Technical Note TN-5).*

Molin, J. P., & Faulin, G. D. C. (2013). Spatial and temporal variability of soil electrical conductivity related to soil moisture. *Scientia Agricola, 70*(1), 01-05.

Mondal, P., & Tewari, V. K. (2007). Present status of precision farming: A review. International Journal of Agricultural Research, 5(12), 1124-1133.

Neely, H. L., Morgan, C. L., Hallmark, C. T., McInnes, K. J. & Molling, C. C. (2016). Apparent electrical conductivity response to spatially variable vertisol properties. *Geoderma, 263,* 168-175.

Pan, L., Adamchuk, V. I., Prasher, S., Gebbers, R., Taylor, R. S., & Dabas, M. (2014). Vertical soil profiling using a galvanic contact resistivity scanning approach. *Sensors, 14*(7), 13243-13255.

Peralta, N. R., & Costa, J. L. (2013). Delineation of management zones with soil apparent electrical conductivity to improve nutrient management. *Computers and Electronics in Agriculture, 99*, 218–226.

Rhoades, J. D., Raats, P. A., & Prather, R. J. (1976). Effects of liquid-phase electrical conductivity, water content, and surface conductivity on bulk soil electrical conductivity. *Soil Science Society of America Journal, 40*, 651–655.

Rhoades, J. D., Manteghi, N. A., Shouse, P. J., & Alves, W. J. (1989). Soil electrical conductivity and soil salinity: New formulations and calibrations. *Soil Science Society of America Journal, 53*(2), 433-439.

Robinson, D. A., Lebron, I., Lesch, S. M., & Shouse, P. (2004). Minimizing drift in electrical conductivity measurements in high temperature environments using the EM-38. *Soil Science Society of America Journal, 68*(2), 339-345.

Sanborn, P., Lamontagne, L., & Hendershot, W. (2011). Podzolic soils of Canada: Genesis, distribution, and classification. *Canadian Journal of Soil Science, 91*(5), 843-880.

Serrano, J. M., Shahidian, S., & da Silva, J. R. M. (2013). Apparent electrical conductivity in dry versus wet soil conditions in a shallow soil. *Precision Agriculture, 14*(1), 99–114.

Soil Classification Working Group. (1998). The Canadian System of Soil Classification. The Canadian System of Soil Classification, 3rd ed. *Agriculture and Agri-Food Canada Publication* 1646. NRC Research Press.

Souza, Z. M. D., Marques Júnior, J., & Pereira, G. T. (2009). Spatial variability of the physical and mineralogical properties of the soil from the areas with variation in landscape shapes. *Brazilian Archives of Biology and Technology, 52*(2), 305-316.

Topp, G. C., Davis, J. L., & Annan, A. P. (1980). Electromagnetic determination of soil water content: Measurements in coaxial transmission lines. *Water resources research, 16*(3), 574-582.

Vereecken, H., Huisman, J. A., Pachepsky, Y., Montzka, C., Van Der Kruk, J., Bogena, H., Weihermüller, L., Herbst, M., Martinez, G., & Vanderborght, J. (2014). On the spatio-temporal dynamics of soil moisture at the field scale. *Journal of Hydrology 516,* 76-96.

Walter, J., Lueck, E., Bauriegel, A., Richter, C., & Zeitz, J. (2015). Multi-scale analysis of electrical conductivity of peatlands for the assessment of peat properties. *European Journals of Soil Science, 66*(4), 639-650.

Wang, C., Rees, H. W., & Daigle, J. L. (1984). Classification of Podzolic soils as affected by cultivation. *Canadian Journal of Soil Science, 64*(2), 229-239.

Warrick, A. W., & Nielsen, D. R. (1980). Spatial variability of soil physical properties in the field. 319–44. In: Hillel, D. (Ed.). *Applications of Soil Physics. Academic Press,* New York, NY, USA.

Wijewardana, Y. G. N. S., & Galagedara, L. W. (2010). Estimation of spatio-temporal variability of soil water content in agricultural fields with ground penetrating radar. *Journal of Hydrology, 391*(1–2), 24–33.

Won, I. J. (1980). A wide-band electromagnetic exploration method—Some theoretical and experimental results. *Geophysics, 45*(5), 928–940.

Zhang, Z., He, G., & Jiang, H. (2013). Leaf area index retrieval using red edge parameters based on Hyperion hyper-spectral imagery. *Journal of Theoretical and Applied Information Technology, 48*(2), 957–960.

Zhu, Q., Lin, H., & Doolittle, J. (2010). Repeated electromagnetic induction surveys for determining subsurface hydrologic dynamics in an agricultural landscape. *Soil Science Society of America Journal, 74*(5), 1750-1762.

CHAPTER 3

3.0 SOIL APPARENT ELECTRICAL CONDUCTIVITY (ECa): A PROXY FOR DETERMINATION OF SOIL PROPERTIES IN MANAGED PODZOLS[2].

Abstract

Understanding of the spatial variability of soil apparent electrical conductivity (ECa) in agricultural fields is useful for site specific management. ECa measured using the non-invasive electromagnetic induction (EMI) sensors is widely used to determine the spatial variability of soil physical properties such as texture and bulk density, and hydraulic properties such as soil moisture content (SMC) and available water content (AWC). This study investigated the temporal variability of ECa in relation to SMC in managed podzol soils to demonstrate the spatial variability of soil physical and hydraulic properties. Two different EMI sensors, CMD Mini-explorer and GEM-2, multi-Coil and multi-Frequency, respectively were used for ECa measurements on a 45 m x 8.5 m plot at Pynn's Brook Research Station (PBRS), Pasadena, Newfoundland, Canada. Results show that there is a significant relationship between the ECa mean relative differences (MRD) and the SMC MRD (R^2 = 0.33 to 0.70) for both multi-coil and multi-frequency sensors. The ECa standard deviation of the relative differences (SDRD) varies between 0.015 to 0.09, due to the difference in the depth of investigation (DOE) of the ECa data between CMD Mini-explorer and GEM-2. Also, significant linear relationships were observed

foot note[2]:"Badewa, E., Unc, A., Cheema, M. and Galagedara, L. (2017). Soil apparent electrical conductivity (ECa): A proxy for determination of soil properties in managed podzols (Submitted to Pedosphere (Re.: pedos201710503))".

between ECa MRD and sand (R^2 = 0.35 and 0.53) and silt (R^2 = 0.43), but a non-significant linear relationship with clay (R^2 = 0.06 and 0.16). The spatial variability of the ECa predicted soil properties are relatively consistent, with lower variability (CV = 3.26 to 27.61), compared to the measured soil properties. I conclude that the temporal stability of ECa can be used in a managed podzol to interpret the spatial variability of soil physical and hydraulic properties such as SMC, texture, bulk density and AWC.

Keywords

Apparent electrical conductivity, Electromagnetic induction, Soil properties, Spatial variability, Temporal stability

3.1 Introduction

The knowledge of the variability of soil properties is essential for efficient soil and crop management. This has led to increasing interests in the management of field variability (Serrano et al., 2014) especially with respect to inputs, primarily aimed at achieving higher productivity with minimum environmental effects. The traditional and commonly adopted way of characterizing soil's variability is labour intensive and time consuming (Shibusawa, 2006; Brevik et al., 2016). Indirect techniques such as electromagnetic induction (EMI) have been proven to be a valuable geophysical tool to understand soil variability (Corwin, 2008; Toushmalani, 2010), owing to their speed, volume of data collection and low cost (Doolittle et al., 2014). EMI sensors measure the soil apparent electrical conductivity (ECa) either invasively or non-invasively (Doolittle et al., 2014; Serrano et al., 2014; Neely et al., 2016). ECa measured using EMI sensors is commonly used to provide spatial variability of soil properties such as SMC (Calamita et al., 2015; Altdorff et al., 2017), soil texture (Heil and Schmidhalter, 2012; White et al., 2012), soil bulk density (Altdorff et al., 2016) and available water content (AWC) (Fortes et al., 2015).

Newly adopted EMI sensors such as CMD Mini-explorer and GEM-2 have the ability to measure ECa at different depths due to their multiple coils or multiple frequency options, respectively. CMD Mini-explorer, a multi-coil EMI sensor, which operates at 30 kHz and has one transmitter and three coplanar receiver coils with different distances (32 cm, 71 cm, and 118 cm) that can be oriented in low or high depth range *i.e.* vertical coplanar (VCP) or horizontal coplanar (HCP) coil configuration, respectively (GF Instruments, 2011). GEM-2 is a broadband multi-frequency EMI sensor with one transmitter coil and a receiver coil separated by 166 cm, which can be operated in a frequency band between 30 Hz to about 93 kHz. The GEM-2 sensor can also be operated in VCP and HCP coil configurations (Geophex Ltd., 2004).

Several studies have shown that the spatial patterns of ECa can also indicate temporal stability. Pedrera-Parrilla et al. (2017) investigated the temporal stability between SMC and ECa. They found out that a spatial relationship exists between SMC and ECa, with a linear behaviour, and that the temporal stability of the ECa survey can be used for determining SMC. Laio et al. (2014) also reported the relationship between the temporal stability of ECa and a number of soil properties such as SMC, texture, and depth to the bedrock, noting that the spatial and temporal variations of these soil properties can be identified and assessed from the temporally stable spatial distribution of the ECa.

To assess the full potential of ECa, and fill the literature gap on the temporal stability of ECa, recent studies have targeted the temporal changes of ECa (Pedrera-Parrilla et al., 2017). Most researchers have analyzed the ECa mean relative differences (MRD) through the positive and negative deviations from the spatial mean (Martínez et al., 2010; Zhu et al., 2010; Van Arkel and Kaleita, 2014). Furthermore, literature confirms possible to obtain a better representation of clay distribution than of the sand and silt (Heil and Schmidhalter, 2015). However, podzols, in particular the orthic humic podzols, generally have high sand and silt than clay (Soil Classification Working Group, 1998).

The analyses of the spatial structure of soil properties is widely carried out using the kriging interpolation technique with a variogram model (Pandey and Pandey, 2010). Kriging has the potential to provide spatial estimates for unsampled locations through the interpolation of available sampled locations for soil properties (Rossi et al., 1994). Also, the use of theoretical variogram model (Gaussian, spherical, exponential, or linear) that best fits the experimental variogram is often used with the block kriging technique to improve soil properties mapping (Huang et al., 2013).

The objectives of this study were to investigate the temporal stability of ECa and selected soil physical and hydraulic properties such as SMC, texture, bulk density and AWC under managed podzols, and also to demonstrate the spatial variability of soil properties such as SMC, sand, silt, bulk density and AWC using block kriging and spherical variogram.

3.2 Materials and Methods

3.2.1 Study site

The study was carried out at Pynn's Brook Research Station (PBRS) (49° 04' 20" N, 57° 33' 35" W), Pasadena, Newfoundland, Canada (see Fig. 2.1). The site is a portion of a corn silage experimental field consisting of one variety. The soil, reddish brown to brown, has developed on gravelly sandy fluvial deposit of mixed lithology, with >100 cm depth to the bedrock, and a 2-5 % slope (Kirby, 1988). Soil samples (n = 7) analyzed from the study site revealed a gravelly loamy sand soil (sand = 82.0±3.4%; silt = 11.6±2.4%; clay = 6.4±1.2%), classified as orthic Humo-ferric podzol (Kirby, 1988). The average bulk density and porosity for the site (n = 28) were 1.31±0.07 g cm^{-3} and 51±0.03%, respectively. Based on the 30-year data (1986-2016) of a nearby Deer Lake weather station (Environment Canada, http://climate.weather.gc.ca/), the area receives an average precipitation of 1113 mm per year with less than 410 mm falling as snow, and has an annual mean temperature of 4 °C.

3.2.2 EMI surveys and data processing

Soil ECa was measured using the CMD Mini-explorer (GF instruments, Brno, Czech Republic) and GEM-2 (Geophex, Ltd., Raleigh, USA). The CMD Mini-explorer was used in both VCP and HCP to simultaneously sense different integral depths, also called Pseudo-depths (PDs), of 25, 50 and 90 cm from VCP, and 50, 100, 180 cm from

HCP (Altdorff et al., 2016). Although the depth of exploration (DOE) of GEM-2 frequencies are yet to be determined, the sensor was operated in the HCP configuration, which has the potential to measure at a deeper DOE compared to CMD Mini-explorer (Won, 1980). Based on the preliminary data obtained on the site, I decided to employ the CMD Mini-explorer with the largest coil separation (coil 3 = 118 cm) with PDs 90 and 180 and GEM-2 with a 38-kHz frequency (the coil separation is 166 cm). The CMD Mini-explorer at VCP configuration was represented with ECa-L and at HCP configuration was represented with ECa-H, while GEM-2 at HCP configuration was represented with ECa-38kHz. The surveys with CMD Mini-explorer were carried at a height of 15 cm above ground, while the GEM-2 device was carried with the supplied shoulder strap at an average height of 100 cm above the ground.

Four gridded ECa surveys were conducted in fall 2016 (Sept 22, Sept 30, Oct. 6, and Oct. 30) across the study area of 45 m x 8.5 m. To ensure high data quality, both sensors were allowed a warm up period of at least 30 min before measurements (Robinson et al., 2004), even though, no instrumental drift was expected in the ECa due to the high temperature stability of the CMD Mini-explorer and GEM-2 (Allred et al., 2005; GF Instruments, 2011).

Additionally, the CMD Mini-explorer coil 3 dipole configuration adopted for the study showed the highest local sensitivity between 35 and 75 cm depth according to the sensitivity function by McNeil (1980), which provides a reasonable match between the sensing volume of EMI and the depth range sampled by the HD2-TDR precision soil moisture probe (IMKO, 2016). The largest coil separation in VCP orientation was also less sensitive to variations in instrument height that inevitably occur when EMI measurements was carried out.

3.2.3 Soil sample collection and analysis

Soil samples were collected using a gauge auger and a hammer, in a depth range of 0 − 20 cm. The soil was characterized for SMC, texture, pH, electrical conductivity of extract ($ECw_{(1:2)}$), AWC and soil organic matter (SOM). Standard soil analyses were employed (Gregorich and Carter, 2008). Particle size analysis was evaluated with the hydrometer method, while SMC was measured both gravimetrically (θ_g), by oven drying (OD), and in the field with a 16 cm HD2-TDR probe (θ_v). Soil $ECw_{(1:2)}$ and pH was measured with a portable EC meter (HI9813-6 Portable pH/EC/TDS/Temperature Meter with CAL Check). AWC were estimated using the soil moisture characteristic curve developed with a pressure plate extractor and fitted with the van Genuchten (1980) equation. Readings from 0.2 bar to 7 bar for θ_v were collected with the pressure plate extractor, while the remaining readings, between 0 bar to 0.2 bar, were randomly input at 0.01, 0.02, 0.03, 0.04, 0.05, 0.06, 0.07, 0.08, 0.09, 0.10, 0.125, 0.150 and 0.175 bars before fitting the van Genuchten (1980) model. The porosity values were taken as the saturated θ_v at 0 bar. Since the soil is sandy, AWC was accounted for between 0.1 bar (field capacity) to 15 bar (permanent wilting point) (see appendix 5).

3.2.4 Data analysis

ECa and other soil properties measurements were interpolated across 20 sampling locations (Fig. 3.1) on the study field using block kriging in Surfer 8 (Golden Software Inc., USA) to generate the map for the study area. The linear and spherical variogram models were used to analyze the spatial pattern of the ECa and other soil properties, respectively, also using Surfer 8.

The nugget/sill ratio concept, as described by Zhu et al. (2010), was used to assess the variation in soil properties and the measurement errors of the interpolated soil properties values. Greater variation in soil properties is demonstrated with a higher sill or shorter correlation length (Range), while measurement error was indicated with the nugget, the height of the variogram at the origin (lag 0).

The temporal stability analysis of ECa and SMC were determined similar to Pedrera-Parrilla et al. (2017) using the relative differences (RD), the mean of the relative differences (MRD) and the standard deviation of the relative differences (SDRD), respectively by Eq. 3.1, Eq. 3.2 and Eq. 3.3 as proposed by Vachaud et al. (1985).

$$RD_{ij} = \left(X_{ij} - (X)_j\right)/(X)_J, \quad (3.1)$$

$$\mathrm{MRD_i} = \frac{1}{\mathrm{N}}\sum_{j=1}^{j=N} RD_{ij} \quad (3.2)$$

$$\mathrm{SDRD}_i = \sqrt{\frac{1}{\mathrm{N}-1}\sum_{\mathrm{j}=1}^{\mathrm{j}=\mathrm{N}}(\mathrm{RDij} - \mathrm{MRDi})^2} \tag{3.3}$$

where *i* stands for location, *j* for the survey number, *X* for ECa or SMC, *Xi* for the spatial average, and *N* for the number of surveys.

For analysis, the ECa data from ECa-L, ECa-H and ECa-38kHz EMI surveys and SMC measured at the 20 locations during the 4 surveys were used. Positive or negative MRD indicates that the location *i* has greater or smaller ECa/SMC than the average of the study area, respectively. The SDRD is the temporal stability of ECa/SMC at location *i*. Greater SDRD indicates temporal unstability, while small SDRD means temporally stable. The maps of ECa MRD and SDRD were thus generated. The MRD and SDRD of ECa were then statistically compared with the SMC.

The descriptive statistics – min, max, mean, median, variance, standard deviation (SD) and coefficient of variation (CV), coefficient of determination (R^2), simple linear regression and backward stepwise multiple linear regression (MLR) were performed in Minitab 17 (Minitab 17 statistical software). Interpolated maps were generated using Surfer 8 (Golden Software, 2002).

3.3 Results

3.3.1 Interpolation and temporal stability analysis of ECa

The interpolated maps of ECa for different dates, obtained by block kriging, are shown in Figure 3.1. Generally, the spatial pattern shows ECa to be highest for ECa-H followed by ECa-L and lowest for ECa-38kHz (Fig. 3.1). With respect to the spatial pattern of ECa, the lowest ECa values (< 3.3 mS m^{-1}) are at the center of the study site (20 – 30 m North) (Fig. 3.1). Maps of ECa temporal stability are shown in Figures 3.2 and 3.3. The most negative ECa MRD can be observed at the center of the study area (generally < -0.05), while the most positive ECa MRD was found at the ends of the study area (generally > 0) (Fig. 3.2a). The variation in the ECa SDRD is shown in Figure 3.2b. ECa-L gives a large ECa SDRD (generally > 0.06) at the center of study site, while a small ECa SDRD (generally < 0.06) spreads to the ends of the study site. ECa-H gives a small ECa SDRD (generally < 0.06) at the middle area with large ECa SDRD (generally > 0.06) spreading out from the center to both ends of the study site (Fig. 3.2). ECa-38kHz gives a small ECa SDRD (generally < 0.06) of ECa on the entire study site.

3.3.2 Relationship between temporal stability of ECa and soil physical properties

The comparison of the temporal stabilities of ECa values and SMC is given in Figure 3.3. Larger ECa MRD always corresponds with the larger SMC MRD, regardless the PD in which the SMC measurements were taken (Fig. 3.3a). Similarly, locations with a great ECa SDRD (*e.g.*, > 0.06) also have a great SMC SDRD except for ECa-L (Fig. 3.3b).

Table 3.1 shows the correlation between the ECa MRD and the soil physical properties such as soil texture, AWC and bulk density. The ECa MRD (ECa-H, and ECa-38kHz) are positively correlated with silt (R^2 = 0.55 and 0.66) and negatively correlated with sand (R^2 = -0.59 and -0.73), both significant at a p-value = 0.05, with ECa-L MRD for silt and sand (R^2 = 0.47 and -0.52) significant at a p-value = 0.10 (Table 3.1). The linear relationship between the texture and MRD are shown in Figure 3.4. A significant relationship was observed between sand versus ECa-H MRD (R^2 = 0.35, p-value = 0.032), sand versus ECa-38kHz MRD (R^2 = 0.53, p-value = 0.005) and silt versus ECa-38kHz MRD (R^2 = 0.43, p-value = 0.015). However, no significant relationship between clay versus ECa MRD was observed (*e.g*. clay versus ECa-38kHz MRD, R^2 = 0.16, p-value = 0.179). The ECa MRD values are positively correlated with AWC and negatively correlated with bulk density, except for ECa-L MRD and bulk density (R^2 = -0.40), significant at a p-value = 0.10. A significant relationship was observed between AWC and ECa MRD (R^2 = 0.49 to 0.77, p-value = 0.000 to 0.008). For bulk density, only the relationship with ECa-H MRD was significant (R^2 = 0.33, p-value = 0.042).

Table 3.1 Pearson's correlation coefficients of the ECa MRD and soil texture at the study site (n = 13). Significance is reported at the 0.1 (*), 0.05 (**), and 0.001 (***) p-values for correlation.

	ECa-L MRD	ECa-H MRD	ECa-38kHz MRD	Sand	Silt	Clay	AWC	Bulk Density
ECa-L MRD	1							
ECa-H MRD	0.89^{***}	1						
ECa-38kHz MRD	0.80^{***}	0.77^{**}	1					
Sand	-0.52^{*}	-0.59^{**}	-0.73^{**}	1				
Silt	0.47^{*}	0.55^{**}	0.66^{**}	-0.98^{**}	1			
Clay	0.29	0.25	0.40	-0.08	-0.09	1		
AWC	0.88***	0.70***	0.78***	-0.52*	0.45	0.40	1	
Bulk Density	-0.40	-0.57^{*}	-0.49^{*}	0.33	-0.33	0.02	-0.36	1

3.3.3 Influence of soil properties on ECa

The simple linear regression analysis (Table 3.2) indicates that only θ_v had a significant relationship with ECa, thus confirming SMC as the dominant factor influencing ECa variability of the soil at the study site. The step-wise MLR shows there is a slight increase in the R^2 when all, θ_v, sand, $ECw_{(1:2)}$ and pH are compared with ECa versus when the soil properties were considered individually or in two with θ_v (Table 3.2). The MLR of sand, $ECw_{(1:2)}$ and pH without θ_v is not significant at $p = 0.05$.

Table 3.2 Simple and step wise MLR analysis between ECa data of CMD Mini-explorer and GEM-2 and θ_v at the study site to show the influence of soil properties on ECa measurements. Significance is reported at 0.05 (*) p-value (n=20)

Selected variable	ECa-L	ECa-H	ECa-38kHz
	Simple Linear Regression		
θ_v	0.74*	0.47*	0.25*
Sand	0.15	0.11	0.009
pH	0.07	0.03	0.002
$EC_{1:2}$	0.08	0.08	0.14
	Stepwise Multiple Linear Regression		
θ_v+ Sand	0.77*	0.50*	0.29
θ_v + pH	0.78*	0.52*	0.31*
θ_v + pH+ Sand	0.80*	0.53*	0.33
θ_v + $EC_{1:2}$	0.75*	0.47*	0.28
θ_v + pH + $EC_{1:2}$	0.79*	0.52*	0.38*
θ_v + Sand + $EC_{1:2}$	0.77*	0.50*	0.36
θ_v + Sand + pH + $EC_{1:2}$	0.80*	0.55*	0.44
Sand + pH + $EC_{1:2}$	0.31	0.26	0.34

The MLR using stepwise backward elimination on the selected soil properties (see Appendix 3) determination at the study site shows sand, silt, bulk density, AWC and SMC as the factors influencing ECa at the study site (Table 3.3). The equations generated after MLR were used to predict the soil properties using measured ECa values. The descriptive statistics for the measured and the predicted soil properties using ECa are presented in

Table 3.4. Means for measured and ECa predicted soil properties are almost the same, while the measured SD and CV are higher than the predicted values with ECa. For instance, for measured and predicted silt; mean = 15.27 and 15.28, SD = 6.38 and 4.22, variance = 40.70 and 17.78, CV = 41.77 and 27.61, respectively (Table 3.4).

Table 3.3 The MLR models for different soil properties after backward stepwise MLR with R^2, adjusted R^2 and p-value (n = 13).

Soil property	Equation	R^2	R^2 adjusted	p-value
Sand	114.8 - 8.66 ECa-H	0.53	0.49	0.005
Silt	-17.6 + 7.84 ECa-H	0.44	0.38	0.014
SMC	-0.0130 + 0.0540 ECa-L	0.35	0.29	0.032
Bulk Density	1.650 - 0.0791 ECa-H	0.34	0.28	0.038
AWC	0.0838 + 0.05321 ECa-L	0.77	0.75	0.000

Table 3.4 Descriptive statistics of measured and ECa predicted soil properties (n = 13).

Soil property	Observations	Min	Max	Median	Mean	Variance	SD	CV
SMC (m^3m^{-3})	Measured	0.13	0.22	0.19	0.18	0.00	0.03	17.82
	Predicted	0.14	0.20	0.19	0.18	0.00	0.02	9.96
Sand (%)	Measured	68.10	87.88	81.16	78.47	40.64	1.77	8.12
	Predicted	72.50	84.92	76.70	78.49	21.70	1.29	5.94
Silt (%)	Measured	7.52	25.30	12.92	15.27	40.70	6.38	41.77
	Predicted	9.45	20.69	16.90	15.28	17.78	4.22	27.61
Bulk Density ($g\ cm^{-3}$)	Measured	1.20	1.47	1.34	1.32	0.01	0.07	5.56
	Predicted	1.26	1.38	1.30	1.32	0.00	0.04	3.26
AWC ($m^3\ m^{-3}$)	Measured	0.24	0.31	0.29	0.27	0.00	0.02	7.81
	Predicted	0.23	0.30	0.28	0.27	0.00	0.02	6.86

3.3.4 Spatial variability of soil properties influencing ECa

Interpolation of maps of measured soil properties and ECa predicted soil properties as a result of MLR were carried out using block kriging in Surfer 8. The plotted experimental variogram fitted (see Appendix 4) with the spherical model for the soil properties show zero nugget with different parameter fittings of semivariogram (Table 3.5). Figure 3.5 shows the trend and pattern of both measured and ECa predicted soil properties. The trend of the prediction shows lower spatial variability of the soil properties than measured.

Table 3.5 Different parameters of the fitted model of semivariogram for selected soil properties.

Soil property	Observations	Type of model	Range	Nugget	Sill	Nugget as % of sill	Spatial dependence
SMC	Measured	Spherical	4.8	0	0.00062	0	Strong
	Predicted	Spherical	6	0	0.00015	0	Strong
Sand	Measured	Spherical	5	0	11.9	0	Strong
	Predicted	Spherical	10	0	4.5	0	Strong
Silt	Measured	Spherical	6.5	0	6	0	Strong
	Predicted	Spherical	10	0	3.5	0	Strong
Bulk Density	Measured	Spherical	6	0	0.0047	0	Strong
	Predicted	Spherical	9	0	0.00036	0	Strong
AWC	Measured	Spherical	2	0	0.0002	0	Strong
	Predicted	Spherical	5	0	0.00015	0	Strong

3.4 Discussion

Liao Liao et al. (2014) observed a moderate spatial dependence of ECa based on the nugget/sill ratio of variogram analysis for spatial dependence classification of variables (Zhu and Lin, 2010). However, in this study, for high quality analysis, the experimental variogram for each measuring day was calculated for the temperature corrected interpolated ECa and fitted using a linear model. The use of the linear variogram models was decided due to a linear behaviour at larger lag distances with zero nugget by all experimental variograms (Appendix 4). The zero-nugget effect implies that the spatial variability of ECa is well resolved and that there is minimal measurement error of the interpolated ECa values (Liao et al., 2014).

The variation in EMI- ECa can be attributed to their different PD of measurements (Allred et al., 2005; Von Hebel et al., 2014; Altdorff et al., 2016). In this study, the spatial patterns of the soil ECa on different days were consistent, which could be attributed to the fact that the distribution of soil ECa was largely controlled by differences in relatively stable soil properties (*e.g.* particle size distribution) (Zhu et al., 2010). Similar to Liao et al. (2014), visual observations at the site show that the soil is much more gravelly sand, which implies the soil in the area has low clay. Also, at the ends of the study site, with the lowest elevation points, had the greatest ECa values (Fig. 3.1). Furthermore, Sherlock and McDonnell (2003) also showed the greatest ECa values with high water table, while Zhu and Lin (2009) established the soil ECa to be temporally unstable in humid areas. This implies that temporal variations in soil ECa at the study site can be attributed to the dynamics of SMC and related soil water movement (Liao et al., 2014).

A temporal stability analysis proposed by Vachaud et al. (1985) has been widely used to study the temporal persistence of spatial patterns of soil properties such as SMC and ECa. Liao et al. (2014) observed that high soil ECa values corresponded to areas with temporally unstable ECa and vice versa. However, this is not the case with these results (Fig. 2 and 3), which show that low soil ECa values corresponded to areas with temporally unstable ECa (*e.g.* the center of the study area, 20 -30 m North) and vice versa. In addition, according to Vachaud et al. (1985), It can also deduce that the first 20 m north of the area is suitable for representing the entire area for future measurement of soil ECa in the region, since this area had relative differences of ECa close to zero and small SD. The variation in the temporal stability between ECa-L (> 0.06) compared with ECa-H and ECa-38kHz (< 0.06) at the center of the study area is best explained by the low clay content at the PDs of measurement, parent material (reddish brown sandy fluvial deposit of mixed lithology) and depth to bedrock (<100 cm) (Kirby, 1988).

According to a general consensus in the literature, soil ECa values are affected by a few soil properties including clay content (King et al., 2005; Cockx et al., 2009), depth to the bedrock (Mueller et al., 2003), SMC (Korsaeth et al., 2008; Tromp-van Meerveld and McDonnell, 2009), salinity (Mankin and Karthikeyan, 2002; Williams et al., 2006), and soil organic matter (SOM) (Huang et al., 2017). However, Liao et al. (2014) assumed that the clay content, depth to the bedrock, salinity, and SOM are temporally more stable than SMC, as SMC is strongly affected by temporally unstable weather factors including evapotranspiration and precipitation. The authors further observed that the temporal variations of soil ECa values can reflect the temporal change of SMC assuming that the soil properties other than SMC were stable during the period of measurements. Similarly, these results showed that other soil properties are relatively stable, while SMC as the major controlling factor (Table 3.1). Temporal variations of soil ECa values therefore can also reflect the temporal change of SMC (ECa-L, $R^2 = 0.42$, $p = 0.00$) even though not significant for ECa-H and ECa-38kHz ($R^2 = 0.05$ and 0.02 $p = 0.33$ and 0.59, respectively) (Fig. 3.3b). In addition, the temporal variation of soil ECa measured from repeated EMI surveys from September to October 2016 can reflect the temporal variation of SMC during this period (Fig. 3.3), which was correspondence to the local precipitation data (data not shown). Also, the soil ECa at unstable sites is similar to the SMC at unstable sites (Fig. 3.3b).

Reports by several authors established that the spatial patterns of SMC are temporally persistent (*e.g.* Vachaud et al., 1985; Mohanty and Skaggs 2001; Grant et al., 2004; Pachepsky et al., 2005; Lin, 2006), which implies that spatial patterns of SMC measured at different days can be used to represent the spatial patterns of SMC on days with ECa measurements but no SMC measurements (Liao et al., 2014). However, SMCs used in this study were measured on the same day where the soil ECa data collections were also carried out. Also, Liao et al. (2014) observed that there was no significant correlation ($p < 0.05$) and regression with great R^2 values (*e.g.*, > 0.6) between soil ECa values and SMC. However, in this study, there is a significant correlation ($p < 0.05$) and regression with great R^2 values (*e.g.*, 0.74) between soil ECa values and SMC (Table 3.2).

Furthermore, numerous studies have documented the potential for using soil ECa values to interpret the SMC (*e.g.* Sherlock and McDonnell, 2003; Reedy and Scanlon, 2003), while others (*e.g*. Kachanoski et al., 1990; Sudduuth et al., 2003) reported lack of success. Sherlock and McDonnell (2003) reported that soil ECa measurements using EM38 vertical dipole mode could explain over 70% of the gravimetrically determined soil-moisture variance. Kachanoski et al. (1990) found that soil ECa measured by EM38 and SMC were not correlated at scales < 40 m. Nevertheless, in this study, ECa-L could explain over 70% of the HD2-TDR 16 cm probe measurement, while ECa-H and ECa-38kHz could explain over 40% and 30%, respectively (Table 3.2).

The significant negative correlation between sand vs. ECa MRD ($R = -0.52$ to -0.73, $R^2 = 0.35$ to 0.53) shown in Table 3.1 and Figure 3.2a implies that ECa MRD decreases with increasing sand content. The positive significant correlation between silt vs ECa MRD ($R = 0.47$ to 0.66, $R^2 = 0.30$ to 0.43) shown in Table 3.1 and Figure 3.3b implies that ECa MRD increases with increasing silt content. Similarly, Laio et al. (2014) reported a positive relationship between silt and ECa ($R^2 = 0.47$). Furthermore, Heil and Schmidhalter (2015) found a significant relationship between soil texture and ECa with adjusted R^2 ranging from 0.16 to 0.85, with silt having the lowest adjusted R^2. This is similar to this study where the adjusted R^2 ranged between 0.28 to 0.49 (Table 3.3), even though no significant relationship with clay was found.

Fortes et al. (2015) reported a significant relationship between AWC and ECa (R^2 = 0.67 to 0.70). Hedley and Yule (2009) also reported a significant relationship between AWC and ECa (R^2 = 0.8). Likewise, this study reported positive significant relationship of AWC vs. ECa MRD (R^2 = 0.49 to 0.77), which implies that ECa MRD increases with increasing AWC. Also, the negative significant correlation between bulk density vs ECa MRD (R^2 = 0.24 to 0.33, p-value = 0.042 to 0.180) implies that ECa MRD decreases with increasing bulk density.

Souza et al. (2009) showed high spatial dependence and spherical model fitting with low nugget effect for soil property variables such as clay, silt, sand and bulk density. Pandey and Pandey (2010) also showed high spatial dependence for SMC, while Fortes et al. (2015) found the same for AWC. This is similar to this study, with high spatial dependence and spherical model fit even though without nugget effect (Table 3.5). Generally, the ECa predicted soil properties have lower sill and longer range (correlation length) than measured soil properties (Fig. 3.5), which implies reduction in the spatial variability, more consistency and reliability of the maps (Pandey and Pandey, 2010). The lower value of the CV (3.26 to 27.61) for ECa predicted soil properties (Table 3.4) indicates there have been consistency in the kriging estimates. The zero-nugget observed (Table 3.5) implies strong spatial dependence and no error of estimation of parameters at the smallest sampling interval. In relation to the above discussion, contour maps developed with ECa predicted soil properties would be more precise than those developed with measured soil properties.

3.5 Conclusions

The spatial pattern of ECa can be used to determine the spatial pattern of SMC. The temporal variation of ECa can be related to SMC, soil texture, bulk density, and AWC. The relationship between the MRD of ECa versus sand and silt were explored with significant correlations observed. The backward elimination MLR were sufficient to identify and derive the equation for the ECa predicted soil properties. The addition of variables such as topography can improve the correlation of the soil properties, which was not carried out in this study. Based on findings of this study, it can be stated that ECa predicted soil properties are more consistent and representative of soil properties values. The ECa predicted soil properties can help in site specific agronomic management, especially fertilizer application or irrigation, which are fundamental components of precision agriculture.

3.6 Acknowledgments

Financial supports from Research and Development Corporation, NL (RDC-Ignite) for field research and Research Office of Grenfell Campus, Memorial University of Newfoundland for equipment purchase are greatly appreciated. An MSc-BEAS graduate fellowship from Memorial University to E. Badewa, and data-collection support by Marli Vermooten, Dinushika Wanniarachchi and Kamaleswaran Sadatcharam are acknowledged.

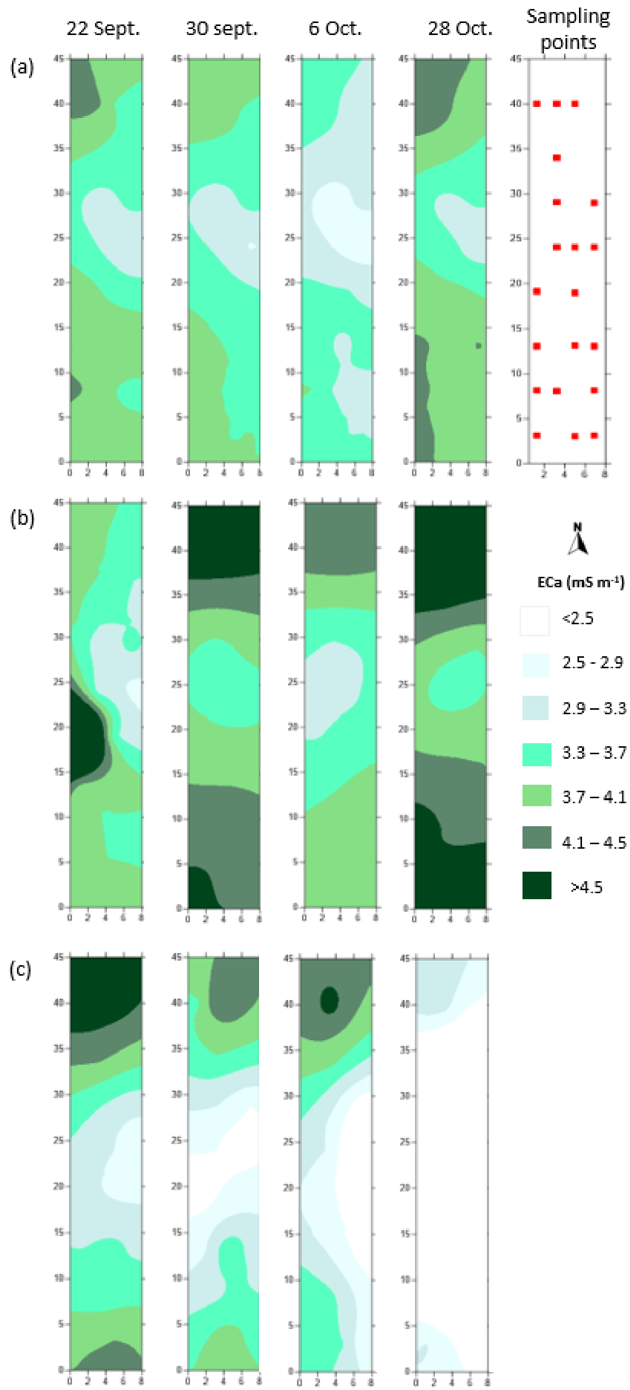

Figure 3.1 Sampling points and interpolated soil ECa maps for ECa measurements on 22 Sept., 30 Sept., 6 Oct. and 28 Oct., 2016 (a) ECa-L (b) ECa-H (c) ECa-38kHz.

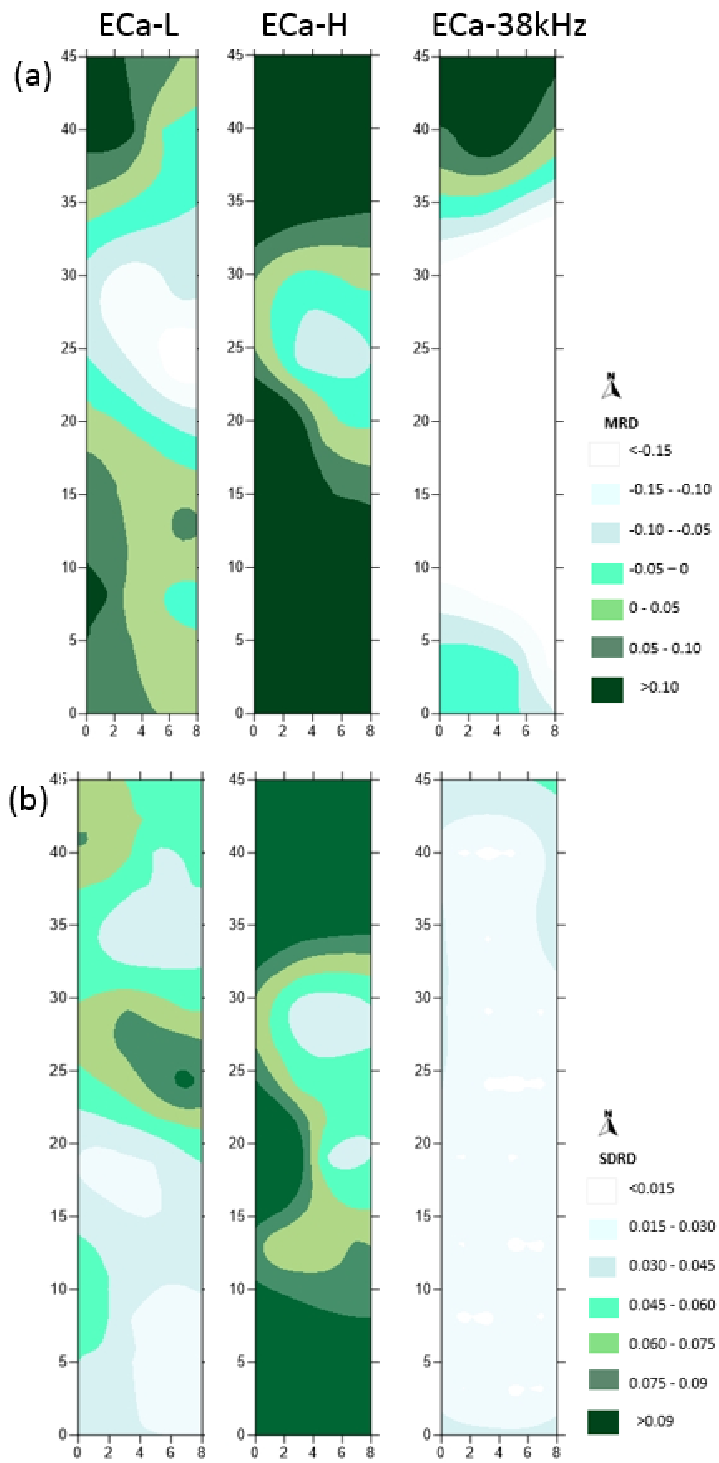

Figure 3.2 Maps of ECa measurements (a) MRD of soil ECa and (b) SDRD of soil ECa.

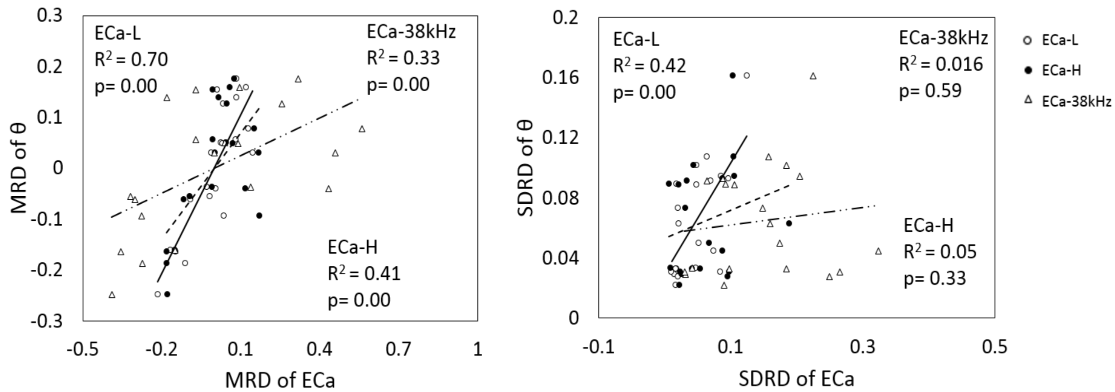

Figure 3.3 The temporal stability of soil apparent electrical conductivity (ECa) for CMD Mini-explorer and GEM-2 surveys in 2016 using (a) SMC MRD vs ECa MRD (B) SMC SDRD vs ECa SDRD.

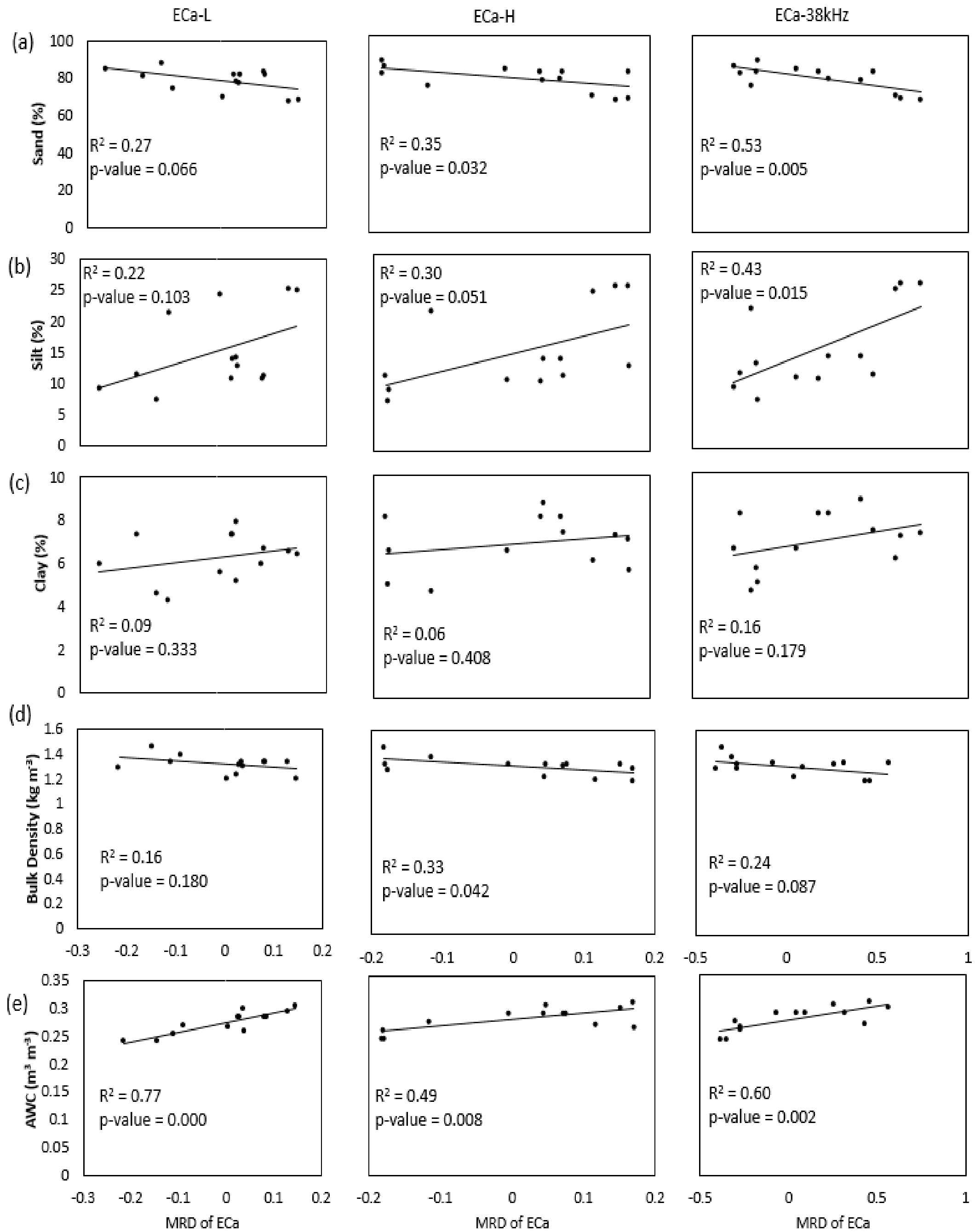

Figure 3.4 The relationship between ECa MRD and (a) sand (b) silt (c) clay (d) Bulk density (e) AWC.

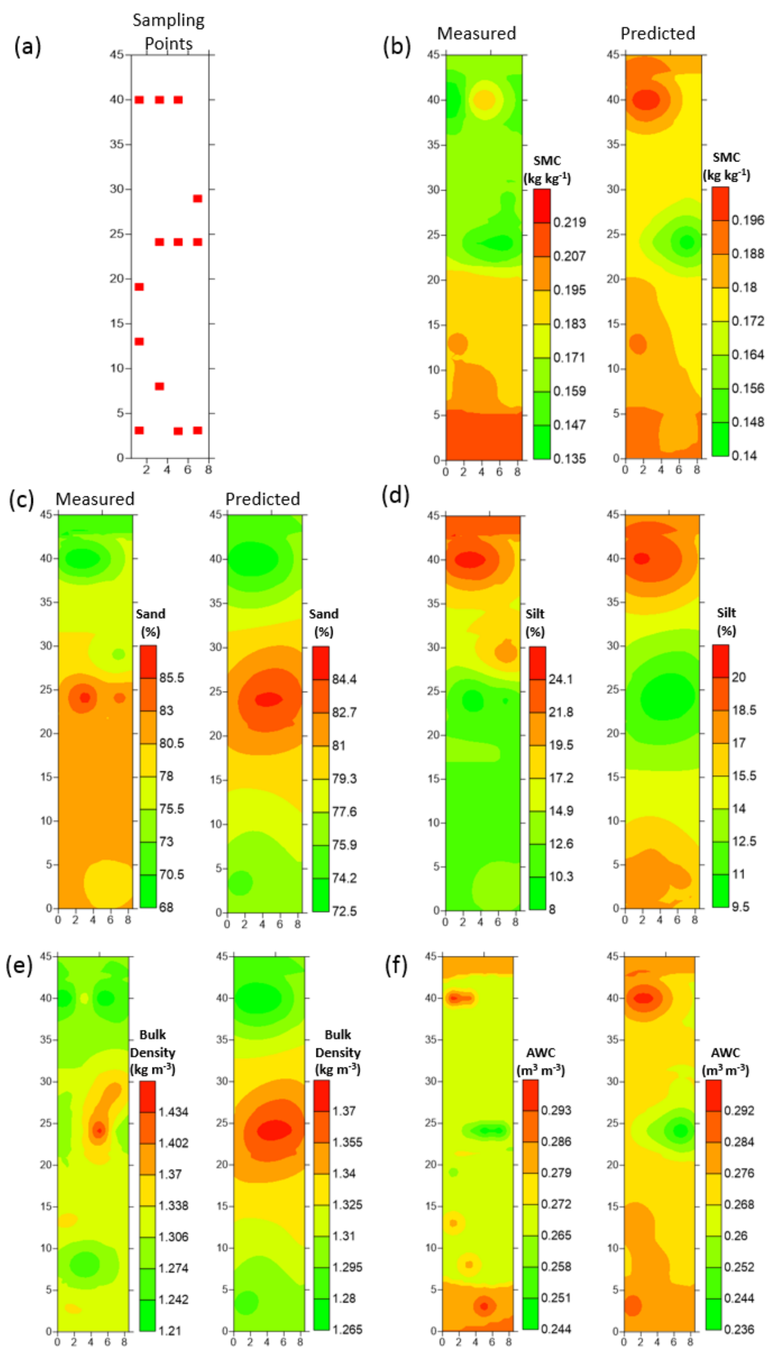

Figure 3.5 Measured and predicted interpolated maps (a) sampling points, (b) SMC (c) sand (d) silt (e) bulk density (f) AWC.

3.7 References

Allred, B. J., Ehsani, M. R., & Saraswat, D. (2005). The Impact of Temperature and Shallow Hydrologic Conditions on The Magnitude and Spatial Pattern Consistency of Electromagnetic Induction Measured Soil Electrical Conductivity. *American Society of Agricultural Engineers,* 48(6), 2123–2135.

Altdorff, D., Bechtold, M., van der Kruk, J., Vereecken, H., & Huisman, J. A. (2016). Mapping peat layer properties with multi-coil offset electromagnetic induction and laser scanning elevation data. *Geoderma,* 261, 178–189.

Altdorff, D., von Hebel, C., Borchard, N., van der Kruk, J., Bogena, H. R., Vereecken, H., & Huisman, J. A. (2017). Potential of catchment-wide soil water content prediction using electromagnetic induction in a forest ecosystem. *Environmental Earth Sciences,* 76(3), 111.

Brevik E. C., Calzolari C., Miller B. A., Pereira P., Kabala C., Baumgarten A., & Jordán A. (2016). Soil mapping, classification, and modeling: history and future directions. *Geoderma*, 264, 256-274.

Calamita, G., Perrone, A., Brocca, L., Onorati, B., & Manfreda, S. (2015). Field test of a multi-frequency electromagnetic induction sensor for soil moisture monitoring in southern Italy test sites. *Journal of Hydrology*, 529, 316-329.

Corwin, D. L. (2008). Past, present, and future trends in soil electrical conductivity measurements using geophysical methods. *In: Allred, B.J., Daniels, J.J., Ehsani, M.R. (Eds.), Handbook of Agricultural Geophysics.* CRC Press, Taylor and Francis Group, Boca Raton, Florida, pp. 17–44.

Doolittle, J. A., & Brevik, E. C. (2014). The use of electromagnetic induction techniques in soils studies. *Geoderma*, 223, 33–45.

Fortes, R., Millán, S., Prieto, M. H., & Campillo, C. (2015). A methodology based on apparent electrical conductivity and guided soil samples to improve irrigation zoning. *Precision Agriculture*, 16(4), 441–454.

Geophex Ltd., 2004. GEM-2 User's Manual, *Version 3.8.* Geophex Ltd., Raleigh, USA. Available at: http://www.geophex.com/Downloads/GEM-2%20Operator's%20Manual.pdf.

GF Instruments., 2011. CMD Electromagnetic conductivity meter user manual *V. 1.5.* Geophysical Equipment and Services, Czech Republic Available at: http://www.gfinstruments.cz/index.php?menu=gi&smenu=iem&cont=cmd_&ear=ov.

Grant, L., Seyfried, M., & McNamara, J. (2004). Spatial variation and temporal stability of soil water in a snow-dominated, mountain catchment. *Hydrological Processes*, 18(18), 3493-3511.

Gregorich, E. G., & Carter, M. R. (2008). Soil Sampling and Methods of Analysis (second ed) Canadian Society of Soil Science. CRC Press: Boca Raton, FL, USA.

Hedley, C. B., & Yule, I. J. (2009). Soil water status mapping and two variable-rate irrigation scenarios. *Precision Agriculture*, *10*(4), 342-355.

Heil, K., & Schmidhalter, U. (2012). Characterisation of soil texture variability using the apparent soil electrical conductivity at a highly variable site. *Computers and geosciences*, 39, 98-110.

Heil, K., & Schmidhalter, U., (2015). Comparison of the EM38 and EM38-MK2 electromagnetic induction-based sensors for spatial soil analysis at field scale. *Computers and Electronics in Agriculture*, 110, 267-280.

Huang, H. H., Adamchuk, V. I., Boiko, I. I., & Ferguson, R. F. (2013). Effect of sampling patterns and interpolation methods on prediction quality of soil variability mapping. *In Precision agriculture'13 (pp. 243-250).* Wageningen Academic Publishers, Wageningen.

Huang, J., Pedrera-Parrilla, A., Vanderlinden, K., Taguas, E. V., Gómez, J. A., & Triantafilis, J. (2017). Potential to map depth-specific soil organic matter content across an olive grove using quasi-2d and quasi-3d inversion of DUALEM-21 data. *Catena,* 152, 207-217.

Kachanoski, R. G., Wesenbeeck, I. V., Jong, E. D. (1990). Field scale patterns of soil water storage from non-contacting measurements of bulk electrical conductivity. *Canadian Journal of Soil Science, 70*(3), 537-542.

King, J. A., Dampney, P. M. R., Lark, R. M., Wheeler, H. C., Bradley, R. I., & Mayr, T. R. (2005). Mapping potential crop management zones within fields: use of yield-map series and patterns of soil physical properties identified by electromagnetic induction sensing. *Precision Agriculture* 6(2), 167-181.

Kirby, G. E. (1988). Soils of the Pasadena-Deer Lake area, Newfoundland. St. John's. *Retrieved from http://sis.agr.gc.ca/cansis/publications/surveys/nf/nf17/nf17_report.pdf*

Korsaeth, A., Riley, H., Kværnø, S. H., & Vestgarden, L. S. (2008). Relations between a Commercial Soil Survey Map Based on Soil Apparent Electrical Conductivity (ECa) and Measured Soil Properties on a Morainic Soil in Southeast Norway. *Handbook of Agricultural Geophysics (Eds. Barry J. Allred, Jeffrey J. Daniels, and M. Reza Ehsani), pp.225-231.*

Liao, K. H., Zhu, Q., & Doolittle, J. (2014). Temporal stability of *apparent soil electrical conductivity measured by electromagnetic induction techniques. Journal of Mountain Science,* 11(1), 98.

Lin, H. (2006). Temporal stability of soil moisture spatial pattern and subsurface preferential flow pathways in the Shale Hills Catchment. *Vadose Zone Journal, 5*(1), 317-340.

Mankin, K. R., & Karthikeyan, R. (2002). Field assessment of saline seep remediation using electromagnetic induction. *Transactions of the American Society of Agricultural and Biological Engineers,* 45(1), 99.

Martínez, G., Vanderlinden, K., Giráldez, J. V., Espejo, A. J., & Muriel, J. L. (2010). Field-scale soil moisture pattern mapping using electromagnetic induction. *Vadose Zone Journal,* 9(4), 871-881.

McNeill, J. D. (1980). Electromagnetic terrain conductivity measurement at low induction numbers. *(Geonics Ltd., Mississauga, Ontario, Canada, Technical Note TN-5).*

Mohanty, B. P., & Skaggs, T. H. (2001). Spatio-temporal evolution and time-stable characteristics of soil moisture within remote sensing footprints with varying soil, slope, and vegetation. *Advances in water resources*, 24(9), 1051-1067.

Mueller, T. G., Hartsock, N. J., Stombaugh, T. S., Shearer, S. A., Cornelius, P. L., Barnhisel, R. I. (2003). Soil electrical conductivity map variability in limestone soils overlain by loess. *Agronomy Journal,* 95(3), 496-507.

Neely, H. L., Morgan, C. L., Hallmark, C. T., McInnes, K. J. & Molling, C. C. (2016). Apparent electrical conductivity response to spatially variable vertisol properties. *Geoderma, 263,* 168-175.

Pachepsky, Y. A., Guber, A. K., & Jacques, D. (2005). Temporal persistence in vertical distributions of soil moisture contents. *Soil Science Society of America Journal,* 69(2), 347-352.

Pandey, V., & Pandey, P. K. (2010). Spatial and temporal variability of soil moisture. *International Journal of Geosciences,* 1(02), 87.

Pedrera-Parrilla, A., Pachepsky, Y. A., Taguas, E. V., Martos-Rosillo, S., Giráldez, J. V., Vanderlinden, K. (2017). Concurrent temporal stability of the apparent electrical conductivity and soil water content. *Journal of Hydrology,* 544, 319-326.

Reedy, R. C., & Scanlon, B. R. (2003). Soil water content monitoring using electromagnetic induction. *Journal of Geotechnical and Geoenvironmental Engineering,* 129(11), 1028-1039.

Robinson, D. A., Lebron, I., Lesch, S. M., & Shouse, P. (2004). Minimizing drift in electrical conductivity measurements in high temperature environments using the EM-38. *Soil Science Society of America Journal,* 68(2), 339-345.

Rossi, R. E., Dungan, J. L., & Beck, L. R. (1994). Kriging in the shadows: geostatistical interpolation for remote sensing. *Remote Sensing of Environment*, 49(1), 32-40.

Serrano, J., Shahidian, S., & Silva, J. M. D. (2014). Spatial and temporal patterns of apparent electrical conductivity: DUALEM vs. Veris sensors for monitoring soil properties. *Sensors,* 14(6), 10024-10041.

Sherlock, M. D., & McDonnell, J. J. (2003). A new tool for hillslope hydrologists: spatially distributed groundwater level and soil water content measured using electromagnetic induction. *Hydrological Processes,* 17(10), 1965-1977.

Shibusawa, S. (2006). Soil Sensors for Precision Farming. *In Handbook of Precision Agriculture, Principles and Applications; Srinivasan, A., Ed.; The Haworth Press: New York, NY, USA,* pp. 57–90.

Soil Classification Working Group. (1998). The Canadian System of Soil Classification. *The Canadian System of Soil Classification, 3rd ed. Agriculture and Agri-Food Canada Publication* 1646. NRC Research Press.

Soil Survey Standard Test Method: Organic Carbon. (n.d). *Retrieved from http://www.environment.nsw.gov.au/resources/soils/testmethods/oc.pdf.*

Souza, Z. M. D., Marques Júnior, J., & Pereira, G. T. (2009). Spatial variability of the physical and mineralogical properties of the soil from the areas with variation in landscape shapes. *Brazilian Archives of Biology and Technology*, 52(2), 305-316.

Sudduth, K. A., Kitchen, N. R., Bollero, G. A., Bullock, D. G., & Wiebold, W. J. (2003). Comparison of electromagnetic induction and direct sensing of soil electrical conductivity. *Agronomy Journal,* 95(3), 472-482.

Toushmalani, R. (2010). Application of geophysical methods in agriculture. Australian Journal of *Basic and Applied Sciences*, 4(12), 6433–6439.

Tromp-van Meerveld, H. J., & McDonnell, J. J. (2009). Assessment of multi-frequency electromagnetic induction for determining soil moisture patterns at the hillslope scale. *Journal of Hydrology*, 368(1), 56-67.

Vachaud, G., Passerat de Silans, A., Balabanis, P., & Vauclin, M. (1985). Temporal stability of spatially measured soil water probability density function. *Soil Science Society of America Journal*, 49(4), 822-828.

Van Arkel, Z., & Kaleita, A.L. (2014). Identifying sampling locations for field-scale soil moisture estimation using K-means clustering. *Water Resources Research,* 50(8), 7050-7057.

Van Genuchten, M.T. (1980). A closed-form equation for predicting the hydraulic conductivity of unsaturated soils. *Soil Science Society of America Journal*, 44(5), 892-898.

von Hebel, C., Rudolph, S., Mester, A., Huisman, J.A., Kumbhar, P., Vereecken, H., & van der Kruk, J. (2014). Three-dimensional imaging of subsurface structural patterns using quantitative large-scale multiconfiguration electromagnetic induction data. *Water Resources Research,* 50(3), 2732-2748.

White, M.L., Shaw, J.N., Raper, R.L., Rodekohr, D., & Wood, C.W. (2012). A multivariate approach for high-resolution soil survey development. *Soil science*, 177(5), 345-354.

Williams, B., Walker, J., & Anderson, J. (2006). Spatial variability of regolith leaching and salinity in relation to whole farm planning. *Australian Journal of Experimental Agriculture,* 46(10), 1271-1277.

Won, I. J. (1980). A wide-band electromagnetic exploration method—Some theoretical and experimental results. *Geophysics,* 45(5), 928–940.

Zhu, Q., & Lin, H. S. (2009). Simulation and validation of concentrated subsurface lateral flow paths in an agricultural landscape. *Hydrology and Earth System Sciences,* 13(8), 1503-1518.

Zhu, Q., & Lin, H. S. (2010). Comparing ordinary kriging and regression kriging for soil properties in contrasting landscapes. *Pedosphere,* 20(5), 594-606.

Zhu, Q., Lin, H., & Doolittle, J. (2010). Repeated electromagnetic induction surveys for determining subsurface hydrologic dynamics in an agricultural landscape. *Soil Science Society of America Journal,* 74(5), 1750-1762.

CHAPTER 4

4.0 GENERAL DISCUSSION AND CONCLUSION

4.1 General discussion

Multi-coil and multi-frequency non-invasive EMI sensors provide high resolution field scale ECa measurements, due to their multiple DOE, rapid response, non-destructive and large-scale mapping ability of collecting georeferenced data connecting with a GPS. ECa measurements can be correlated with spatio-temporal variability of soil properties because of the influence of several factors such as SMC, AWC, temperature, clay content and bulk density. The EMI sensors measure the ECa through the transmission of a low frequency (kHz) electromagnetic field into the soil subsurface so as to induce current loops that is proportional to the soil subsurface's electrical properties. The current loops in turn induce secondary magnetic field loops, which makes headway back the total field to the receiver of the instrument. Multi-coil such as CMD Mini-explorer operates at a 30kHz frequency with one transmitter and three receiver coils that can be oriented in the vertical and horizontal dipole orientation while multi-frequency sensors such as GEM-2 operates between 30 Hz to about 93 kHz with one transmitter and receiver coil that can also be oriented in the vertical and horizontal dipole orientation. According to time laps EMI data, the range of ECa on the study site is low ($0 \sim 7$ mS m^{-1}). The DOE of CMD Mini-explorer is known, while that of GEM-2 is yet unknown even though it can sense deeper than CMD Mini-explorer.

EMI surveys were carried out on a small study field (45 m to 8.5 m) with 0.7m interval gridded lines, while the large study field (0.45 ha) was carried out with a GPS for georeferenced ECa measurements. The data quality of EMI survey with gridded lines is less noisy than GPS connected ECa data. This can be attributed to instability of the GPS when the survey was carried out and comparatively smaller survey area related to the accuracy of the GPS.

Furthermore, gridded ECa measurements were collected in four different days using CMD Mini-explorer and GEM-2 on a 45 m by 8.5 m silage corn plot at PBRS, Pasadena in western Newfoundland. This was used to investigate the spatial and temporal variation of soil properties such as texture even though the use of EMI mapping is challenging in soils with low ECa. The temporal stability analysis was carried out using MRD and SDRD of ECa, after which the backward elimination MLR was used to identify the soil properties influencing ECa and the ones that ECa can predict for the study site. The comparison between the measured and ECa predicted soil properties were evaluated using spherical semivariogram model with block kriging. The ECa predicted soil properties is consistency even though the variability is low.

4.2 Conclusion

The application of ECa data from CMD Mini-explorer and GEM-2 can be used to measure the spatial and temporal variability of soil moisture in managed and unmanaged fields. A study was conducted for site specific calibration of ECa measurements from CMD Mini-explorer (multi-coil) and GEM-2 (multi-frequency) to investigate their potential in soil moisture mapping on managed podzols. The model generated for SMC prediction from CMD Mini-explorer is best for shallow prediction, while GEM-2 is best for deeper. The prediction using HD2-TDR probes is sufficiently accurate for SMC measurements and model prediction with ECa data. The study also found out that the HD2-TDR probes performance matches that of the gravimetrically determined soil moisture.

Overall, ECa measurements using multi-frequency and multi-coil EMI Sensors, CMD Mini-explorer and GEM-2 can sufficiently account for soil properties such as SMC, texture, bulk density and AWC in managed podzols.

4.3 Recommendations

The application of the study to different managed fields with various soil types and different land use systems is needful since the study was deliberately carried out on a small study area with uniform soils so has to minimize the influence of factors apart from SMC on the ECa.

Further recommendations include, but not limited to:

- Monitoring the SMC variation across the depth using the EMI sensors will further provide detailed potential of their multi depth measurement ability.
- Measurement of the terrain indices such as slope, topographic wet index (TWI) and profile curvature and depth to water table can help to

understanding the ECa influencing variables and help improve the ECa predicted soil properties.

BIBLIOGRAPHY AND REFERENCES

Allred, B. J., Ehsani, M. R., & Daniels, J. J. (2008). General considerations for geophysical methods applied to agriculture. *Handbook of Agricultural Geophysics. CRC Press, Taylor and Francis Group, Boca Raton, Florida*, 3-16.

Allred, B. J., Ehsani, M. R., & Saraswat, D. (2005). The Impact of Temperature and Shallow Hydrologic Conditions on The Magnitude and Spatial Pattern Consistency of Electromagnetic Induction Measured Soil Electrical Conductivity. *American Society of Agricultural Engineers, 48*(6), 2123–2135.

Altdorff, D., Bechtold, M., van der Kruk, J., Vereecken, H., & Huisman, J. A. (2016). Mapping peat layer properties with multi-coil offset electromagnetic induction and laser scanning elevation data. *Geoderma, 261*, 178–189.

Altdorff D, Galagedara L, & Unc A. (2017a). Impact of projected land conversion on water balance of boreal soils in western Newfoundland. *Journal of Water and Climate Change,* (In press).

Altdorff, D., von Hebel, C., Borchard, N., van der Kruk, J., Bogena, H. R., Vereecken, H., & Huisman, J. A. (2017b). Potential of catchment-wide soil water content prediction using electromagnetic induction in a forest ecosystem. *Environmental Earth Sciences*, *76*(3), 111.

Bittelli, M. (2011). Measuring soil water content: A review. *HortTechnology, 21*(3), 293-300.

Bonsall, J., Fry, R., Gaffney, C., Armit, I., Beck, A., & Gaffney, V. (2013). Assessment of the CMD Mini-Explorer, a New Low-frequency Multi-coil Electromagnetic Device, for Archaeological Investigations. *Archaeological Prospection, 20*(3), 219–231.

Brevik, E. C., Calzolari, C., Miller, B. A., Pereira, P., Kabala, C., Baumgarten, A., & Jordán, A. (2016). Soil mapping, classification, and pedologic modeling: History and future directions. *Geoderma*, *264*, 256-274.

Brevik, E. C., & Fenton, T. E. (2002). The relative influence of soil water, clay, temperature, and carbonate minerals on soil electrical conductivity readings with an EM-38 along a Mollisol catena in central Iowa. *Soil Survey Horizon*, *43*, 9–13.

Brevik, E. C., Fenton, T. E., & Lazari, A. (2006). Soil electrical conductivity as a function of soil water content and implications for soil mapping. *Precision Agriculture, 7*(6), 393–404.

Calamita, G., Perrone, A., Brocca, L., Onorati, B., & Manfreda, S. (2015). Field test of a multi-frequency electromagnetic induction sensor for soil moisture monitoring in southern Italy test sites. *Journal of Hydrology, 529*, 316-329.

Callegary, J. B., Ferré, T. P. A., & Groom, R.W. (2007). Vertical spatial sensitivity and exploration depth of low-induction-number electromagnetic induction instruments. *Vadose Zone Journal, 6*, 158–167.

Corwin, D. L., & Lesch, S. M. (2003). Application of soil electrical conductivity to precision agriculture. *Agronomy Journal, 95*(3), 455–471.

Corwin, D. L., & Lesch, S. M. (2005a). Characterizing soil spatial variability with apparent soil electrical conductivity Part II. Case study. *Computers and Electronics in Agriculture, 46*, 135–152.

Corwin, D. L., & Lesch, S. M. (2005b). Apparent soil electrical conductivity measurements in agriculture. *Computers and electronics in agriculture, 46*(1), 11-43.

Corwin, D. L., & Lesch, S. M. (2005c). Characterizing soil spatial variability with apparent soil electrical conductivity: I. Survey protocols. *Computers and Electronics in Agriculture, 46*(1), 103-133.

Corwin, D. L., Lesch, S. M., Oster, J. D., & Kaffka, S. R. (2006). Monitoring management-induced spatio–temporal changes in soil quality through soil sampling directed by apparent electrical conductivity. *Geoderma*, *131*(3), 369-387.

Corwin, D. L. (2008). Past, present, and future trends in soil electrical conductivity measurements using geophysical methods. In: *Allred, B.J., Daniels, J.J., Ehsani, M.R. (Eds.), Handbook of Agricultural Geophysics*. CRC Press, Taylor and Francis Group, Boca Raton, Florida, pp. 17–44.

Dalton, F.N. (1992). Development of time domain reflectometry for measuring soil water content and bulk soil electrical conductivity. In: Topp, G.C., Reynolds,W.D., Green, R.E. (Eds.), *Advances in Measurement of Soil Physical Properties: Bringing Theory into Practice. SSSA Spec. Publ. 30. Soil Science Society of America*, Madison, WI, USA, 143–167.

Daniels, J. J., Allred, B., Collins, M., & Doolittle, J. (2003). Geophysics in soil science. *Encyclopedia of Soil Science, Second edition. Marcel Dekker, New York*, 1-5.

Delefortrie, S., Saey, T., Van De Vijver, E., De Smedt, P., Missiaen, T., Demerre, I., & Van Meirvenne, M. (2014). Frequency domain electromagnetic induction survey in the intertidal zone: Limitations of low-induction-number and depth of exploration. *Journal of Applied Geophysics, 100*, 14-22.

Desilets, D., Zreda, M., & Ferre, T. P. A. (2010). Nature's neutron probe: Land surface hydrology at an elusive scale with cosmic rays, *Water Resource Research 46,* W11505, doi:10.1029/2009WR008726.

Dominati, E., Patterson, M., & Mackay, A. (2010). A framework for classifying and quantifying the natural capital and ecosystem services of soils. *Ecological Economics*, *69*(9), 1858-1868.

Doolittle, J. A., & Brevik, E. C. (2014). The use of electromagnetic induction techniques in soils studies. *Geoderma, 223*, 33–45.

Driessen, P., Deckers, J., Spaargaren, O., & Nachtergaele, F. (2001). Lecture notes on the major soils of the world. Food and Agriculture Organization of the United Nations. World Soil Resources Report No. 94. 334 pp.

FAO Soils Portal. (2016). Soil survey. Retrieved from http://www.fao.org/soils-portal/soil-survey/en/

FAO Soils Portal. (2017). Acid soils. Retrieved from http://www.fao.org/soils-portal/soil-management/management-of-some-problem-soils/acid-soils/en/

Ferré, P. A., Redman, J. D., Rudolph, D. L., & Kachanoski, R. G. (1998). The Dependence of the Electrical Conductivity Measured by Time Domain Reflectometry on the Water Content of a Sand. *Water Resources Research, 34*(5), 1207-1213.

Ferré, P. A., & Topp, G. C. (2002). Time domain reflectometry. In: Dane, J.H., Topp, G.C. (Eds.), Methods of Soil Analysis. Part 4. Physical Methods. *American Society of Agronomy, Madison, WI*, 434–445.

Franz, T. E., Zreda, M., Ferre, P. A., & Rosolem, R. (2013). An assessment of the effect of horizontal soil moisture heterogeneity on the area-average measurement of cosmic-ray neutrons. *Water Resources Research, 49*(10), 1-10.

Fortes, R., Millán, S., Prieto, M. H., & Campillo, C. (2015). A methodology based on apparent electrical conductivity and guided soil samples to improve irrigation zoning. *Precision Agriculture, 16*(4), 441–454.

Friedman, S. P. (2005). Soil properties influencing apparent electrical conductivity: a review. *Computers and electronics in agriculture, 46*(1), 45-70.

Galagedara, L. W., Parkin, G. W., Redman, J. D. von Bertoldi, P., & Endres, A. L. (2005). Field studies of the GPR ground wave method for estimating soil water content during irrigation and drainage. *Journal of Hydrology, 301*, 182-197.

Geophex Ltd., 2004. GEM-2 User's Manual, *Version 3.8.* Geophex Ltd., Raleigh, USA. *Available at: http://www.geophex.com/Downloads/GEM-2%20Operator's%20Manual.pdf.*

GF Instruments., 2011. CMD Electromagnetic conductivity meter user manual *V. 1.5.* Geophysical Equipment and Services, Czech Republic. *Available at: http://www.gfinstruments.cz/index.php?menu=gi&smenu=iem&cont=cmd_&ear=ov.*

Goff, A., Huang, J., Wong, V. N. L., Monteiro Santos, F. A., Wege, R., & Triantafilis, J. (2014). Electromagnetic Conductivity Imaging of Soil Salinity in an Estuarine–Alluvial Landscape. *Soil Science Society of America Journal, 78*(5), 1686.

Grant, L., Seyfried, M., & McNamara, J. (2004). Spatial variation and temporal stability of soil water in a snow-dominated, mountain catchment. *Hydrological Processes, 18*(18), 3493-3511.

Gregorich, E. G., & Carter, M. R. (2008). Soil Sampling and Methods of Analysis (second ed) Canadian Society of Soil Science. CRC Press: Boca Raton, FL, USA.

Hedley, C. B., & Yule, I. J. (2009). Soil water status mapping and two variable-rate irrigation scenarios. *Precision Agriculture*, *10*(4), 342-355.

Heil, K., & Schmidhalter, U. (2012). Characterisation of soil texture variability using the apparent soil electrical conductivity at a highly variable site. *Computers and geosciences, 39*, 98-110.

Heil, K., & Schmidhalter, U., (2015). Comparison of the EM38 and EM38-MK2 electromagnetic induction-based sensors for spatial soil analysis at field scale. *Computers and Electronics in Agriculture, 110*, 267-280.

Hendrickx, J. M. H., & Kachanoski, R. G. (2002). Nonintrusive electromagnetic induction. *Methods of soil analysis. Part, 4*, 1297-1306.

Hignett, C., & Evett, S. (2008). Direct and surrogate measures of soil water content (*No. IAEA-TCS--30).*

Huang, H. H., Adamchuk, V. I., Boiko, I. I., & Ferguson, R. F. (2013). Effect of sampling patterns and interpolation methods on prediction quality of soil variability mapping. In *Precision agriculture'13* (pp. 243-250). Wageningen Academic Publishers, Wageningen.

Huang, J., Nhan, T., Wong, V. N. L., Johnston, S. G., Lark, R. M., & Triantafilis, J. (2014). Digital soil mapping of a coastal acid sulfate soil landscape. *Soil Research, 52*, 327–339.

Huang, J., Scudiero, E., Bagtang, M., Corwin, D. L., & Triantafilis, J. (2016). Monitoring scale-specific and temporal variation in electromagnetic conductivity images. *Irrigation Science, 34*(3), 187–200.

Huang, J., Pedrera-Parrilla, A., Vanderlinden, K., Taguas, E. V., Gómez, J. A., & Triantafilis, J. (2017). Potential to map depth-specific soil organic matter content across an olive grove using quasi-2d and quasi-3d inversion of DUALEM-21 data. *Catena, 152*, 207-217.

Ibáñez, J. J., Sánchez Díaz, J., De Alba, S., López Árias, M., & Boixadera, J. (2005). Collection of Soil Information in Spain: a review in 2003. *Soil Resources of Europe, second edition. Jones, RJA, Houšková, B., Bullock, P. et Montanarella, L.(eds). European Soil Bureau Research Report*, (9), 345-356.

Ibáñez, J. J., Pérez-Gómez, R., Oyonarte, C., & Brevik, E. C. (2015). Are there arid land soilscapes in Southwestern Europe?. *Land Degradation & Development*, *26*(8), 853-862.

Imko. (2016). About TRIME-TDR. Retrieved from https://imko.de/en/about-trime-tdr

IMKO. (2016). TRIME-TDR user manual. Retrieved from https://imko.de/en/about-trime-tdr

IUSS Working Group WRB (2014). World reference base for soil resources 2014. *International soil classification system for naming soils and creating legends for soil maps. FAO, Rome. World Soil Resources Reports No*. 106.

Jacobsen, O. H., & Schjønning, P. (1993). A laboratory calibration of time domain reflectometry for soil water measurement including effects of bulk density and texture. *Journal of Hydrology*, *151*(2-4), 147-157.

Jay, S. C., Lawrence, R. L., Repasky, K. S., & Rew, L. J. (2010 July). Detection of leafy spurge using hyper-spectral-spatial-temporal imagery. In *Geoscience and Remote Sensing Symposium (IGARSS) 2010 IEEE International* (pp. 4374-4376). IEEE.

Jones, S. B., Wraith, J. M., & Or, D. (2002). Time domain reflectometry measurement principles and applications. *Hydrological processes*, *16*(1), 141-153.

Kachanoski, R. G., Gregorich, E. G., & vanWesenbeeck, I. J. (1988). Estimating spatial variations of soil water content using non contacting electromagnetic inductive methods. *Canadian Journal of Soil Science, 68*, 715–722.

Kachanoski, R. G., Wesenbeeck, I. V., Jong, E. D. (1990). Field scale patterns of soil water storage from non-contacting measurements of bulk electrical conductivity. *Canadian Journal of Soil Science, 70*(3), 537-542.

Kaufman, A. (1983). Geophysical field theory and method: *Part C, Electromagnetic Fields II. Elsevier, New York, USA*.

Khan, F. S., Zaman, Q. U., Chang, Y. K., Farooque, A. A., Schumann, A. W., & Madani, A. (2016). Estimation of the rootzone depth above a gravel layer (in wild blueberry fields) using electromagnetic induction method. *Precision agriculture, 17*(2), 155-167.

Khosla, R., Inman, D., Westfall, D. G., Reich, R. M., Frasier, M., Mzuku, M., Koch, B., & Hornung, A. (2008). A synthesis of multi-disciplinary research in precision agriculture: site-specific management zones in the semi-arid western Great Plains of the USA. *Precision Agriculture, 9*(1-2), 85-100.

King, J. A., Dampney, P. M. R., Lark, R. M., Wheeler, H. C., Bradley, R. I., & Mayr, T. R. (2005). Mapping potential crop management zones within fields: use of yield-map series and patterns of soil physical properties identified by electromagnetic induction sensing. *Precision Agriculture 6*(2), 167-181.

Kirby, G. E. (1988). *Soils of the Pasadena-Deer Lake area, Newfoundland.* St. John's. Retrieved from http://sis.agr.gc.ca/cansis/publications/surveys/nf/nf17/nf17_report.pdf

Korsaeth, A., Riley, H., Kværnø, S. H., & Vestgarden, L. S. (2008). Relations between a Commercial Soil Survey Map Based on Soil Apparent Electrical Conductivity (ECa) and Measured Soil Properties on a Morainic Soil in Southeast Norway. *Handbook of Agricultural Geophysics (Eds. Barry J. Allred, Jeffrey J. Daniels, and M. Reza Ehsani)*, pp.225-231.

Kyaw, T., Ferguson, R. B., Adamchuk, V. I., Marx, D. B., Tarkalson, D. D., & McCallister, D. L. (2008). Delineating site-specific management zones for pH-induced iron chlorosis. *Precision Agriculture, 9*(1–2), 71–84.

Lesch, S. M., Strauss, D. J., & Rhoades, J. D. (1995). Spatial prediction of soil salinity using electromagnetic induction techniques. Part 1. Statistical prediction models: a comparison of multiple linear regression and cokriging. *Water Resources Research, 31*, 373–386.

Lesch, S. M., & Corwin, D. L. (2003). Predicting EM/soil property correlation estimates via the dual pathway parallel conductance model. *Agronomy Journal, 95*(2), 365–379.

Lesch, S. M., Corwin, D. L., & Robinson, D. A. (2005). Apparent soil electrical conductivity mapping as an agricultural management tool in arid zone soils. *Computers and Electronics in Agriculture, 46*(1), 351-378.

Liao, K. H., Zhu, Q., & Doolittle, J. (2014). Temporal stability of apparent soil electrical conductivity measured by electromagnetic induction techniques. *Journal of Mountain Science, 11*(1), 98.

Lin, H. (2006). Temporal stability of soil moisture spatial pattern and subsurface preferential flow pathways in the Shale Hills Catchment. *Vadose Zone Journal, 5*(1), 317-340.

Liu, T. L., Juang, K. W., & Lee, D. Y. (2006). Interpolating soil properties using kriging combined with categorical information of soil maps. *Soil Science Society of America Journal, 70*(4), 1200-1209.

Lück, E., Gebbers, R., Ruehlmann, J., & Spangenberg, U. (2009). Electrical conductivity mapping for precision farming. *Near Surface Geophysics*, *7*(1), 15-25.

Ma, R., McBratney, A., Whelan, B., Minasny, B., & Short, M. (2011). Comparing temperature correction models for soil electrical conductivity measurement. *Precision Agriculture, 12*(1), F55–F66.

Mankin, K. R., & Karthikeyan, R. (2002). Field assessment of saline seep remediation using electromagnetic induction. *Transactions of the American Society of Agricultural and Biological Engineers, 45*(1), 99.

Martínez, G., Vanderlinden, K., Giráldez, J. V., Espejo, A. J., & Muriel, J. L. (2010). Field-scale soil moisture pattern mapping using electromagnetic induction. *Vadose Zone Journal, 9*(4), 871-881.

Martini, E., Werban, U., Zacharias, S., Pohle, M., Dietrich, P., & Wollschläger, U. (2017). Repeated electromagnetic induction measurements for mapping soil moisture at the field scale: validation with data from a wireless soil moisture monitoring network. *Hydrology and Earth System Sciences, 21*(1), 495.

McNeill, J. D. (1980). Electromagnetic terrain conductivity measurement at low induction numbers. (*Geonics Ltd., Mississauga, Ontario, Canada, Technical Note TN-5*).

Mohanty, B. P., & Skaggs, T. H. (2001). Spatio-temporal evolution and time-stable characteristics of soil moisture within remote sensing footprints with varying soil, slope, and vegetation. *Advances in water resources, 24*(9), 1051-1067.

Molin, J. P., & Faulin, G. D. C. (2013). Spatial and temporal variability of soil electrical conductivity related to soil moisture. *Scientia Agricola, 70*(1), 01-05.

Mondal, P., & Tewari, V. K. (2007). Present status of precision farming: A review. *International Journal of Agricultural Research, 5*(12), 1124-1133.

Mueller, T. G., Hartsock, N. J., Stombaugh, T. S., Shearer, S. A., Cornelius, P. L., Barnhisel, R. I. (2003). Soil electrical conductivity map variability in limestone soils overlain by loess. *Agronomy Journal, 95*(3), 496-507.

Neely, H. L., Morgan, C. L., Hallmark, C. T., McInnes, K. J. & Molling, C. C. (2016). Apparent electrical conductivity response to spatially variable vertisol properties. *Geoderma, 263*, 168-175.

Pachepsky, Y. A., Guber, A. K., & Jacques, D. (2005). Temporal persistence in vertical distributions of soil moisture contents. *Soil Science Society of America Journal, 69*(2), 347-352.

Pan, L., Adamchuk, V. I., Prasher, S., Gebbers, R., Taylor, R. S., & Dabas, M. (2014). Vertical soil profiling using a galvanic contact resistivity scanning approach. *Sensors, 14*(7), 13243-13255.

Pandey, V., & Pandey, P. K. (2010). Spatial and temporal variability of soil moisture. *International Journal of Geosciences, 1*(02), 87.

Pedrera-Parrilla, A., Pachepsky, Y. A., Taguas, E. V., Martos-Rosillo, S., Giráldez, J. V., Vanderlinden, K. (2017). Concurrent temporal stability of the apparent electrical conductivity and soil water content. *Journal of Hydrology*, *544*, 319-326.

Peralta, N. R., & Costa, J. L. (2013). Delineation of management zones with soil apparent electrical conductivity to improve nutrient management. *Computers and Electronics in Agriculture, 99*, 218–226.

Reedy, R. C., & Scanlon, B. R. (2003). Soil water content monitoring using electromagnetic induction. *Journal of Geotechnical and Geoenvironmental Engineering, 129*(11), 1028-1039.

Rhoades, J. D., Raats, P. A., & Prather, R. J. (1976). Effects of liquid-phase electrical conductivity, water content, and surface conductivity on bulk soil electrical conductivity. *Soil Science Society of America Journal, 40,* 651–655.

Rhoades, J. D., Manteghi, N. A., Shouse, P. J., & Alves, W. J. (1989). Soil electrical conductivity and soil salinity: New formulations and calibrations. *Soil Science Society of America Journal, 53*(2), 433-439.

Robinson, D. A., Jones, S. B., Wraith, J. M., Or, D., & Friedman, S. P. (2003). A review of advances in dielectric and electrical conductivity measurement in soils using time domain reflectometry. *Vadose Zone Journal*, *2*(4), 444-475.

Robinson, D. A., Lebron, I., Lesch, S. M., & Shouse, P. (2004). Minimizing drift in electrical conductivity measurements in high temperature environments using the EM-38. *Soil Science Society of America Journal, 68*(2), 339-345.

Rossi, R. E., Dungan, J. L., & Beck, L. R. (1994). Kriging in the shadows: geostatistical interpolation for remote sensing. *Remote Sensing of Environment, 49*(1), 32-40.

Sanborn, P., Lamontagne, L., & Hendershot, W. (2011). Podzolic soils of Canada: Genesis, distribution, and classification. *Canadian Journal of Soil Science, 91*(5), 843-880.

Schaap, M. G., De Lange, L., & Heimovaara, T. J. (1997). TDR calibration of organic forest floor media. *Soil Technology*, *11*(2), 205-217.

Serrano, J. M., Shahidian, S., & da Silva, J. R. M. (2013). Apparent electrical conductivity in dry versus wet soil conditions in a shallow soil. *Precision Agriculture, 14*(1), 99–114.

Serrano, J., Shahidian, S., & Silva, J. M. D. (2014). Spatial and temporal patterns of apparent electrical conductivity: DUALEM vs. Veris sensors for monitoring soil properties. *Sensors, 14*(6), 10024-10041.

Sherlock, M. D., & McDonnell, J. J. (2003). A new tool for hillslope hydrologists: spatially distributed groundwater level and soil water content measured using electromagnetic induction. *Hydrological Processes, 17*(10), 1965-1977.

Shibusawa, S. (2006). Soil Sensors for Precision Farming. In *Handbook of Precision Agriculture, Principles and Applications; Srinivasan, A., Ed.*; The Haworth Press: New York, NY, USA, pp. 57–90.

Soil Classification Working Group. (1998). The Canadian System of Soil Classification. The Canadian System of Soil Classification, 3rd ed. *Agriculture and Agri-Food Canada Publication* 1646. NRC Research Press.

Soil Survey Standard Test Method: Organic Carbon. (n.d). Retrieved from http://www.environment.nsw.gov.au/resources/soils/testmethods/oc.pdf.

Souza, Z. M. D., Marques Júnior, J., & Pereira, G. T. (2009). Spatial variability of the physical and mineralogical properties of the soil from the areas with variation in landscape shapes. *Brazilian Archives of Biology and Technology, 52*(2), 305-316.

Sudduth, K. A., Drummond, S. T., & Kitchen, N. R. (2001). Accuracy issues in electromagnetic induction sensing of soil electrical conductivity for precision agriculture. *Computers and electronics in agriculture*, *31*(3), 239-264.

Sudduth, K. A., Kitchen, N. R., Bollero, G. A., Bullock, D. G., & Wiebold, W. J. (2003). Comparison of electromagnetic induction and direct sensing of soil electrical conductivity. *Agronomy Journal, 95*(3), 472-482.

Terraplus Inc., (2013). Gem 2 Multi-Frequency EM Sensor. http://terraplus.ca/products/electromagnetics/gem2.aspx

Topp, G. C., Davis, J. L., & Annan, A. P. (1980). Electromagnetic determination of soil water content: Measurements in coaxial transmission lines. *Water resources research, 16*(3), 574-582.

Toushmalani, R. (2010). Application of geophysical methods in agriculture. *Australian Journal of Basic and Applied Sciences, 4*(12), 6433–6439.

Triantafilis, J., & Santos, F. M. (2013). Electromagnetic conductivity imaging (EMCI) of soil using a DUALEM-421 and inversion modelling software (EM4Soil). *Geoderma*, *211*, 28-38.

Tromp-van Meerveld, H. J., & McDonnell, J. J. (2009). Assessment of multi-frequency electromagnetic induction for determining soil moisture patterns at the hillslope scale. *Journal of Hydrology, 368*(1), 56-67.

USDA-NRCS. (2016). Soil Health.

Vachaud, G., Passerat de Silans, A., Balabanis, P., & Vauclin, M. (1985). Temporal stability of spatially measured soil water probability density function. *Soil Science Society of America Journal, 49*(4), 822-828.

Van Arkel, Z., & Kaleita, A.L. (2014). Identifying sampling locations for field-scale soil moisture estimation using K-means clustering. *Water Resources Research, 50*(8), 7050-7057.

Van Genuchten, M.T. (1980). A closed-form equation for predicting the hydraulic conductivity of unsaturated soils. *Soil Science Society of America Journal, 44*(5), 892-898.

Vereecken, H., Huisman, J. A., Pachepsky, Y., Montzka, C., Van Der Kruk, J., Bogena, H., Weihermüller, L., Herbst, M., Martinez, G., & Vanderborght, J. (2014). On the spatio-temporal dynamics of soil moisture at the field scale. *Journal of Hydrology 516*, 76-96.

von Hebel, C., Rudolph, S., Mester, A., Huisman, J.A., Kumbhar, P., Vereecken, H., & van der Kruk, J. (2014). Three-dimensional imaging of subsurface structural patterns using quantitative large-scale multiconfiguration electromagnetic induction data. *Water Resources Research, 50*(3), 2732-2748.

Walter, J., Lueck, E., Bauriegel, A., Richter, C., & Zeitz, J. (2015). Multi-scale analysis of electrical conductivity of peatlands for the assessment of peat properties. *European Journals of Soil Science, 66*(4), 639-650.

Wang, C., Rees, H. W., & Daigle, J. L. (1984). Classification of Podzolic soils as affected by cultivation. *Canadian Journal of Soil Science, 64*(2), 229-239.

Warrick, A. W., & Nielsen, D. R. (1980). Spatial variability of soil physical properties in the field. 319–44. In: Hillel, D. (Ed.). *Applications of Soil Physics. Academic Press*, New York, NY, USA.

White, M.L., Shaw, J.N., Raper, R.L., Rodekohr, D., & Wood, C.W. (2012). A multivariate approach for high-resolution soil survey development. *Soil science*, *177*(5), 345-354.

Wijewardana, Y. G. N. S., & Galagedara, L. W. (2010). Estimation of spatio-temporal variability of soil water content in agricultural fields with ground penetrating radar. *Journal of Hydrology, 391*(1–2), 24–33.

Williams, B., Walker, J., & Anderson, J. (2006). Spatial variability of regolith leaching and salinity in relation to whole farm planning. *Australian Journal of Experimental Agriculture, 46*(10), 1271-1277.

Won, I. J. (1980). A wide-band electromagnetic exploration method—Some theoretical and experimental results. *Geophysics, 45*(5), 928–940.

Zhang, Z., He, G., & Jiang, H. (2013). Leaf area index retrieval using red edge parameters based on Hyperion hyper-spectral imagery. *Journal of Theoretical and Applied Information Technology, 48*(2), 957–960.

Zhu, Q., & Lin, H. S. (2009). Simulation and validation of concentrated subsurface lateral flow paths in an agricultural landscape. *Hydrology and Earth System Sciences, 13*(8), 1503-1518.

Zhu, Q., & Lin, H. S. (2010). Comparing ordinary kriging and regression kriging for soil properties in contrasting landscapes. *Pedosphere, 20*(5), 594-606.

Zhu, Q., Lin, H., & Doolittle, J. (2010). Repeated electromagnetic induction surveys for determining subsurface hydrologic dynamics in an agricultural landscape. *Soil Science Society of America Journal, 74*(5), 1750-1762.

APPENDIXES

(A) MULTILINEAR REGRESSION USING BACKWARD ELIMINATION

DEPENDENT VARIABLE: $\theta_{v(0\text{-}11)}$, $\theta_{v(0\text{-}16)}$, $\theta_{v(0\text{-}30)}$, $\theta_{g(0\text{-}10)}$, $\theta_{g(10\text{-}20)}$, $\theta_{g(0\text{-}20)}$ VMC-16cm, Sand, Silt, Clay, SMC, AWC, Bulk density,

INDEPENDENT VARIABLE: ECa-L, ECa-H, ECa-38kHz, ECa-LH, ECa-LH38

Regression Analysis: $\theta_{v(0\text{-}16)}$ versus ECa-L, ECa-H, ECa-LH, ECa-38kHz, ECa-LH38

```
The following terms cannot be estimated and were removed:
   ECa-LH, ECa-LH38


Backward Elimination of Terms

Candidate terms: ECa-L, ECa-H, ECa-LH, ECa-38kHz, ECa-LH38

             ------Step 1------    ------Step 2------    ------Step 3------
                Coef          P       Coef          P       Coef          P
Constant     -0.0988               -0.1090               -0.0988
ECa-L         0.1410      0.000     0.1308      0.000     0.0983      0.000
ECa-H        -0.0444      0.175    -0.0256      0.208
ECa-38kHz     0.0097      0.448

S                     0.0191246             0.0189017             0.0192711
R-sq                     77.38%                76.53%                74.17%
R-sq(adj)                73.14%                73.77%                72.73%
R-sq(pred)               66.28%                69.88%                68.27%

α to remove = 0.1


Analysis of Variance

Source      DF    Adj SS    Adj MS  F-Value  P-Value
Regression   1  0.019191  0.019191    51.68    0.000
  ECa-L      1  0.019191  0.019191    51.68    0.000
Error       18  0.006685  0.000371
Total       19  0.025876


Model Summary

        S    R-sq  R-sq(adj)  R-sq(pred)
0.0192711  74.17%     72.73%      68.27%
```

Coefficients

Term	Coef	SE Coef	T-Value	P-Value	VIF
Constant	-0.0988	0.0491	-2.01	0.059	
ECa-L	0.0983	0.0137	7.19	0.000	1.00

Regression Equation

VMC-16cm = -0.0988 + 0.0983 ECa-L

Fits and Diagnostics for Unusual Observations

Obs	VMC-16cm	Fit	Resid	Std Resid		
18	0.30550	0.26291	0.04259	2.27	R	
19	0.16370	0.17559	-0.01189	-0.77		X

R Large residual
X Unusual X

Regression Analysis: $\theta_{v(0\text{-}16)}$ versus ECa-L, ECa-H, ECa-LH, ECa-38kHz, ECa-LH38

The following terms cannot be estimated and were removed:
ECa-LH, ECa-LH38

Backward Elimination of Terms

Candidate terms: ECa-L, ECa-H, ECa-LH, ECa-38kHz, ECa-LH38

	------Step 1------		------Step 2------		------Step 3------	
	Coef	P	Coef	P	Coef	P
Constant	-0.0988		-0.1090		-0.0988	
ECa-L	0.1410	0.000	0.1308	0.000	0.0983	0.000
ECa-H	-0.0444	0.175	-0.0256	0.208		
ECa-38kHz	0.0097	0.448				
S		0.0191246		0.0189017		0.0192711
R-sq		77.38%		76.53%		74.17%
R-sq(adj)		73.14%		73.77%		72.73%
R-sq(pred)		66.28%		69.88%		68.27%

α to remove = 0.1

Analysis of Variance

Source	DF	Adj SS	Adj MS	F-Value	P-Value
Regression	1	0.019191	0.019191	51.68	0.000
ECa-L	1	0.019191	0.019191	51.68	0.000
Error	18	0.006685	0.000371		

```
Total       19  0.025876


Model Summary

        S    R-sq  R-sq(adj)  R-sq(pred)
0.0192711  74.17%     72.73%      68.27%


Coefficients

Term         Coef  SE Coef  T-Value  P-Value   VIF
Constant  -0.0988   0.0491    -2.01    0.059
ECa-L      0.0983   0.0137     7.19    0.000  1.00


Regression Equation

VMC-16cm = -0.0988 + 0.0983 ECa-L


Fits and Diagnostics for Unusual Observations

Obs  VMC-16cm      Fit     Resid  Std Resid
 18   0.30550  0.26291   0.04259       2.27  R
 19   0.16370  0.17559  -0.01189      -0.77     X

R  Large residual
X  Unusual X
```

Regression Analysis: $\theta_{g(0-10)}$ versus ECa-L, ECa-H, ECa-LH, ECa-38kHz, ECa-LH38

```
The following terms cannot be estimated and were removed:
   ECa-LH, ECa-LH38


Backward Elimination of Terms

Candidate terms: ECa-L, ECa-H, ECa-LH, ECa-38kHz, ECa-LH38

             ------Step 1------    ------Step 2------    ------Step 3------
                Coef          P       Coef          P       Coef          P
Constant     -0.0739               -0.0889               -0.0824
ECa-L         0.1124      0.010     0.0975      0.012     0.0771      0.000
ECa-H        -0.0436      0.269    -0.0161      0.511
ECa-38kHz     0.0142      0.365

S                     0.0232986             0.0232090             0.0228518
R-sq                     59.02%                56.79%                55.65%
R-sq(adj)                51.34%                51.71%                53.19%
R-sq(pred)               30.31%                43.69%                47.63%

α to remove = 0.1
```

Analysis of Variance

Source	DF	Adj SS	Adj MS	F-Value	P-Value
Regression	1	0.011795	0.011795	22.59	0.000
ECa-L	1	0.011795	0.011795	22.59	0.000
Error	18	0.009400	0.000522		
Total	19	0.021194			

Model Summary

S	R-sq	R-sq(adj)	R-sq(pred)
0.0228518	55.65%	53.19%	47.63%

Coefficients

Term	Coef	SE Coef	T-Value	P-Value	VIF
Constant	-0.0824	0.0582	-1.42	0.174	
ECa-L	0.0771	0.0162	4.75	0.000	1.00

Regression Equation

0-10cm = -0.0824 + 0.0771 ECa-L

Fits and Diagnostics for Unusual Observations

Obs	0-10cm	Fit	Resid	Std Resid		
12	0.25115	0.20036	0.05079	2.29	R	
19	0.14033	0.13268	0.00765	0.42		X

R Large residual
X Unusual X

Regression Analysis: $\theta_{g(10-20)}$ versus ECa-L, ECa-H, ECa-LH, ECa-38kHz, ECa-LH38

The following terms cannot be estimated and were removed:
ECa-LH, ECa-LH38

Backward Elimination of Terms

Candidate terms: ECa-L, ECa-H, ECa-LH, ECa-38kHz, ECa-LH38

	Step 1		Step 2		Step 3	
	Coef	P	Coef	P	Coef	P
Constant	0.0709		0.0589		0.1084	
ECa-L	0.0790	0.208	0.0186	0.592		
ECa-H	-0.0724	0.244				
ECa-38kHz	0.0385	0.127	0.0162	0.307	0.0215	0.081

```
S                    0.0366326          0.0371252          0.0363947
R-sq                    24.31%             17.40%             15.95%
R-sq(adj)               10.12%              7.69%             11.28%
R-sq(pred)               0.00%              0.00%              1.59%

α to remove = 0.1
```

```
Analysis of Variance

Source         DF    Adj SS    Adj MS  F-Value  P-Value
Regression      1  0.004526  0.004526     3.42    0.081
  ECa-38kHz     1  0.004526  0.004526     3.42    0.081
Error          18  0.023842  0.001325
Total          19  0.028368
```

```
Model Summary

        S    R-sq  R-sq(adj)  R-sq(pred)
0.0363947  15.95%     11.28%       1.59%
```

```
Coefficients

Term           Coef  SE Coef  T-Value  P-Value   VIF
Constant     0.1084   0.0382     2.84    0.011
ECa-38kHz    0.0215   0.0116     1.85    0.081  1.00
```

```
Regression Equation

10-20cm = 0.1084 + 0.0215 ECa-38kHz
```

```
Fits and Diagnostics for Unusual Observations

Obs  10-20cm     Fit    Resid  Std Resid
  5   0.0623  0.1871  -0.1249      -3.56  R

R  Large residual
```

Regression Analysis: $\theta_{g(0-20)}$ versus ECa-L, ECa-H, ECa-LH, ECa-38kHz, ECa-LH38

```
The following terms cannot be estimated and were removed:
   ECa-LH, ECa-LH38
```

```
Backward Elimination of Terms

Candidate terms: ECa-L, ECa-H, ECa-LH, ECa-38kHz, ECa-LH38
```

	Step 1 Coef	Step 1 P	Step 2 Coef	Step 2 P	Step 3 Coef	Step 3 P
Constant	-0.0015		-0.0111		-0.0265	
ECa-L	0.0957	0.030	0.0473	0.057	0.0592	0.004
ECa-H	-0.0580	0.166				
ECa-38kHz	0.0264	0.118	0.0084	0.430		
S		0.0244368		0.0252199		0.0249768
R-sq		47.50%		40.59%		38.30%
R-sq(adj)		37.66%		33.60%		34.87%
R-sq(pred)		7.45%		21.14%		22.69%

α to remove = 0.1

Analysis of Variance

Source	DF	Adj SS	Adj MS	F-Value	P-Value
Regression	1	0.006970	0.006970	11.17	0.004
ECa-L	1	0.006970	0.006970	11.17	0.004
Error	18	0.011229	0.000624		
Total	19	0.018199			

Model Summary

S	R-sq	R-sq(adj)	R-sq(pred)
0.0249768	38.30%	34.87%	22.69%

Coefficients

Term	Coef	SE Coef	T-Value	P-Value	VIF
Constant	-0.0265	0.0636	-0.42	0.682	
ECa-L	0.0592	0.0177	3.34	0.004	1.00

Regression Equation

0-20cm = -0.0265 + 0.0592 ECa-L

Fits and Diagnostics for Unusual Observations

Obs	0-20cm	Fit	Resid	Std Resid	
5	0.1341	0.2099	-0.0758	-3.27	R
19	0.1378	0.1389	-0.0010	-0.05	X

R Large residual
X Unusual X

Regression Analysis: $\theta_{v(0-11)}$ versus ECa-L, ECa-H, ECa-LH, ECa-38kHz, ECa-LH38

The following terms cannot be estimated and were removed:
ECa-LH, ECa-LH38

Backward Elimination of Terms

Candidate terms: ECa-L, ECa-H, ECa-LH, ECa-38kHz, ECa-LH38

	------Step 1------		------Step 2------		------Step 3------	
	Coef	P	Coef	P	Coef	P
Constant	-0.0301		-0.0349		-0.0301	
ECa-L	0.1087	0.001	0.1039	0.000	0.0888	0.000
ECa-H	-0.0207	0.440	-0.0119	0.473		
ECa-38kHz	0.0046	0.669				
S		0.0159973		0.0156115		0.0154104
R-sq		79.48%		79.24%		78.58%
R-sq(adj)		75.63%		76.79%		77.39%
R-sq(pred)		65.49%		70.90%		73.85%

α to remove = 0.1

Analysis of Variance

Source	DF	Adj SS	Adj MS	F-Value	P-Value
Regression	1	0.015679	0.015679	66.02	0.000
ECa-L	1	0.015679	0.015679	66.02	0.000
Error	18	0.004275	0.000237		
Total	19	0.019953			

Model Summary

S	R-sq	R-sq(adj)	R-sq(pred)
0.0154104	78.58%	77.39%	73.85%

Coefficients

Term	Coef	SE Coef	T-Value	P-Value	VIF
Constant	-0.0301	0.0393	-0.77	0.453	
ECa-L	0.0888	0.0109	8.13	0.000	1.00

Regression Equation

VMC-11cm = -0.0301 + 0.0888 ECa-L

Fits and Diagnostics for Unusual Observations

Std

Obs	VMC-11cm	Fit	Resid	Resid	
1	0.33610	0.30626	0.02984	2.01	R
19	0.22590	0.21787	0.00803	0.65	X

R Large residual
X Unusual X

Regression Analysis: $\theta_{v(0\text{-}30)}$ versus ECa-L, ECa-H, ECa-LH, ECa-38kHz, ECa-LH38

The following terms cannot be estimated and were removed:
ECa-LH, ECa-LH38

Backward Elimination of Terms

Candidate terms: ECa-L, ECa-H, ECa-LH, ECa-38kHz, ECa-LH38

	------Step 1------	
	Coef	P
Constant	-0.053	
ECa-L	0.1992	0.007
ECa-H	-0.1359	0.051
ECa-38kHz	0.0466	0.088
S		0.0393584
R-sq		49.22%
R-sq(adj)		39.70%
R-sq(pred)		17.73%

α to remove = 0.1

Analysis of Variance

Source	DF	Adj SS	Adj MS	F-Value	P-Value
Regression	3	0.024026	0.008009	5.17	0.011
ECa-L	1	0.014692	0.014692	9.48	0.007
ECa-H	1	0.006905	0.006905	4.46	0.051
ECa-38kHz	1	0.005103	0.005103	3.29	0.088
Error	16	0.024785	0.001549		
Total	19	0.048811			

Model Summary

S	R-sq	R-sq(adj)	R-sq(pred)
0.0393584	49.22%	39.70%	17.73%

Coefficients

Term	Coef	SE Coef	T-Value	P-Value	VIF
Constant	-0.053	0.105	-0.50	0.623	
ECa-L	0.1992	0.0647	3.08	0.007	5.37
ECa-H	-0.1359	0.0644	-2.11	0.051	11.05
ECa-38kHz	0.0466	0.0257	1.82	0.088	4.18

Regression Equation

VMC-30CM = -0.053 + 0.1992 ECa-L - 0.1359 ECa-H + 0.0466 ECa-38kHz

PLS Regression: $\theta_{g(0\text{-}10)}$, $\theta_{g(10\text{-}20)}$, $\theta_{v(0\text{-}20)}$... versus ECa-L, ECa-H, ECa-LH, ...

Method

Cross-validation	Leave-one-out
Components to evaluate	Adjusted
Number of components evaluated	3
Number of components selected	2

Analysis of Variance for 0-10cm

Source	DF	SS	MS	F	P
Regression	2	0.0112076	0.0056038	9.54	0.002
Residual Error	17	0.0099869	0.0005875		
Total	19	0.0211945			

Analysis of Variance for 10-20cm

Source	DF	SS	MS	F	P
Regression	2	0.0041204	0.0020602	1.44	0.263
Residual Error	17	0.0242474	0.0014263		
Total	19	0.0283678			

Analysis of Variance for 0-20cm

Source	DF	SS	MS	F	P
Regression	2	0.0066750	0.0033375	4.92	0.021
Residual Error	17	0.0115245	0.0006779		
Total	19	0.0181995			

Analysis of Variance for VMC-11cm

Source	DF	SS	MS	F	P
Regression	2	0.0153280	0.0076640	28.17	0.000
Residual Error	17	0.0046254	0.0002721		
Total	19	0.0199534			

Analysis of Variance for VMC-16cm

Source	DF	SS	MS	F	P
Regression	2	0.0185719	0.0092860	21.61	0.000
Residual Error	17	0.0073038	0.0004296		
Total	19	0.0258757			

Analysis of Variance for VMC-30CM

Source	DF	SS	MS	F	P
Regression	2	0.0150326	0.0075163	3.78	0.044
Residual Error	17	0.0337786	0.0019870		
Total	19	0.0488112			

Model Selection and Validation for 0-10cm

Components	X Variance	Error	R-Sq	PRESS	R-Sq (pred)
1	0.894409	0.0117598	0.445150	0.0146683	0.307917
2	0.986297	0.0099869	0.528797	0.0132706	0.373867
3		0.0086852	0.590213	0.0147697	0.303134

Model Selection and Validation for 10-20cm

Components	X Variance	Error	R-Sq	PRESS	R-Sq (pred)
1	0.894409	0.0243660	0.141068	0.0321606	0
2	0.986297	0.0242474	0.145249	0.0337725	0
3		0.0214711	0.243117	0.0395157	0

Model Selection and Validation for 0-20cm

Components	X Variance	Error	R-Sq	PRESS	R-Sq (pred)
1	0.894409	0.0117681	0.353384	0.0151865	0.165556
2	0.986297	0.0115245	0.366769	0.0157715	0.133408
3		0.0095545	0.475013	0.0168435	0.074509

Model Selection and Validation for VMC-11cm

Components	X Variance	Error	R-Sq	PRESS	R-Sq (pred)
1	0.894409	0.0074852	0.624867	0.0094753	0.525130
2	0.986297	0.0046254	0.768190	0.0064286	0.677821
3		0.0040946	0.794791	0.0068863	0.654881

Model Selection and Validation for VMC-16cm

Components	X Variance	Error	R-Sq	PRESS	R-Sq (pred)
1	0.894409	0.0114335	0.558137	0.0147574	0.429681
2	0.986297	0.0073038	0.717735	0.0102018	0.605737
3		0.0058520	0.773841	0.0087265	0.662752

Model Selection and Validation for VMC-30CM

Components	X Variance	Error	R-Sq	PRESS	R-Sq (pred)

1	0.894409	0.0357872	0.266823	0.0439985	0.098599
2	0.986297	0.0337786	0.307975	0.0444998	0.088329
3		0.0247853	0.492221	0.0401557	0.177327

Coefficients

	0-10cm	10-20cm	0-20cm	VMC-11cm	VMC-16cm	VMC-30CM
Constant	-0.0782087	0.0646665	-0.0067711	-0.0328140	-0.103296	-0.0639204
ECa-L	0.0524757	0.0021806	0.0273282	0.0645619	0.075087	0.0577695
ECa-H	0.0039502	0.0078489	0.0058995	0.0038423	0.003211	0.0052818
ECa-LH	0.0216033	0.0065884	0.0140958	0.0258253	0.029105	0.0244737
ECa-38kHz	-0.0055791	0.0062370	0.0003290	-0.0077207	-0.010038	-0.0053564
ECa-LH38	0.0005402	0.0076622	0.0041012	-0.0003471	-0.001654	0.0015223

	0-10cm standardized	10-20cm standardized	0-20cm standardized	VMC-11cm standardized	VMC-16cm standardized
Constant	0.000000	0.000000	0.000000	0.000000	0.000000
ECa-L	0.508040	0.018248	0.285517	0.644196	0.657915
ECa-H	0.055161	0.094738	0.088903	0.055298	0.040586
ECa-LH	0.247888	0.065345	0.174546	0.305411	0.302247
ECa-38kHz	-0.119974	0.115931	0.007634	-0.171113	-0.195354
ECa-LH38	0.008452	0.103627	0.069248	-0.005598	-0.023416

	VMC-30CM standardized
Constant	0.000000
ECa-L	0.368544
ECa-H	0.048602
ECa-LH	0.185049
ECa-38kHz	-0.075901
ECa-LH38	0.015696

(B) PAIRED T-TEST

Paired T-Test and CI: ECa-L, ECa-H

Paired T for ECa-L - ECa-H

	N	Mean	StDev	SE Mean
ECa-L	20	3.576	0.323	0.072
ECa-H	20	4.139	0.466	0.104
Difference	20	-0.5634	0.2380	0.0532

95% CI for mean difference: (-0.6748, -0.4520)
T-Test of mean difference = 0 (vs ≠ 0): T-Value = -10.58 P-Value = 0.000

Paired T-Test and CI: ECa-L, ECa-H

Paired T for ECa-L - ECa-H

	N	Mean	StDev	SE Mean
ECa-L	20	3.576	0.323	0.072
ECa-H	20	4.139	0.466	0.104
Difference	20	-0.5634	0.2380	0.0532

95% CI for mean difference: (-0.6748, -0.4520)
T-Test of mean difference = 0 (vs ≠ 0): T-Value = -10.58 P-Value = 0.000

Paired T-Test and CI: ECa-L, ECa-38kHz

Paired T for ECa-L – ECa-38kHz

	N	Mean	StDev	SE Mean
ECa-L	20	3.576	0.323	0.072
ECa-38kHz	20	3.214	0.718	0.161
Difference	20	0.362	0.571	0.128

95% CI for mean difference: (0.095, 0.629)
T-Test of mean difference = 0 (vs ≠ 0): T-Value = 2.84 P-Value = 0.010

Paired T-Test and CI: 0-10cm, VMC-11cm

Paired T for 0-10cm - VMC-11cm

	N	Mean	StDev	SE Mean
0-10cm	20	0.19312	0.03340	0.00747
VMC-11cm	20	0.28755	0.03241	0.00725
Difference	20	-0.09444	0.01704	0.00381

95% CI for mean difference: (-0.10241, -0.08646)
T-Test of mean difference = 0 (vs ≠ 0): T-Value = -24.78 P-Value = 0.000

Paired T for 0-10cm - 10-20cm

	N	Mean	StDev	SE Mean
0-10cm	20	0.19312	0.03340	0.00747
10-20cm	20	0.17751	0.03864	0.00864
Difference	20	0.01561	0.03722	0.00832

95% CI for mean difference: (-0.00181, 0.03303)
T-Test of mean difference = 0 (vs ≠ 0): T-Value = 1.88 P-Value = 0.076

Paired T-Test and CI: 0-10cm, 0-20cm

Paired T for 0-10cm - 0-20cm

	N	Mean	StDev	SE Mean
0-10cm	20	0.19312	0.03340	0.00747
0-20cm	20	0.18531	0.03095	0.00692
Difference	20	0.00780	0.01861	0.00416

95% CI for mean difference: (-0.00091, 0.01652)
T-Test of mean difference = 0 (vs ≠ 0): T-Value = 1.88 P-Value = 0.076

Paired T-Test and CI: VMC-11cm, VMC-16cm

Paired T for VMC-11cm - VMC-16cm

	N	Mean	StDev	SE Mean
VMC-11cm	20	0.28755	0.03241	0.00725
VMC-16cm	20	0.25268	0.03690	0.00825
Difference	20	0.03487	0.01174	0.00263

95% CI for mean difference: (0.02938, 0.04036)
T-Test of mean difference = 0 (vs ≠ 0): T-Value = 13.28 P-Value = 0.000

Paired T-Test and CI: VMC-11cm, VMC-30CM

Paired T for VMC-11cm - VMC-30CM

	N	Mean	StDev	SE Mean
VMC-11cm	20	0.2876	0.0324	0.0072
VMC-30CM	20	0.2471	0.0507	0.0113
Difference	20	0.04044	0.03380	0.00756

95% CI for mean difference: (0.02462, 0.05626)
T-Test of mean difference = 0 (vs ≠ 0): T-Value = 5.35 P-Value = 0.000

Paired T-Test and CI: 0-20cm, VMC-16cm

Paired T for 0-20cm - VMC-16cm

	N	Mean	StDev	SE Mean
0-20cm	20	0.18531	0.03095	0.00692
VMC-16cm	20	0.25268	0.03690	0.00825
Difference	20	-0.06737	0.02082	0.00466

95% CI for mean difference: (-0.07712, -0.05763)
T-Test of mean difference = 0 (vs ≠ 0): T-Value = -14.47 P-Value = 0.000

Paired T-Test and CI: VMC-16cm, VMC-30CM

Paired T for VMC-16cm - VMC-30CM

	N	Mean	StDev	SE Mean
VMC-16cm	20	0.2527	0.0369	0.0083
VMC-30CM	20	0.2471	0.0507	0.0113
Difference	20	0.00557	0.03152	0.00705

95% CI for mean difference: (-0.00918, 0.02033)
T-Test of mean difference = 0 (vs ≠ 0): T-Value = 0.79 P-Value = 0.439

Paired T-Test and CI: ECa-H, ECa-38kHz

Paired T for ECa-H – ECa-38kHz

	N	Mean	StDev	SE Mean
ECa-H	20	4.139	0.466	0.104
ECa-38kHz	20	3.214	0.718	0.161
Difference	20	0.9256	0.4109	0.0919

```
95% CI for mean difference: (0.7333, 1.1180)
T-Test of mean difference = 0 (vs ≠ 0): T-Value = 10.07  P-Value = 0.000
```

Paired T-Test and CI: ECa-L, VMC-16cm

```
Paired T for ECa-L - VMC-16cm

             N    Mean   StDev  SE Mean
ECa-L       20  3.5760  0.3234   0.0723
VMC-16cm    20  0.2527  0.0369   0.0083
Difference  20  3.3233  0.2922   0.0653


95% CI for mean difference: (3.1866, 3.4601)
T-Test of mean difference = 0 (vs ≠ 0): T-Value = 50.87  P-Value = 0.000
```

(C) MULTILINEAR REGRESSION USING BACKWARD ELIMINATION

<u>DEPENDENT VARIABLE</u>: Sand, Silt, Clay, SMC, AWC, Bulk density, pH, CEC, ECw, Organic matter, NH4-N (ppm)

<u>INDEPENDENT VARIABLE</u>: ECa-L, ECa-H, ECa-38kHz

Regression Analysis: Sand versus ECa-L, ECa-H, ECa-38kHz

```
Backward Elimination of Terms

Candidate terms: ECa-L, ECa-H, ECa-38kHz

             ----Step 1----    -----Step 2----    ----Step 3----
              Coef        P      Coef        P     Coef        P
Constant     109.6              110.2              114.8
ECa-L         3.62    0.721      4.00    0.640
ECa-H        -10.2    0.357    -10.99    0.072    -8.66    0.005
ECa-38kHz    -0.37    0.933

S                   4.96984           4.71673            4.54909
R-sq                 54.42%            54.39%             53.33%
R-sq(adj)            39.23%            45.26%             49.08%
R-sq(pred)           14.07%            30.43%             36.02%
Mallows' Cp            4.00              2.01               0.22

α to remove = 0.1
```

Analysis of Variance

Source	DF	Adj SS	Adj MS	F-Value	P-Value
Regression	1	260.1	260.10	12.57	0.005
ECa-H	1	260.1	260.10	12.57	0.005
Error	11	227.6	20.69		
Total	12	487.7			

Model Summary

S	R-sq	R-sq(adj)	R-sq(pred)
4.54909	53.33%	49.08%	36.02%

Coefficients

Term	Coef	SE Coef	T-Value	P-Value	VIF
Constant	114.8	10.3	11.13	0.000	
ECa-H	-8.66	2.44	-3.55	0.005	1.00

Regression Equation

Sand = 114.8 - 8.66 ECa-H

Regression Analysis: Silt versus ECa-L, ECa-H, ECa-38kHz

Backward Elimination of Terms

Candidate terms: ECa-L, ECa-H, ECa-38kHz

	----Step 1----		----Step 2----		----Step 3----	
	Coef	P	Coef	P	Coef	P
Constant	-14.8		-14.3		-17.6	
ECa-L	-3.2	0.778	-2.87	0.761		
ECa-H	10.1	0.410	9.52	0.147	7.84	0.014
ECa-38kHz	-0.28	0.955				
S		5.49861		5.21741		4.99876
R-sq		44.29%		44.26%		43.72%
R-sq(adj)		25.71%		33.12%		38.61%
R-sq(pred)		0.00%		17.57%		24.45%
Mallows' Cp		4.00		2.00		0.09

α to remove = 0.1

Analysis of Variance

Source	DF	Adj SS	Adj MS	F-Value	P-Value
Regression	1	213.5	213.54	8.55	0.014

ECa-H	1	213.5	213.54	8.55	0.014
Error	11	274.9	24.99		
Total	12	488.4			

Model Summary

S	R-sq	R-sq(adj)	R-sq(pred)
4.99876	43.72%	38.61%	24.45%

Coefficients

Term	Coef	SE Coef	T-Value	P-Value	VIF
Constant	-17.6	11.3	-1.55	0.148	
ECa-H	7.84	2.68	2.92	0.014	1.00

Regression Equation

Silt = -17.6 + 7.84 ECa-H

Regression Analysis: Clay versus ECa-L, ECa-H, ECa-38kHz

* NOTE * There are no terms in the model.

Backward Elimination of Terms

Candidate terms: ECa-L, ECa-H, ECa-38kHz

	----Step 1----		----Step 2----		----Step 3----		----Step 4----	
	Coef	P	Coef	P	Coef	P	Coef	P
Constant	5.20		5.26		4.33		6.252	
ECa-L	-0.47	0.840	-0.35	0.783				
ECa-H	0.15	0.952						
ECa-38kHz	0.651	0.527	0.703	0.201	0.600	0.112		
S		1.13340		1.07547		1.02952		1.11150
R-sq		22.02%		21.98%		21.36%		0.00%
R-sq(adj)		0.00%		6.38%		14.21%		0.00%
R-sq(pred)		0.00%		0.00%		0.00%		0.00%
Mallows’ Cp		4.00		2.00		0.08		0.54

α to remove = 0.1
Backward elimination removed all terms from the model.

Regression Analysis: AWC versus ECa-L, ECa-H, ECa-38kHz

Backward Elimination of Terms

α to remove = 0.1

Analysis of Variance

Source	DF	Adj SS	Adj MS	F-Value	P-Value
Regression	1	0.004256	0.004256	36.93	0.000
ECa-L	1	0.004256	0.004256	36.93	0.000
Error	11	0.001268	0.000115		
Total	12	0.005523			

Model Summary

S	R-sq	R-sq(adj)	R-sq(pred)
0.0107344	77.05%	74.96%	68.37%

Coefficients

Term	Coef	SE Coef	T-Value	P-Value	VIF
Constant	0.0838	0.0315	2.66	0.022	
ECa-L	0.05321	0.00876	6.08	0.000	1.00

Regression Equation

AWC = 0.0838 + 0.05321 ECa-L

Fits and Diagnostics for Unusual Observations

Obs	AWC	Fit	Resid	Std Resid	
12	0.24000	0.23235	0.00765	1.00	X

X Unusual X

Regression Analysis: pH versus ECa-L, ECa-H, ECa-38kHz

* NOTE * There are no terms in the model.

Backward Elimination of Terms

Candidate terms: ECa-L, ECa-H, ECa-38kHz

```
             -----Step 1-----    -----Step 2-----    ------Step 3-----    -----
Step 4-----
               Coef         P      Coef         P       Coef         P
Coef         P
```

	Step 1 Coef	Step 1 P	Step 2 Coef	Step 2 P	Step 3 Coef	Step 3 P	Step 4 Coef	Step 4 P
Constant	6.809		6.809		6.582		6.5231	
ECa-L	-0.000	0.999						
ECa-H	-0.130	0.605	-0.130	0.355	-0.0141	0.812		
ECa-38kHz	0.0806	0.439	0.0806	0.360				
S		0.113852		0.108010		0.107613		0.103311
R-sq		8.91%		8.91%		0.54%		0.00%
R-sq(adj)		0.00%		0.00%		0.00%		0.00%
R-sq(pred)		0.00%		0.00%		0.00%		0.00%
Mallows’ Cp		4.00		2.00		0.83		-1.12

α to remove = 0.1
Backward elimination removed all terms from the model.

Regression Analysis: EC (Hanna) versus ECa-L, ECa-H, ECa-38kHz

* NOTE * There are no terms in the model.

Backward Elimination of Terms

Candidate terms: ECa-L, ECa-H, ECa-38kHz

	----Step 1----		----Step 2----		----Step 3----		----Step 4---	
	Coef	P	Coef	P	Coef	P	Coef	P
Constant	4.2		9.1		-1.54		5.92	
ECa-L	8.5	0.460						
ECa-H	-11.9	0.340	-4.48	0.522				
ECa-38kHz	6.57	0.209	4.87	0.278	2.33	0.220		
S		5.56437		5.45112		5.31049		5.46140
R-sq		22.15%		16.98%		13.33%		0.00%
R-sq(adj)		0.00%		0.38%		5.45%		0.00%
R-sq(pred)		0.00%		0.00%		0.00%		0.00%
Mallows’ Cp		4.00		2.60		1.02		0.56

α to remove = 0.1
Backward elimination removed all terms from the model.

Regression Analysis: Organic Carbon (%) versus ECa-L, ECa-H, ECa-38kHz

* NOTE * There are no terms in the model.

Backward Elimination of Terms

Candidate terms: ECa-L, ECa-H, ECa-38kHz

	-----Step 1----		-----Step 2-----		-----Step 3----		-----Step 4----	
	Coef	P	Coef	P	Coef	P	Coef	P
Constant	1.33		0.67		0.99		2.540	
ECa-L	1.52	0.409	1.10	0.480	0.434	0.532		
ECa-H	-1.32	0.501	-0.497	0.626				
ECa-38kHz	0.405	0.614						
S		0.887116		0.854266		0.824715		0.804373
R-sq		8.78%		6.01%		3.64%		0.00%
R-sq(adj)		0.00%		0.00%		0.00%		0.00%
R-sq(pred)		0.00%		0.00%		0.00%		0.00%
Mallows' Cp		4.00		2.27		0.51		-1.13

α to remove = 0.1
Backward elimination removed all terms from the model.

Regression Analysis: Organic Matter versus ECa-L, ECa-H, ECa-38kHz

* NOTE * There are no terms in the model.

Backward Elimination of Terms

Candidate terms: ECa-L, ECa-H, ECa-38kHz

	----Step 1----		----Step 2----		----Step 3---		----Step 4----	
	Coef	P	Coef	P	Coef	P	Coef	P
Constant	2.32		1.16		1.71		4.420	
ECa-L	2.65	0.409	1.92	0.480	0.75	0.532		
ECa-H	-2.30	0.501	-0.87	0.626				
ECa-38kHz	0.71	0.614						
S		1.54358		1.48642		1.43500		1.39961
R-sq		8.78%		6.01%		3.64%		0.00%

R-sq(adj)	0.00%	0.00%	0.00%	0.00%
R-sq(pred)	0.00%	0.00%	0.00%	0.00%
Mallows’ Cp	4.00	2.27	0.51	-1.13

α to remove = 0.1
Backward elimination removed all terms from the model.

Regression Analysis: NH4-N (ppm) versus ECa-L, ECa-H, ECa-38kHz

* NOTE * There are no terms in the model.

Backward Elimination of Terms

Candidate terms: ECa-L, ECa-H, ECa38kHz

	------Step 1------		------Step 2------		------Step 3------	
	Coef	P	Coef	P	Coef	P
Constant	-0.0823		-0.0991		-0.0675	
ECa-L	0.1149	0.082	0.1044	0.064	0.0377	0.152
ECa-H	-0.0704	0.293	-0.0495	0.164		
ECa-38kHz	0.0103	0.702				
S		0.0297078		0.0284271		0.0300067
R-sq		34.01%		32.87%		17.72%
R-sq(adj)		12.02%		19.44%		10.24%
R-sq(pred)		0.00%		4.26%		0.00%
Mallows’ Cp		4.00		2.16		2.22

	------Step 4------	
	Coef	P
Constant	0.06754	
ECa-L		
ECa-H		
ECa-38kHz		
S		0.0316718
R-sq		0.00%
R-sq(adj)		0.00%
R-sq(pred)		0.00%
Mallows’ Cp		2.64

α to remove = 0.1
Backward elimination removed all terms from the model.

Regression Analysis: Soil bulk Density versus ECa-L, ECa-H, ECa-38kHz

Backward Elimination of Terms

Candidate terms: ECa-L, ECa-H, ECa-38kHz

	------Step 1-----		------Step 2------		------Step 3------	
	Coef	P	Coef	P	Coef	P
Constant	1.677		1.785		1.650	
ECa-L	0.188	0.135				
ECa-H	-0.311	0.032	-0.1477	0.085	-0.0791	0.038
ECa-38kHz	0.0855	0.125	0.0478	0.349		
S		0.0577632		0.0624738		0.0623764
R-sq		53.47%		39.53%		33.69%
R-sq(adj)		37.96%		27.43%		27.66%
R-sq(pred)		5.99%		0.00%		0.00%
Mallows' Cp		4.00		4.70		3.83

α to remove = 0.1

Analysis of Variance

Source	DF	Adj SS	Adj MS	F-Value	P-Value
Regression	1	0.02174	0.021743	5.59	0.038
ECa-H	1	0.02174	0.021743	5.59	0.038
Error	11	0.04280	0.003891		
Total	12	0.06454			

Model Summary

S	R-sq	R-sq(adj)	R-sq(pred)
0.0623764	33.69%	27.66%	0.00%

Coefficients

Term	Coef	SE Coef	T-Value	P-Value	VIF
Constant	1.650	0.141	11.67	0.000	
ECa-H	-0.0791	0.0335	-2.36	0.038	1.00

Regression Equation

Soil bulk Density = 1.650 - 0.0791 ECa-H

Regression Analysis: SOIL VMC versus ECa-L, ECa-H, ECa-38kHz

```
* NOTE * There are no terms in the model.


Backward Elimination of Terms

Candidate terms: ECa-L, ECa-H, ECa-38kHz

             ------Step 1------    ------Step 2------    ------Step 3-----
                Coef         P        Coef         P       Coef         P
Constant       0.095                  0.018                0.035
ECa-L         0.1395     0.113      0.0914     0.241     0.0564     0.114
ECa-H        -0.1211     0.189     -0.0260     0.602
ECa-38kHz     0.0467     0.215

S                    0.0401227             0.0416488             0.0402833
R-sq                    35.97%                23.34%                21.11%
R-sq(adj)               14.62%                 8.00%                13.94%
R-sq(pred)               0.00%                 0.00%                 0.00%
Mallows' Cp               4.00                  3.78                  2.09

             ------Step 4-----
               Coef          P
Constant     0.2370
ECa-L
ECa-H
ECa-38kHz

S                   0.0434230
R-sq                    0.00%
R-sq(adj)               0.00%
R-sq(pred)              0.00%
Mallows' Cp              3.06

α to remove = 0.1
Backward elimination removed all terms from the model.
```

Regression Analysis: CEC (cmol/kg) versus ECa-L, ECa-H, ECa-38kHz

```
* NOTE * There are no terms in the model.


Backward Elimination of Terms

Candidate terms: ECa-L, ECa-H, ECa-38kHz

             ----Step 1----    ----Step 2----    -----Step 3----    -----Step
4----
              Coef        P     Coef        P      Coef        P      Coef
P
Constant     14.44              13.71               15.72              13.076
ECa-L         2.22    0.552      1.76    0.576
ECa-H        -2.56    0.523     -1.66    0.428    -0.630    0.498
```

```
ECa-38kHz     0.44    0.786

S                  1.81648          1.73074          1.67751
1.64150
R-sq                 8.16%            7.36%            4.27%
0.00%
R-sq(adj)            0.00%            0.00%            0.00%
0.00%
R-sq(pred)           0.00%            0.00%            0.00%
0.00%
Mallows' Cp           4.00             2.08             0.38              -
1.20

α to remove = 0.1
Backward elimination removed all terms from the model.
```

Regression Analysis: Gravi Moisture content versus ECa-L, ECa-H, ECa-38kHz

```
Backward Elimination of Terms

Candidate terms: ECa-L, ECa-H, ECa-38kHz

             ------Step 1------    ------Step 2-----    ------Step 3------
                Coef          P       Coef          P       Coef          P
Constant      0.0236                0.0055               -0.0130
ECa-L         0.0798      0.192    0.0432      0.212     0.0540      0.032
ECa-H        -0.0484      0.446
ECa-38kHz     0.0230      0.382    0.0063      0.649

S                  0.0285895           0.0280628            0.0270491
R-sq                  40.80%              36.62%               35.23%
R-sq(adj)             21.06%              23.94%               29.34%
R-sq(pred)             0.00%               2.56%                9.06%
Mallows' Cp             4.00                2.63                 0.85

α to remove = 0.1


Analysis of Variance

Source      DF    Adj SS    Adj MS  F-Value  P-Value
Regression   1  0.004377  0.004377     5.98    0.032
  ECa-L      1  0.004377  0.004377     5.98    0.032
Error       11  0.008048  0.000732
Total       12  0.012425


Model Summary

        S    R-sq  R-sq(adj)  R-sq(pred)
0.0270491  35.23%     29.34%       9.06%


Coefficients
```

Term	Coef	SE Coef	T-Value	P-Value	VIF
Constant	-0.0130	0.0795	-0.16	0.873	
ECa-L	0.0540	0.0221	2.45	0.032	1.00

Regression Equation

Gravi Moisture content = -0.0130 + 0.0540 ECa-L

Fits and Diagnostics for Unusual Observations

Obs	Gravi Moisture content	Fit	Resid	Std Resid		
4	0.1341	0.2024	-0.0683	-2.80	R	
12	0.1378	0.1377	0.0002	0.01		X

R Large residual
X Unusual X

(D) SEMIVARIOGRAM ANALYSIS FOR SELECTED SOIL PROPERTIES

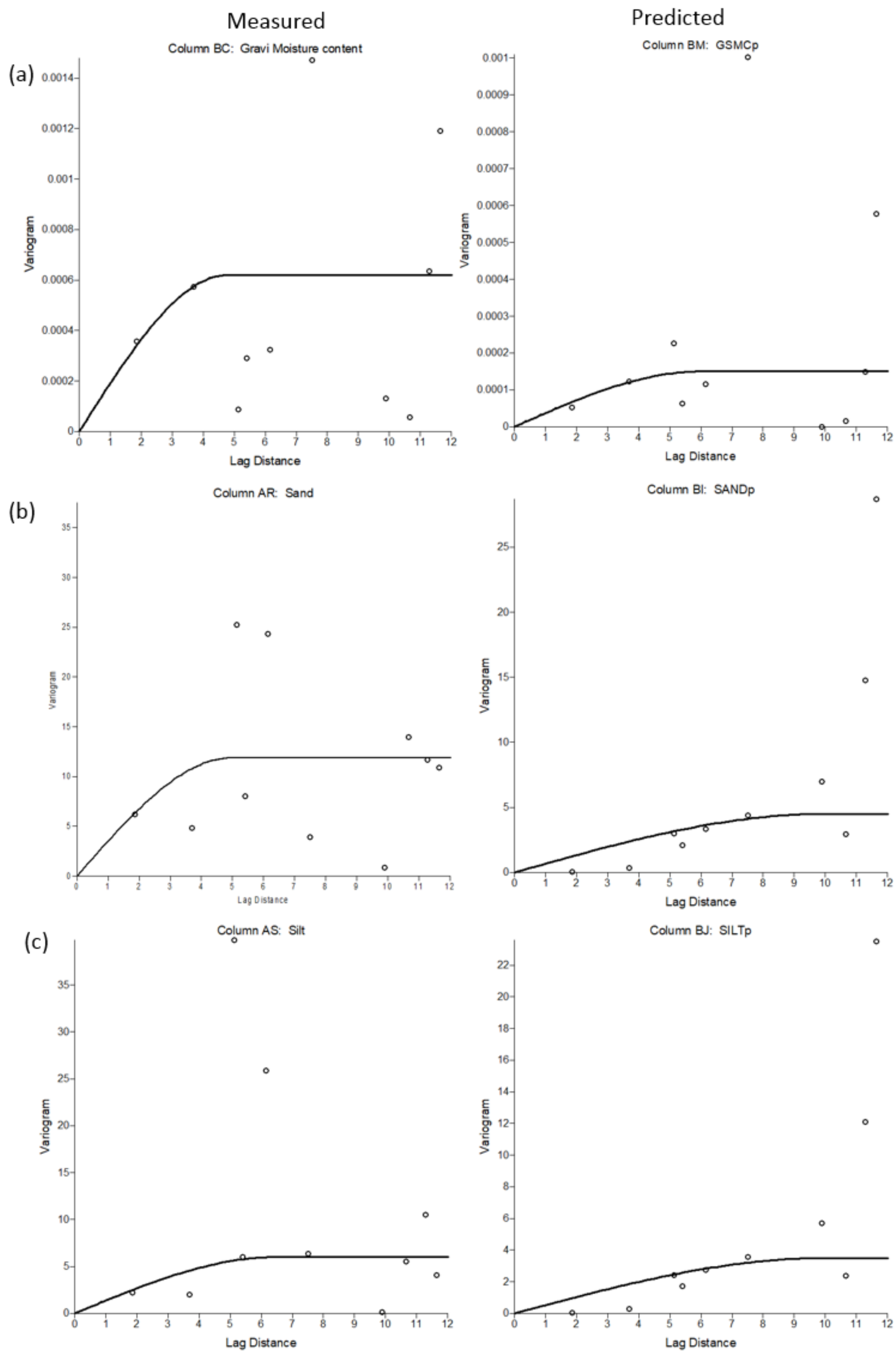

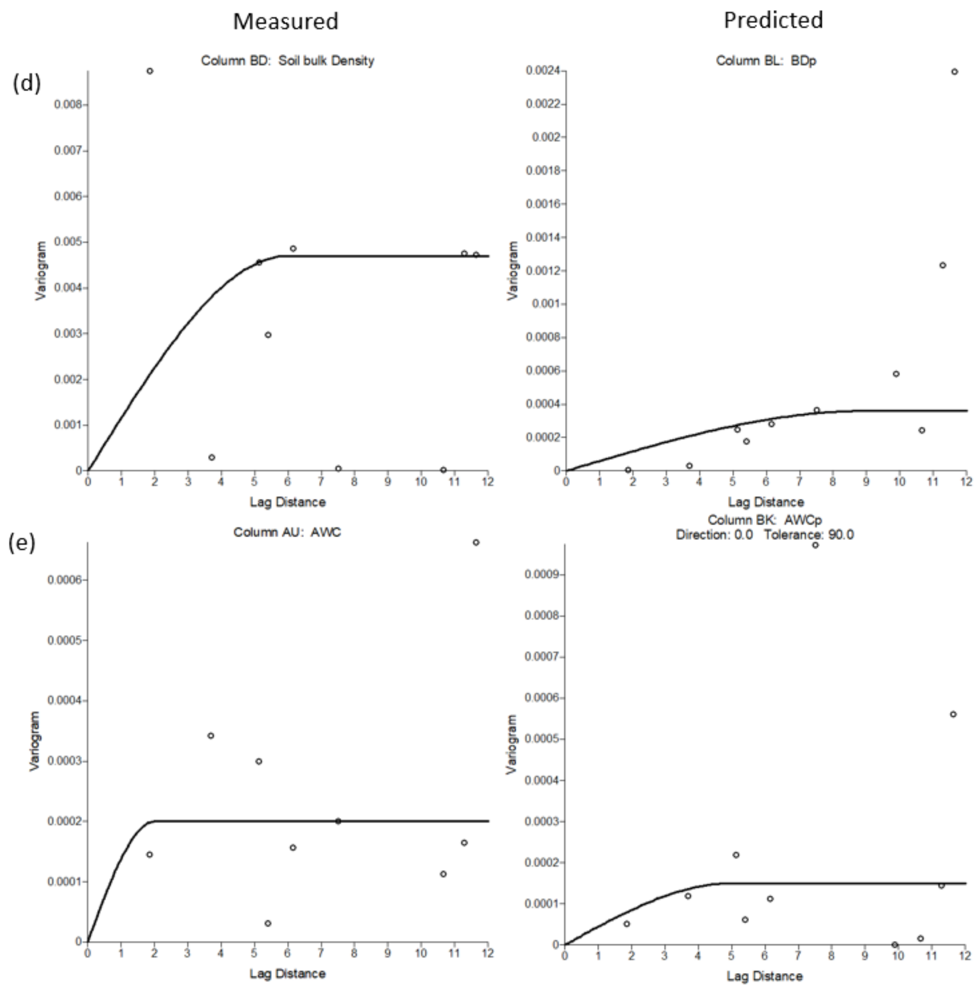

Measured and predicted semi variogram analysis (a) SMC (b) sand (c) silt (d) bulk density (e) AWC.

(E) AWC estimated using soil moisture characteristic curve developed with pressure plate extractor and fitted with van Genuchten (1980) model

0-10 cm	Sampling Plot	FC	PWP (1 m)	AWC (153 m)	10-20 cm	FC	PWP (1 m)	AWC (153 m)	AVERAGE AWC
1	R1P1	0.37	0.10	0.27	15	0.37	0.07	0.30	0.29
2	R1P4	0.37	0.10	0.27	16	0.32	0.07	0.25	0.26
3	R1P5	0.37	0.10	0.27	17	0.29	0.06	0.23	0.25
4	R1P8	0.41	0.10	0.31	18	0.37	0.07	0.30	0.31
5	R2P1	0.42	0.10	0.32	19	0.32	0.07	0.25	0.29
6	R2P5	0.36	0.09	0.27	20	0.30	0.06	0.24	0.26
7	R2P8	0.39	0.10	0.29	21	0.37	0.07	0.30	0.30
8	R3P1	0.38	0.07	0.31	22	0.37	0.08	0.29	0.30
9	R3P5	0.34	0.07	0.27	23	0.28	0.07	0.21	0.24
10	R3P8	0.36	0.07	0.29	24	0.32	0.08	0.24	0.27
11	R4P1	0.37	0.07	0.30	25	0.35	0.08	0.27	0.29
12	R4P5	0.30	0.06	0.24	26	0.31	0.07	0.24	0.24
13	R4P6	0.37	0.07	0.30	27	0.34	0.10	0.24	0.27
14	R4P8	0.34	0.06	0.28	28	0.34	0.07	0.27	0.28

All the average AWC was used for analysis except the average of 14 and 28

FC- Field Capacity

PWP – Permanent Wilting Point

AWC – Available Water Content

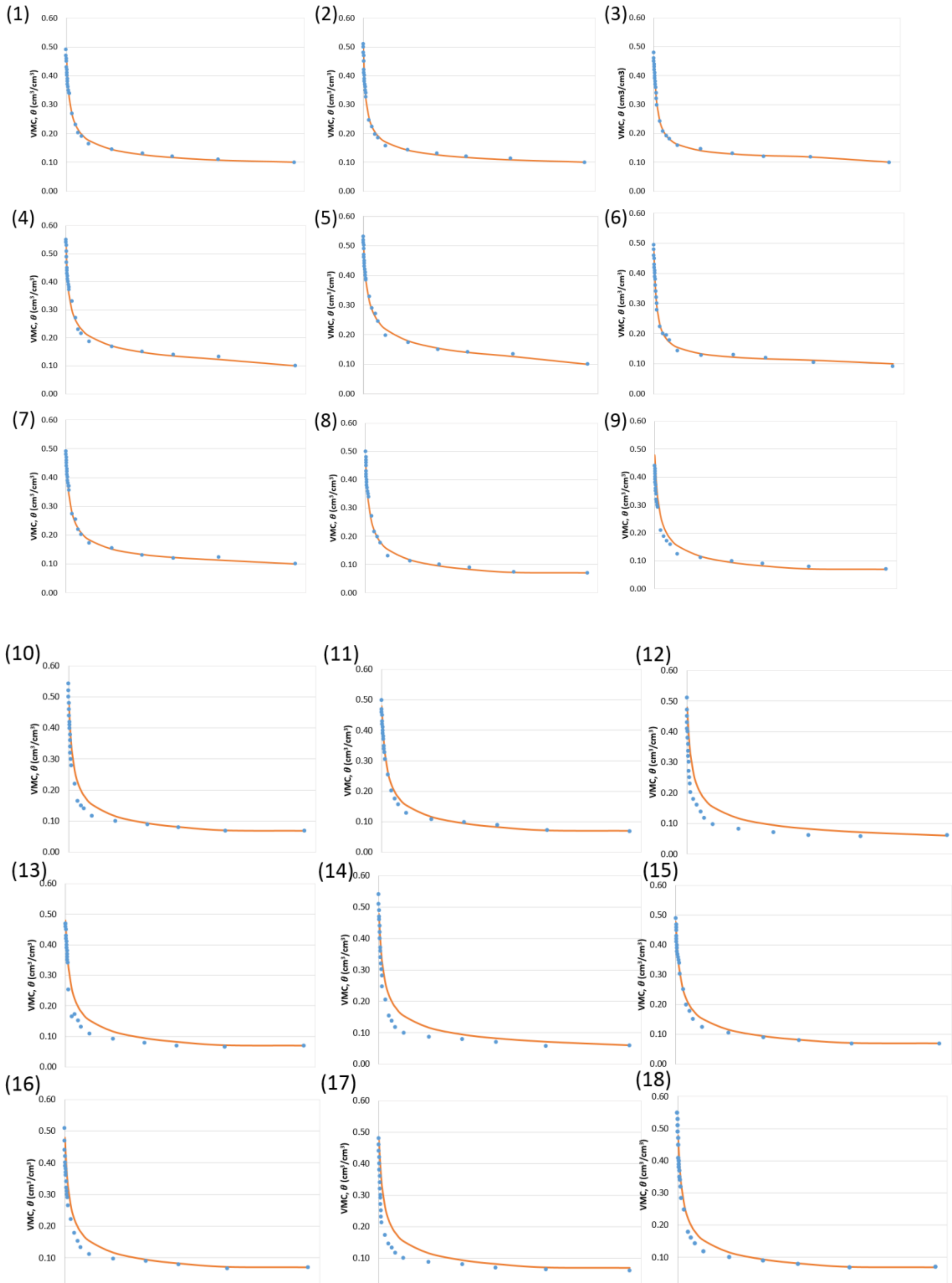
(1)
(2)
(3)
(4)
(5)
(6)
(7)
(8)
(9)
(10)
(11)
(12)
(13)
(14)
(15)
(16)
(17)
(18)
VMC, θ (cm³/cm³)

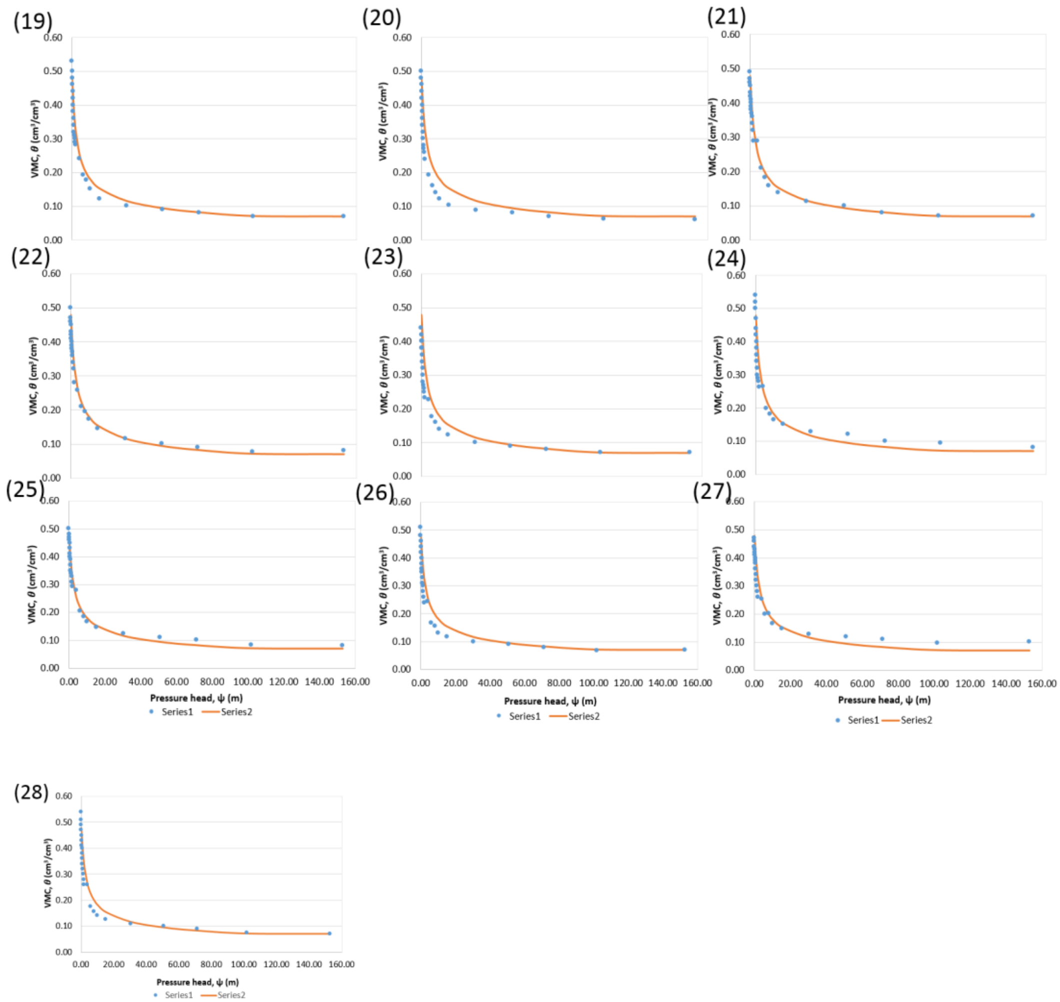
(19)
(20)
(21)
(22)
(23)
(24)
(25)
(26)
(27)
(28)
VMC, θ (cm³/cm³)
Pressure head, ψ (m)
Series1
Series2